REGULATION OF THE TRANSFORMING IMMORTALIZED MAMMARY PROTEIN AND ITS HOMOLOGS BY AUTO-INHIBITION AND TYROSINE PHOSPHORYLATION

Marielle E. Yohe

A dissertation submitted to the faculty of the University of North Carolina at Chapel Hill in partial fulfillment of the requirements for the degree of Doctor of Philosophy in the Department of Pharmacology.

Chapel Hill
2007

Approved by:

Keith Burridge, Ph.D.

Channing J. Der, Ph.D.

Lee M. Graves, Ph.D.

David P. Siderovski, Ph.D.

John Sondek, Ph.D.

ABSTRACT

MARIELLE E. YOHE: Regulation of the Transforming Immortalized Mammary Protein and its Homologs by Auto-inhibition and Tyrosine Phosphorylation
(Under the direction of John Sondek)

Dbl-related oncoproteins are guanine nucleotide exchange factors (GEFs) specific for Rho-family GTPases and typically possess tandem Dbl (DH) and pleckstrin homology (PH) domains that act in concert to catalyze exchange. The exchange activities of many Dbl-proteins are regulated by phosphorylation or constitutively activated by truncations preceding their DH domains. However, exact mechanisms of regulation remain poorly understood. Here we show that a sub-group of Dbl-family proteins, including Tim, Ngef, and Wgef, are auto-inhibited by a highly conserved helix immediately N-terminal to the DH domain that directly occludes the catalytic interface of the DH domain to prevent GTPase activation. Similar to the distantly related Vav isozymes, auto-inhibition is relieved by truncation, mutation, or phosphorylation of the auto-inhibitory helix. Furthermore, substitutions within a highly conserved surface of the DH domain designed to disrupt interactions with the auto-inhibitory helix also fully activates the exchange process. Therefore, the regulated auto-inhibition of DH domains by direct steric exclusion using short N-terminal segments likely represents a general mode of regulation within the large family of Dbl-family proteins. The C-terminal SH3 domain binding to a poly-proline region N-terminal to the DH domain of this subgroup of Dbl-family proteins provides a unique mechanism of regulated auto-inhibition of exchange activity that is functionally linked to the interactions between the auto-inhibitory helix and the DH domain.

for owen

ACKNOWLEDGEMENTS

I am greatly troubled by the fact that although the published manuscripts derived from the work presented in this dissertation have many authors, I am permitted to only list my name on the title page here. I would therefore like to thank the many people who have contributed to this work.

I would first like to thank the members of the Sondek lab for their advice and support, emotionally and experimentally. Kent Rossman served as my rotation mentor when first I joined the lab, and continued to provide advice and help with experiments long after my rotation had ended. This work could not have been accomplished without the efforts of Svetlana Gershburg, who keeps everything running. Cynthia Holley was a critical reader for everything I have written in the Sondek lab, including this dissertation, and I cannot thank her enough for that. Also, I am grateful to Rafael Rojas for his assistance with the *in vitro* exchange assays.

The cellular transformation and GTPase activation assays described here were performed with the guidance of Channing Der and the assistance of many people in his lab, including Patti Solski, Que Lambert and Natalia Mitin. In addition, the *in vitro* kinase assays described here were performed in the laboratory of Lee Graves, by Olivia Gardner and Brian Dewar. All of the work with dissociated neurons in culture was performed by Paul Barnes in the laboratory of Franck Polleux. Ashutosh Tripathy in the Macromolecular Interactions core facility performed the analytical ultracentrifugation experiments. I would like to thank Christopher Johnston and Melinda Willard in the

laboratory of David Siderovski for their help with surface plasmon resonance experiments and antibody characterization, respectively, and Michael Allingham in the laboratory of Keith Burridge for help with fluorescence microscopy experiments.

I would like to thank John Sondek for his enthusiasm for this project and for allowing me the freedom to follow this project in several unexpected directions. I would also like to thank my dissertation committee, the Pharmacology department and the MD/PhD program for all of their support and assistance.

Last but not least, I would like to thank my family and friends for the sacrifices they have made that have allowed me to achieve this goal.

TABLE OF CONTENTS

LIST OF TABLES

LIST OF FIGURES

LIST OF ABBREVIATIONS

Abl	Ableson tyrosine kinase
Abp1	Actin binding protein 1
ACK1	Activated Cdc42-associated kinase 1
AKAP	A-kinase anchoring protein
Ala, A	Alanine
ALS	Amyotrophic lateral scelrosis
AML	Acute myelogenous leukemia
APC	Adenomatous polyposis coli
Asef	APC-stimulated exchange factor
ATP	Adenosine triphosphate
BAR	Bin, amphiphysin, RVS
bFGF	Basic fibroblast growth factor
BNDF	Brain-derived neurotrophic factor
BODIPY	Dipyrromethene boron difluoride
BRCT	BRCA1 C-terminal repeat
CA	Constitutively active
CaMKII	Calcium and calmodulin-modulated kinase II
Cbl	Casistas B-lymphoma
Ccpg1	Cell cycle progression protein 1
CD47	Cluster of differentiation 47
CDEP	Chonrocyte-derived ezrin-like domain containing protein
Cdk	Cyclin dependent kinase

cDNA	Complementary deoxyribonucleic acid
CH	Calponin homology
CHIP	C-terminus of Hsc70 interacting protein
CML	Chronic myelogenous leukemia
COS 7	African green monkey SV40 kidney fibroblast cell line
CRD	Cysteine rich domain
C-terminus	Carboxy-terminus
Dbl	Diffuse B-cell lymphoma
Dbs	Dbl's big sister
DEP	Disheveled, EGL-10, Pleckstrin
DH	Dbl homology
DIV	Days *in vitro*
DMEM	Dulbecco's modified Eagle's medium
DTT	Dithiothreitol
Ect2	Epithelial cell transforming protein 2
EDTA	Ethylenediaminetetraacetic acid
EGF	Epidermal growth factor
EGTA	Ethyelene glycol acetic acid
EH	Eps homology
ERK	Externally regulated kinase
FAK	Focal adhesion kinase
FBS	Fetal bovine serum
FERM	Band 4.1, ezrin, radixin, moesin

Fgd	Faciogenital dysplasia
Frg	Fgd1-related GEF
FYVE	Fab-1, YGL023, Vps37, EEA1
GAP	GTPase activating protein
GDI	Guanine nucleotide dissociation inhibitor
GEF	Guanine nucleotide exchange factor
GFP	Green fluorescent protein
Git	GPCR kinase interactor
Glu, E	Glutamic acid
GPCR	G-protein coupled receptor
Grb2	Growth factor receptor bound protein 2
GST	Glutathione S-transferase
GTP	Guanosine triphosphate
HA	Hemagglutinin
HEK 293T	Human embryonic kidney 293T
HEPES	4-(2-hydroxyethyl)-1-piperazineethanesulfonic acid
Hsp	Heat shock protein
Ile, I	Isoleucine
InsP	Inositol phosphate
IPTG	Isopropyl-β-D-thiogalactopyranoside
IRES	Internal ribosome entry site
ITSN	Intersectin
JNK	c-Jun N-terminal kinase

KD	Kinase dead
kDa	Kilodalton
KGF	Keratinocyte growth factor
LARG	Leukemia-associated RhoGEF
LB	Luria-Bertani
Lbc	Lymphoid blast crisi
Lfc	Lbc's first cousin
LPA	Lysophosphatidic acid
MAD	Multiwavelength anomalous diffraction
Mant	N-methylanthraniloyl
MEK	MAP ERK kinase
MLL	Mixed lineage leukemia
mRNA	Messenger Ribonucleic acid
ND	Not determined
Net1	Neuroepithelial transforming protein
Ngef	Neuronal-specific GEF
NGF	Nerve growth factor
NIH 3T3	National Institutes of Health 3T3
NLS	Nuclear localization signal
NMDA	N-methyl-D-aspartic acid
NMR	Nuclear magnetic resonance
N-terminus	Amino terminus
PAGE	Polyacrylamide gel electrophoresis

Pak	p21-activated kinase
Par	Partitioning defective
PBS	Phosphate buffered saline
PCR	Polymerase chain reaction
PDAC	Pancreatic ductal adenocarcinoma
PDGF	Platelet-derived growth factor
PDZ	PSD95, Discs large, ZO1
Pem2	Posterior end mark 2
PH	Pleckstrin homology
PI	Phosphoinositide
Pix	Pak-interacting exchange factor
PKA	Protein kinase A
PKC	Protein kinase C
PLC	Phospholipase C
P-Rex	PI(3,4,5)P_3-dependent Rac exchanger
PV	Pervanadate
Ras-GRF	Ras guanine nucleotide releasing factor
Rb	Retinoblastoma
RBD	Ras (or Rho) binding domain
REM	Ras exchanger motif
RFU	Relative fluorescence units
RGS	Regulator of G-protein signaling
ROCK	Rho-kinase

ROS	Reactive oxygen species
RTK	Rhotekin
RU	Response units
SDS	Sodium dodecylsulfate
Ser, S	Serine
Sgef	SH3 domain-containing GEF
SH2	Src homology 2
SH3	Src homology 3
Shc	SH2 domain-containing protein
Sos	Son of sevenless
SPR	Surface plasmon resonance
SR	Sarcoplasmic reticulum
Stef	Sif and Tiam1-like exchange factor
SYF	Src/Yes/Fyn triple knock out
TH	Tec homology
Thr, T	Threonine
Tiam	T-cell invasion and metastasis
Tim	Transforming immortalized mammary
Tris	trishydroxymethylaminomethane
TrkB	Tyrosine receptor kinase B
TSS	Tiam1 and Stef similarity region
Tyr, Y	Tyrosine
Vsm-RhoGEF	Vascular smooth muscle cell RhoGEF

WASP	Wiscott-Aldrich syndrome protein
WAVE	WASP-family Verprolin-homology protein
Wgef	Weakly similar to RhoGEF5
WT (wt)	Wild type
Xpln	Exchange factor found in platelets, leukemic and neuronal tissues

CHAPTER 1: REGULATION OF THE EXCHANGE ACTIVITY OF DBL-FAMILY PROTEINS

RhoA, Rac1, and Cdc42 are the best understood of the 22 human Rho-family GTPases, which comprise one of five branches of the Ras superfamily of small GTPases (1). Like Ras, Rho proteins function as binary switches that alternate between inactive, GDP-bound states and active, GTP-bound states. Once activated, Rho GTPases directly engage numerous downstream effectors to modulate their functions. Active Rho GTPases and their effectors orchestrate actin cytoskeleton rearrangement and gene transcription to coordinate diverse cellular processes including adhesion, migration, phagocytosis, cytokinesis, neurite extension and retraction, polarization, growth and survival (2). Not surprisingly, aberrant activation of Rho GTPases promotes various developmental, immunological and proliferative disorders (3).

In the development of the nervous system, Rho GTPases integrate extracellular signals to direct outgrowth of both axons and dendrites; and the formation and dynamics of dendritic spines. Deletion or mutation of crucial components of the Rho signaling pathway renders neurons less responsive to environmental cues, leading to suboptimal neuronal connectivity and plasticity (4).

The activation cycle of Rho GTPases is tightly controlled by three families of proteins: GTPase activating proteins (GAPs), guanine nucleotide dissociation inhibitors (GDIs) and guanine nucleotide exchange factors (GEFs). The Dbl-family of proteins constitutes the largest group of GEFs specific for Rho GTPases. Dbl-family proteins are

characterized by a Dbl-homology (DH) domain, which contacts the Rho GTPase to catalyze nucleotide exchange by promoting and stabilizing an intermediate, nucleotide-free GTPase state, and an associated pleckstrin-homology (PH) domain, which fine-tunes the exchange process by a variety of mechanisms related to the binding of phosphoinositides. The 69 human Dbl-family proteins are divergent in regions outside the DH/PH module, and contain additional protein domains that dictate unique cellular functions (5).

The capacity of DH domains to activate Rho GTPases is tightly regulated through a multitude of diverse mechanisms ranging from alterations in transcript levels and protein expression (6) to subcellular re-distribution (7), post-translation modifications (8) and protein degradation (9). However, despite this large spectrum of regulatory mechanisms, in most cases, truncation of Dbl-family proteins often potently activates their exchange activities (10). Currently, there is no general understanding for why truncation promotes unregulated exchange.

The 69 human Dbl-family proteins can be grouped into 17 different sub-families based on their domain architecture and the sequence similarity of their DH domains (see Figure 1 and (5)). The regulatory mechanisms for each characterized sub-family are reviewed below.

Fgd subfamily:

The Fgd subfamily consists of Fgd1 (**F**acio**g**enital **d**ysplasia protein 1), Fgd2, Fgd3 and Frabin. Each of these proteins possesses a C-terminal FYVE domain in addition to the catalytic DH/PH cassette (5). FYVE domains, named for the proteins

Fab-1, **Y**GL023, **V**ps27 and **E**EA1, which also possess this domain, are small, cysteine-rich, zinc-binding domains known to bind specifically to the phosphoinositide, PI3P (11).

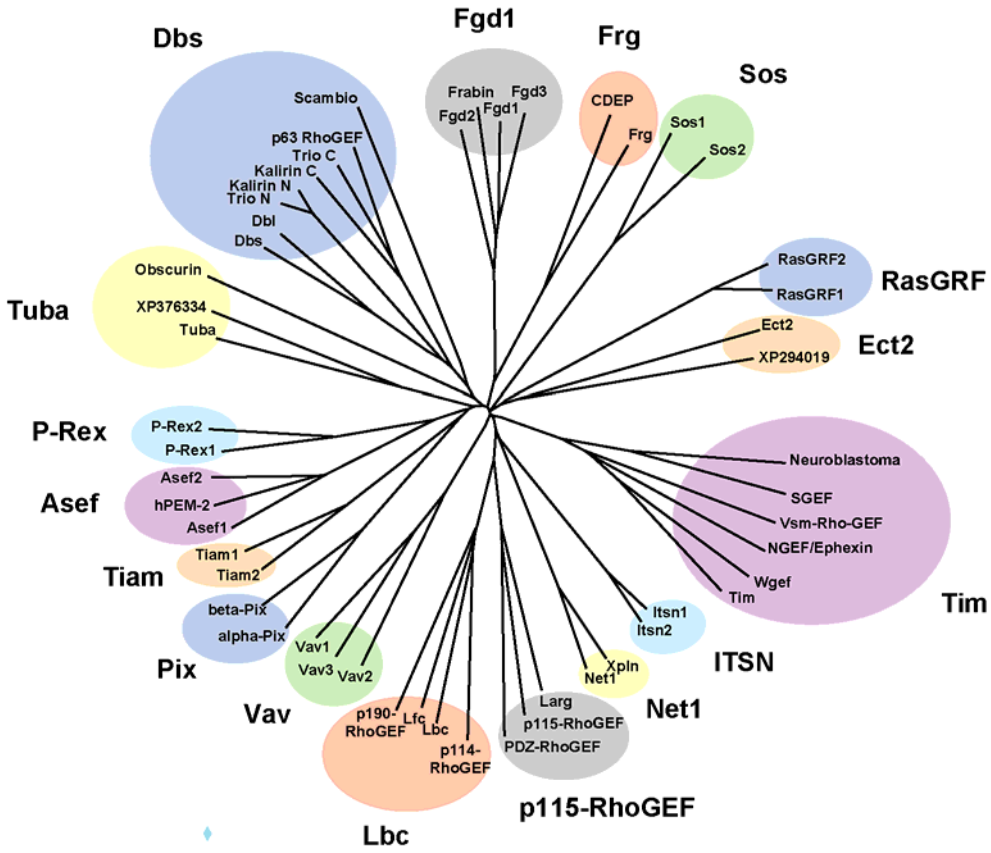

Figure 1: Grouping of Dbl-family proteins into subfamilies.
The 69 human Dbl-family proteins can be grouped into 17 subfamilies based upon their domain architecture and the sequence similarity of their DH domains. Dendrogram adapted from (5).

The genes for the members of the Fgd1 subfamily were originally identified as being responsible for the development of faciogenital dysplasia, or Aasrskog Scott syndrome, a developmental disorder characterized by adverse effects on the formation of skeletal structures as well as mental retardation. Each of these proteins has been shown to specifically activate Cdc42 (12-16).

The best characterized member of this subfamily is Fgd1. Early studies on the regulation of Fgd1 exchange activity showed that while the DH domain alone was incapable of inducing filopodia formation in fibroblasts (17), the DH/PH cassette was able to transform NIH 3T3 cells (18), suggesting that the PH domain of Fgd1 is necessary for it to exchange guanine nucleotide on Cdc42. Indeed, genetic analysis of a family afflicted with faciogenital dysplasia revealed that one mutation responsible for the development of this disorder is a missense mutation of a residue in the PH domain known to be involved in phosphoinositide binding (19), underscoring the importance of a functional PH domain for proper regulation of Fgd1. However, microinjection of the N-terminus of Fgd1 into fibroblasts prevented the formation of Fgd1-induced filopodia (20), indicating that this Dbl-family protein, like many others, may be auto-inhibited by regions N-terminal to the DH domain.

Alterations in sub-cellular localization also play a role in the regulation of Fgd1 exchange activity. A proline-rich region in the N-terminus of Fgd1 is necessary and sufficient for its proper localization to the plasma membrane and the Golgi (20). This region has also been shown to interact with cortactin and Actin Binding Protein 1 (Abp1) (21). The interaction between Fgd1 and these two actin binding proteins localizes Fgd1 to the subcortical actin cytoskeleton in migrating cells. Mutations that prevent this

interaction mislocalize Fgd1 and lead to a decrease in cell motility, indicating that sub-cellular localization is critical for Fgd1 function (21). Finally, Fgd1 has been shown to be regulated by changes in its protein expression level. Fgd1 is poly-ubiquitinated and targeted for degradation by FWD1/β-TrCP, an F-box E3 ubiquitin ligase. Mutant Fgd1, in which both serines in the FWD1 recognition site have been substituted with alanine, is more stably expressed in cells and confers an increase in cell motility (22).

While the regulation of Fgd2 and Fgd3 exchange activity has yet to be studied, the exchange activity of Frabin is also regulated by its sub-cellular localization. While the isolated DH/PH cassette is capable of catalyzing exchange on Cdc42 *in vitro*, an N-terminal portion of Frabin, which is capable of binding F-actin and crosslinking actin filaments, is required for Frabin to induce the formation of microspikes in fibroblasts (15,23), indicating that Frabin must be localized to the actin cytoskeleton to function *in vivo*. However, the products of PI3 kinase are also required for Frabin activity in cells. PI3 kinase has been shown to be necessary for Frabin to induce invadopodia in RPMI7951 human melanoma cells (24), and for Frabin to localize to the plasma membrane during human biliary cell infection by Cryptosporidium parvum (25). The Fgd1 subfamily of Dbl-family proteins, then, is regulated by several distinct mechanisms, including N-terminal auto-inhibition, alteration of sub-cellular localization and alteration in levels of expressed protein.

Frg subfamily:

The Frg subfamily of Dbl-family proteins consists of Frg (**F**gd1-**r**elated **G**EF, also known as FIR or Farp2) and CDEP (**C**hondrocyte-**d**erived **e**zrin-like domain containing **p**rotein, also known as Farp) (5). These proteins each possess an N-terminal FERM

GEF:	Truncation:	Reference:
Asef	Δ SH3	(26)
CDEP	Δ FERM	(27)
Dbl	Δ spectrin repeats	(28)
Dbs	Δ Sec14	(29)
Ect2	Δ BRCT repeats	(30)
Fgd1	Δ N-terminus	(20)
GEF-H1	Δ N- and C-terminus	(31)
ITSN	Δ SH3 domains	(32)
LARG	Δ coiled-coil	(33)
Lbc	Δ C-terminus	(34)
Net1	Δ N-terminus	(35)
Ngef	Δ N-terminus	(36)
p114-RhoGEF	Δ N- and C-terminus	(37)
p115-RhoGEF	Δ coiled-coil	(33)
p190-RhoGEF	Δ N- and C-terminus	(38)
PDZ-RhoGEF	Δ coiled-coil	(33)
Pem2	Δ SH3	(39)
P-Rex	Δ DEP, PH or PDZ	(40)
RasGRF	Δ C-terminus	(41)
Sgef	Δ N-terminus	(42)
Tiam1	Δ PH and TSS	(43)
Tim	Δ N-terminus	(44)
Vav	Δ CH	(45)

Table 1: Dbl-family GEFs that are activated by truncation mutations.

domain and a C-terminal PH domain in addition to the DH/PH cassette. FERM domains, named for Band **4**.1, **E**zrin, **R**adixin and **M**oesin, are thought to bind to both phosphoinositides and adhesion proteins, and in so doing, serve as a link between membrane dynamics and the actin cytoskeleton.

The exchange activity of Frg is activated primarily by direct, Src-dependent tyrosine phosphorylation of Frg, which activates its exchange potential towards Cdc42. Several different signaling pathways lead to Src phosphorylation of Frg. For example, endothelin A, acting through its G-protein coupled receptor, leads to Src phosphorylation of Frg (46). In addition, the binding of nectins, the calcium-independent Ig-like adhesion molecules that initiate the formation of adherens junctions, to their partners on neighboring cells leads to Src-mediated phosphorylation of Frg (47). However, signaling pathways downstream of nectin ligation also lead to activation of the small GTPase Rap1, which is also able to activate Frg, through an as yet undetermined mechanism (48). Finally, the interaction of CD47, an Ig superfamily member, with its ligand, SH2-domain containing protein tyrosine phosphatase, leads to activation of Src and phosphorylation of Frg, which promotes the formation of dendritic filopodia and spines (49).

CDEP has not yet been shown to be a substrate for Src phosphorylation. However, truncation of the N-terminal FERM domain of CDEP has been shown to activate its exchange potential towards RhoA (27). In addition, CDEP is regulated at the transcriptional level. Parathyroid hormone, binding to its G-protein coupled receptor, leads to the formation of the second messenger, cyclic AMP, which induces the expression of CDEP in maturing chondrocytes (27). The two Frg subfamily members, then, are regulated in different ways. Frg is regulated primarily by tyrosine

phosphorylation, while CDEP is regulated by auto-inhibition and alterations in levels of its transcript.

Ras-GRF subfamily:

The Ras-GRF subfamily consists of two highly related isozymes, Ras-GRF1 (Ras **g**uanine nucleotide **r**eleasing **f**actor) and Ras-GRF2 (5). Both Ras-GRF1 and Ras-GRF2 are expressed predominantly in the neuronal cells of the central nervous system. Like the Sos proteins, Ras-GRF1 and 2 are able to catalyze exchange of guanine nucleotides on both GTPases of the Ras family, through a C-terminal Cdc25 domain, and the Rho family, through an N-terminal DH/PH cassette. In addition to the Cdc25 and DH/PH domains, Ras-GRF proteins also contain an N-terminal, non-DH-associated PH domain, and an IQ motif. While the exchange potential of Ras-GRF toward Ras is strongly activated by calcium binding to the IQ motif, the regulation of the exchange potential of Ras-GRF towards Rac1, the cognate GTPase of the DH/PH cassette, is less well understood (41).

Several lines of evidence suggest that regulation of Ras-GRF exchange activity towards Rac1 is regulated by heterotrimeric G-proteins. First, the Rac activity of Ras-GRF is increased in response to LPA (lysophosphatidic acid) (50), which acts through a G-protein coupled receptor (GPCR). In addition, Ras-GRF has been shown to function as a Rac1-specific GEF when it is immunoprecipitated from cells that are also expressing $G\beta\gamma$ (51).

Ras-GRF exchange activity is regulated independently of heterotrimeric G-proteins as well. For example, Ras-GRF is tyrosine phosphorylated in a Src-dependent manner downstream of signaling from the platelet-derived growth factor (PDGF)

receptor, and that phosphorylation increases its exchange activity toward Rac (51). Truncation of the C-terminus of Ras-GRF also activates its exchange potential toward Rac (41). Ras-GRF exchange activity is also regulated by dimerization. Both Ras-GRF1 and Ras-GRF2 form homo- and hetero-dimers through their DH domains, and these dimerization events are required for their transformation activity (52). Finally, the N-terminal region of Ras-GRF has been shown to interact with both microtubules (53) and activated H-Ras (41), although the consequences of these interactions on the exchange potential of Ras-GRF towards Rac have yet to be determined. The mechanisms by which the Rac-specific exchange activity of Ras-GRF isozymes are regulated, then, are incompletely understood. However, these mechanisms include activation downstream of cell surface receptors such as GPCRs and RTKs and other intermolecular interactions.

Sos subfamily:

The Sos subfamily is made up of the highly related isozymes, Sos1 (**S**on **o**f **s**evenless) and Sos2 (5). Sos was originally identified in Drosophila as an exchange factor for Ras in the Sevenless pathway of eye development. Like the RasGRF isozymes, the Sos isozymes are exchange factors for Rac1, through their N-terminal DH/PH cassettes, and Ras, through their C-terminal Cdc25 domains (54).

Unlike the RasGRF isozymes, the molecular context in which the Sos isozymes function as a GEF for Rac as opposed to Ras has been well described. The proline-rich C-terminus of Sos is able to interact with the SH3 domain of the adaptor, Grb2. The SH2 domain of Grb2 localizes the Sos/Grb2 to auto-phosphorylated receptor tyrosine kinases at the cell membrane. This membrane localization enables Sos to catalyze exchange of guanine nucleotides on Ras (54). In contrast, Sos can also form a poly-proline mediated

complex with two scaffold proteins, Eps8 and E3b1. When Sos is in this context, it is able to activate Rac as opposed to Ras (55,56). The transition between the Sos/Grb2 and Sos/Eps8/E3b1 complex is mediated by p66-Shc, an adaptor protein that competes with Grb2 for Sos binding and causes the dissociation of the Sos/Grb2 complex (57).

The Sos isozymes are also unique in that they have been shown to be clearly regulated by the product of PI3 kinase, $PI(3,4,5)P_3$. The exchange activity of Sos is auto-inhibited via steric occlusion of the DH domain by the adjacent PH domain (58). The Sos PH domain has a higher affinity for binding $PI(3,4,5,)P_3$ than it does for $PI(3,4)P_2$ or $PI(4,5)P_2$ (59). However, when the PH domain is bound to $PI(4,5)P_2$ it sterically occludes the GTPase binding site of the DH domain, but when the PH domain is bound to $PI(3,4,5)P_3$, it is not able to bind to the DH domain, and the exchange activity of Sos for Rac is activated (60). Interestingly, the regulatory subunit of PI3 kinase is able to interact with a phosphorylated form of E3b1, and further increase the Rac activity of Sos when it is bound to Eps8/E3b1 (61).

Like many other Dbl-family proteins, Sos is activated by tyrosine phosphorylation. Activation of receptors tyrosine kinase such as the EGFR and PDGFR leads to tyrosine phosphorylation of Sos in an Abl-dependent manner. Phosphorylation by Abl increases the exchange potential of Sos toward Rac1, although Sos must both be tyrosine phosphorylated and bound to Eps8/E3b1 to be fully active (62). Finally, Sos activity towards Rac is activated downstream of signaling from Robo, the repulsive guidance receptor in the nervous system that binds to the ligand, Slit. The mechanism by which Sos is activated in this case has yet to be determined (63). The Sos family

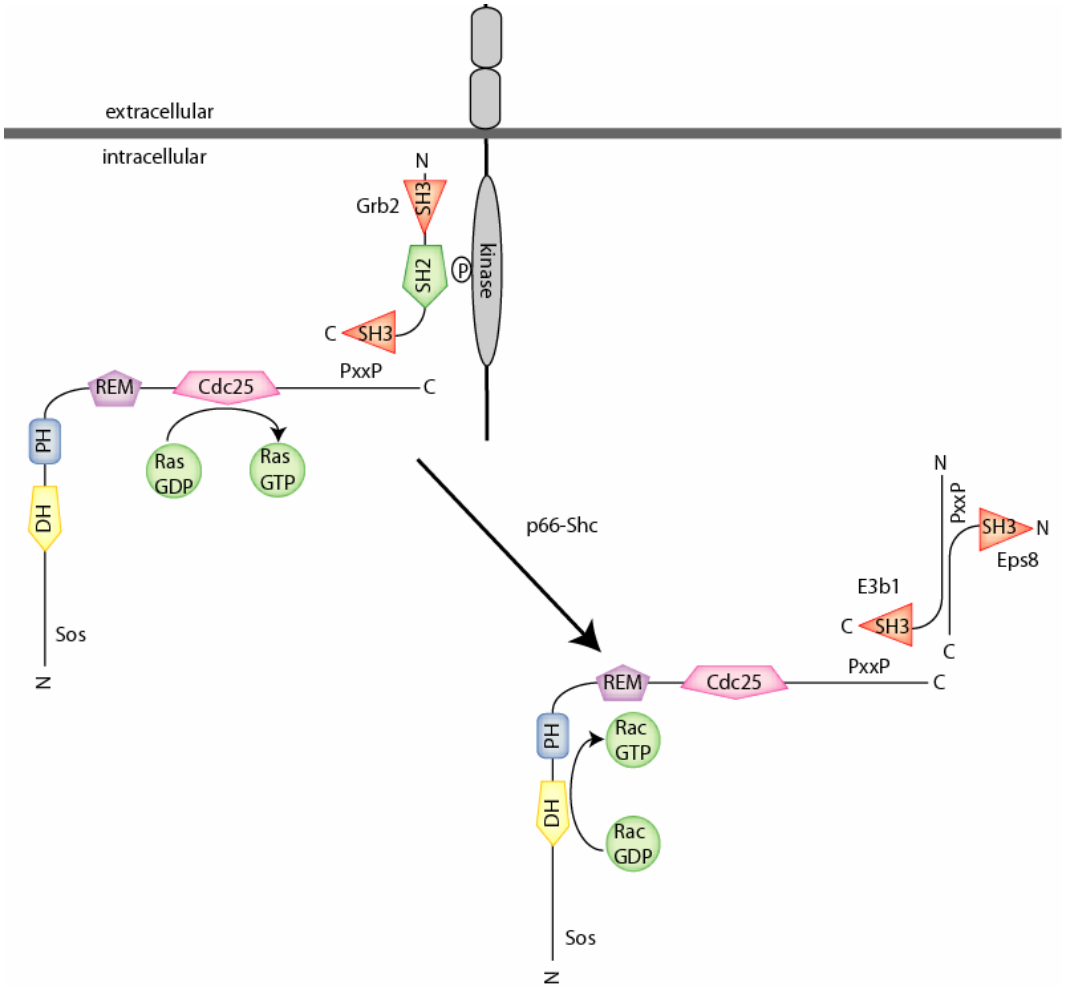

Figure 2: Regulation of Rac-specific exchange activity of Sos by intermolecular interactions.
Sos bound to Grb2 is Ras-specific and localized to the plasma membrane. The activity of p66-Shc causes dissociation of Sos from Grb2. Sos is then able to bind to the complex of E3b1 and Eps8. This trimeric complex is then able to catalyze exchange of guanine nucleotide on Rac.

isozymes, then, are regulated by alterations in their sub-cellular localization, lipid binding to their PH domains, and tyrosine phosphorylation (see Figure 2).

Ect2 Subfamily:

The Ect2 subfamily consists of the protein product of the **e**pithelial **c**ell **t**ransforming gene 2, as well as its uncharacterized isozyme (protein accession number XP294019) (5). A truncated form of Ect2 was originally identified in a screen for mitogenic, signal-transducing genes in epithelial cells (64). Ect2 has subsequently been shown to be the main guanine nucleotide exchange factor active during mitosis (65). Its N-terminus is composed of a novel domain with homology to the yeast cyclin protein, Clb6; followed by two BRCT (**BR**CA1 **C**-**t**erminal repeat) motifs, which are common in checkpoint and repair proteins. The DH/PH cassette, shown to be specific for RhoA (66), is located in the C-terminus of the molecule. A nuclear localization sequence is found in the center of the molecule, in the so-called S domain, between the BRCT repeats and the DH domain (30).

The exchange activity of Ect2 is strongly auto-inhibited by its N-terminus. The BRCT repeats are able to form a direct, intramolecular interaction with the DH domain to prevent activation of RhoA by Ect2 (30,67). In fact, expression of the N-terminus of Ect2 *in trans* inhibits Ect2 to such an extent that accumulation of active RhoA and cytokinesis is blocked (64,65). The extreme C-terminus of Ect2, however, is necessary for cellular transformation by Ect2 expression (30,66).

Ect2 is localized to the nucleus in interphase cells, where it is inactive (64). However, when a cell enters metaphase, Ect2 translocates to the mitotic spindle, and is found at the cleavage furrow during the anaphase and telophase stages of mitosis (64).

Its localization to the central spindle and astral microtubules near the equatorial cortex in the cleavage furrow is mediated by an interaction with centralspindlin (68), a protein complex composed of the mitotic kinesin, MK1p2 and MgcRacGAP, a GTPase activating protein for Rac (69). An intact PH domain, as well as the BRCT repeats, is necessary for proper localization of Ect2 to the cleavage furrow during mitosis (69). When Ect2 is localized to the cleavage furrow, its exchange activity is increased through an allosteric interaction with p0071, an armadillo-repeat containing protein related to p120-catenin (70).

Ect2 is also regulated at the expression level. Expression of Ect2 is induced at the S to M transition during the cell cycle, and is induced by several growth factors, including KGF, EGF and PDGF (30). In contrast, like other genes responsible for cell cycle progression, Ect2 gene expression is down-regulated through the actions of the tumor suppressor and cell cycle checkpoint proteins, p53 and Rb (71,72). Expression of Ect2 is also regulated at the protein level, since Ect2 interacts with an ubiquitin ligase, UBE3A (73). The importance of proper regulation of Ect2 expression is underscored by the fact that amplification of the Ect2 gene is seen in esophageal squamous cell carcinoma (74).

Finally, Ect2 is regulated by phosphorylation. Ect2 is phosphorylated at the G2 to M transition of the cell cycle, and that phosphorylation event is required for Ect2 exchange activity (64). In particular, during metaphase, Ect2 is phosphorylated at Thr 814 by Cyclin dependent kinase 1 (Cdk1). The mitotic kinase, Plk, binds to Ect2 thus phosphorylated, and subsequently phosphorylates Ect2 at Thr 412, activating its exchange potential (75). The Ect2 proto-oncogene, then, is regulated by a variety of

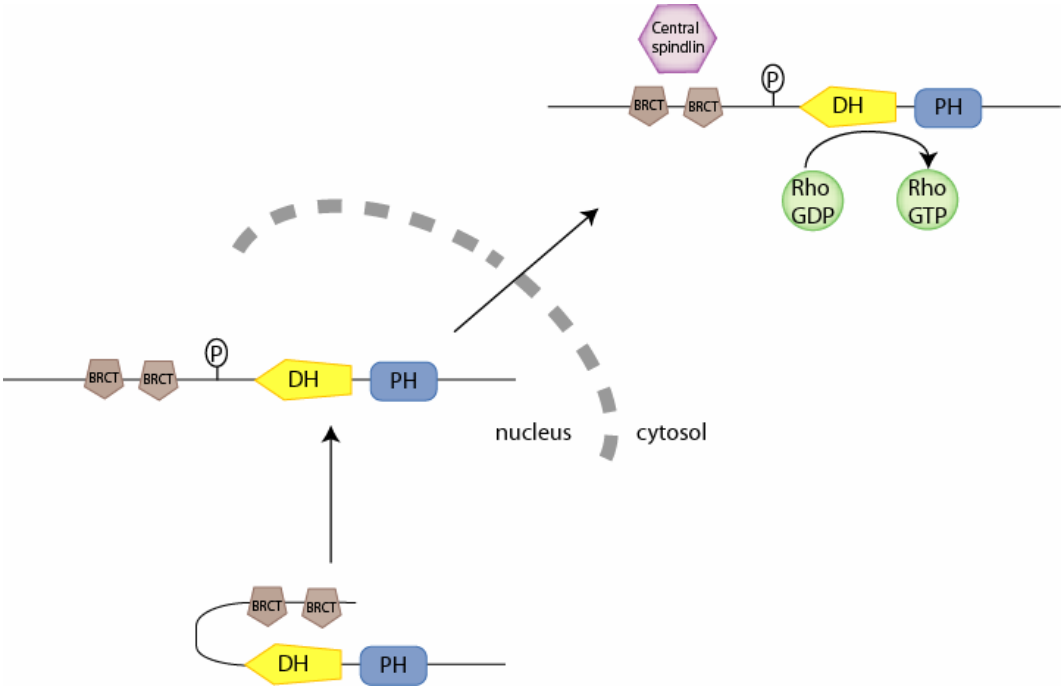

Figure 3: Ect2 is regulated by auto-inhibition, phosphorylation and nuclear sequestration.
During interphase, Ect2 is sequestered in the nucleus, where it is inactive. However, when the cell enters mitosis and the nuclear envelope breaks down, Ect2 is phosphorylated and activated by mitotic kinases. Active Ect2 then translocates to the cleavage furrow, where it is able to activate RhoA.

mechanisms, including auto-inhibition, alteration in sub-cellular localization, tyrosine phosphorylation and alteration in expression levels (see Figure 3).

Tim subfamily:

The Tim subfamily is made up of Tim (**T**ransforming **I**mmortalized **M**ammary), Ngef (**N**euronal-specific **GEF**), Wgef (**W**eakly similar to Rho**GEF**5), Sgef (**S**H3 domain-containing **GEF**), Vsm-RhoGEF (**V**ascular **s**mooth **m**uscle cell specific **GEF**), and neuroblastoma (5). Tim and its closest homologs all possess a divergent N-terminus of low complexity followed by a DH/PH cassette and a C-terminal Src homology 3 (SH3) domain. SH3 domains are known to interact with poly-proline containing ligands, however, no such binding partners have yet been identified for members of the Tim subfamily.

Ngef is expressed primarily in the brain, is localized to chromosome 2q37, and is transforming in cell culture (36,76). The mouse homolog of Ngef, ephexin, is expressed in the central nervous system during development and was originally cloned based upon its ability to interact with the EphA4 receptor tyrosine kinase. Ephexin activates RhoA, Rac1 and Cdc42 in cell-based assays; mediates ephrinA-induced growth cone collapse (77); and is phosphorylated by Src family kinases downstream of EphA4 receptor activation (76). When ephexin is not tyrosine phosphorylated, it activates RhoA, Rac1 and Cdc42; but when ephexin is tyrosine phosphorylated; it activates RhoA exclusively (78). Most recently, ephexin has been shown to be phosphorylated in its N-terminus by Cdk5 downstream of EphA4 receptor activation. Phosphorylation of ephexin by Cdk5 also activates its exchange potential towards RhoA (79). The precise mechanism by

which ephexin undergoes its specificity switch and the mechanisms by which Cdk5 and Src coordinate to modulate ephexin activity are poorly understood.

Vsm-RhoGEF, which is specifically expressed in vascular smooth muscle cells, also associates with the intracellular domain of EphA4. EphA4 signaling leads to phosphorylation of Vsm-RhoGEF and activation of the RhoA specific exchange activity of this protein (80). Sgef is localized to human chromosome 2q25.2, an amplification unit in prostate tumors (81), and generates a novel dorsal ruffling phenotype through activation of RhoG (42). Wgef is expressed primarily in liver, heart and kidney, and activates RhoA, Rac1 and Cdc42 in cell-based activity assays (82).

Tim was originally identified based upon its capacity to induce transformation of NIH 3T3 cells upon truncation (83), and while there are multiple transcripts of TIM (44,83), endogenous Tim is expressed as a 60-kDa protein. mRNA transcripts encoding Tim are ubiquitously expressed in numerous tissues and cancer-derived cell lines; corresponding protein expression has been verified in various cell lines (44,83). The gene encoding human Tim has been localized to chromosomal region 7q33 -7q35, which has been implicated in rearrangements contributing to both acute myelogenous leukemia and breast carcinoma (84). The regulation of Tim and its orthologs, Ngef and Wgef, will be described in later chapters.

GEF:	Binding Partner:	Domain required:	Sub-cellular localization:	Activity at this location:	Reference:
Ect2	centralspindlin	PH domain	Cleavage furrow	Increased	(68)
Fgd1	Actin binding protein 1; cortactin	N-terminal proline rich region	Actin cytoskeleton	Increased	(21)
Frabin	Unknown	N-terminus	Actin cytoskeleton	Increased	(15)
GEF-H1	Microtubules	Zn^{++} finger	Mitotic spindle	Decreased	(85)
Net1	N/A	N-terminal NLS	Nucleus	Decreased	(86)
Tiam1	Par3/Par6/aPKC	RBD	Junctions	Unknown	(87)
Tiam1	Arp 2/3	PH-TSS	Actin rich regions of plasma membrane	Unknown	(88)
Tuba	ZO-1	Unknown	Tight junctions	Unknown	(89)

Table 2: Regulation of Dbl-family GEFs by alteration of their sub-cellular localization.

Intersectin subfamily:

The intersectin subfamily consists of ITSN1 (**in**t**er**secti**n**1) and its ortholog, ITSN2, which is largely unstudied (5). A short splice isoform of ITSN was originally characterized as a scaffold protein that functions in receptor-mediated endocytosis, consisting of two EH domains (**E**ps15 **h**omology), a coiled-coil region and five tandem SH3 domains. The EH domains, which are related to EF hand motifs, helix-loop-helix structural motifs that coordinate calcium and function in protein-protein interactions, target ITSN-S to clathrin-coated pits. Additionally, the SH3 domains bind to the molecular motor for endocytosis, the GTPase, dynamin (90,91).

A longer, neuronal-specific, isoform of ITSN was identified, ITSN-L, which contains a DH/PH cassette in its C-terminus. ITSN-L is an exchange factor specific for Cdc42 (32). While the PH domain of ITSN-L binds to a broad spectrum of phosphoinositides, the binding of phospholipids does not affect the *in vitro* exchange activity of ITSN-L (92). Similarly, ITSN-L is not stimulated by PI3 kinase activity, the DH domain alone exhibits the same *in vitro* exchange activity as the DH/PH tandem (93) and the PH domain makes no contacts with Cdc42 as judged by the crystal structure of the DH/PH cassette bound to Cdc42 (94). Multiple lines of evidence, then, show that the

GEF:	Dimerization domain:	Reference:
β-Pix	Leucine zipper	(95)
Dbl	DH	(96)
LARG	Coiled-coil	(33)
Lbc	Coiled-coil	(97)
p115-RhoGEF	Coiled-coil	(33)
PDZ-RhoGEF	Coiled-coil	(33)
RasGRF	DH	(52)

Table 3: Dbl-family GEFs that form homo-dimers.

exchange activity of ITSN-L is not regulated through the binding of phospholipids to its PH domain.

The exchange activity of ITSN, however, is regulated by auto-inhibition. The SH3 domains of ITSN-L inhibit its *in vitro* exchange activity by sterically occluding the DH domain to prevent binding of nucleotide free Cdc42. The binding of the SH3 domains to the DH domain occurs in a manner independent of the poly-proline binding pocket. However, the binding of proteins, such as N-WASP, which coordinates the formation of actin filaments (32) and Numb, an adaptor protein important in dendritic spine morphogenesis (98), to the SH3 domains leads to an increase in the exchange activity of ITSN-L. Although the SH3 domains mediate ITSN-L auto-inhibition, they are also required for cellular transformation by ITSN-L. The first SH3 domain binds to Sos, which leads to activation of the small GTPase, Ras, and subsequent cellular transformation (99).

Like many other Dbl-family members, the exchange activity ITSN-L also may be regulated by phosphorylation. The kinase domain of the ligand-bound tyrosine kinase, EphB2, interacts with the N-terminus of intersectin. Although phosphorylation of ITSN-L by EphB2 has not yet been studied, the interaction of ITSN-L with EphB2 increases the exchange activity of ITSN-L (100). Therefore, while ITSN subfamily members are not regulated through the binding of phospholipids, they are regulated by auto-inhibition and phosphorylation.

Net1 subfamily:

The Net1 subfamily consists of Net1 (**n**euro**e**pithelial **t**ransforming protein) and Xpln (e**x**change factor found in **p**latelets, **l**eukemic, and **n**euronal tissues). These two

proteins are among the smallest of the Dbl-family, and contain no known domains outside of the conserved DH/PH cassette (5). While Net1 specifically activates RhoA and not Rac1 or Cdc42 (101), Xpln activates RhoA and RhoB but not RhoC (102).

A truncated version of Net1 was originally identified as an oncogene in a genetic screen from a cDNA expression library derived from a human neuroepithelial cell line (35). Indeed, the N-terminus of Net1 inhibits its exchange activity (101), albeit through a unique mechanism. Net1 contains two nuclear localization signals (NLS) in its N-terminus. Removal of these sequences allows Net1 to localize to the cytoplasm, where it is able to activate RhoA. The PH domain of Net1 is necessary and sufficient for its exit from the nucleus, presumably through interactions with other proteins that contain a nuclear export sequence (10). The extreme C-terminus of Net1 forms a consensus PDZ-domain binding site, which has been shown to be critical for the transformation potential of Net1, although no binding partners for this motif have been identified to date (103).

Although binding partners for the PH domain and PDZ-binding motif of Net1 have yet to be identified, Net1 has been shown to bind to several other proteins. The Xenopus ortholog of Net1, xNet1, interacts with Dishevelled, a protein scaffold critical for Wnt signaling. Net1 also interacts with the protein scaffold, CNK1, which leads the RhoA activated by Net1 to activate only the JNK signaling pathway (104). Finally, Net1 is phosphorylated by Pak1 on several serine residues, which decreases its exchange activity (105).

In contrast to Net1, the mechanisms by which the exchange activity of Xpln is regulated are largely unknown. Xpln is not activated by truncation of its N- or C-terminus, although it is transforming (102). In addition, the two NLS in the N-terminus

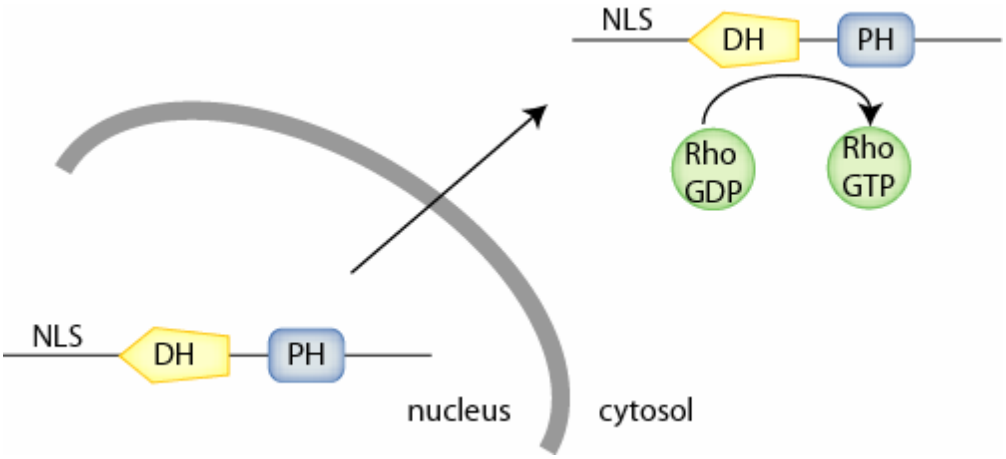

Figure 4: Net1 is regulated by nuclear sequestration.
The nuclear localization sequence on the N-terminus of Net1 targets it to the nucleus, where it is inactive. The mechanisms that allow Net1 to exit from the nucleus to the cytosol, where it is able to activate RhoA, are unclear. Net1, therefore, represents a Dbl-family GEF that is activated in cellular assays by N-terminal truncation, but is not auto-inhibited.

of Net1 are not conserved in Xpln, and as a consequence Xpln is largely expressed in the cytosol (86). Members of the Net1 subfamily, then, are unique in that they are not regulated by auto-inhibition. Net1, but not Xpln, is regulated by sequestration in the nucleus (see Figure 4).

p115-RhoGEF subfamily:

The p115-RhoGEF subfamily is composed of p115-RhoGEF, PDZ-RhoGEF and LARG (for **l**eukemia-**a**ssociated **R**ho **G**EF). Each of these proteins possesses an N-terminal RGS (**r**egulator of **G**-protein **s**ignaling) domain, a DH/PH cassette and a C-terminal coiled-coil domain. PDZ-RhoGEF and LARG also contain a PDZ domain in their extreme N-terminal region, which enables these proteins to interact with the C-termini of various proteins with which p115-RhoGEF is unable to interact, as is discussed below (5). p115-RhoGEF and PDZ-RhoGEF were originally identified based upon their ability to interact with $G\alpha_{13}$ (106,107), while LARG, in contrast, was identified as a fusion partner with **M**ixed **L**ineage **L**eukemia (MLL) protein in an AML patient (108).

All three of these proteins have been shown to be exchange factors specific for RhoA (5). In addition, all three of these proteins have been shown to oligomerize through their C-terminal coiled-coil domain (33). This oligomerization leads to a decrease in exchange activity. Finally, all three of these proteins have been shown to interact directly with activated $G\alpha_{12}$ and $G\alpha_{13}$ (106-108).

The best characterized member of this subfamily is p115-RhoGEF. The RGS domain of p115-RhoGEF has been shown to bind to and act as a GAP (GTPase accelerating protein) for $G\alpha_{12}$ and $G\alpha_{13}$. However, only $G\alpha_{13}$ has been shown to directly activate the exchange potential of p115-RhoGEF for RhoA, although truncation of the

RGS domain is activating (107). Endogenous p115-RhoGEF is localized to the cytosol in serum-starved cells, but translocates to the plasma membrane upon stimulation with LPA (109). LPA acts through a GPCR to activate $G\alpha_{12}$ and $G\alpha_{13}$. Palmitoylated and activated $G\alpha_{12}$ and $G\alpha_{13}$ are able to induce translocation of p115-RhoGEF (110). Interestingly, both the RGS domain and the PH domain are necessary for p115-RhoGEF translocation to the membrane in response to LPA treatment, indicating that the PH domain is also a potential binding site for Gα subunits (111).

The PDZ domain of PDZ-RhoGEF and LARG mediates an interaction of these Dbl-proteins with the C-terminus of Plexin-B2, a transmembrane receptor that transduces both attractive and repulsive signals mediated by the axon-guidance ligands, the semaphorins. Plexin B signaling leads to activation of the exchange potential of PDZ-RhoGEF and LARG through an as yet undefined mechanism (112). An association of the small GTPase, Rnd1, with the C-terminus of Plexin B increases the interaction of plexin B with PDZ-RhoGEF, leading to an increase in Rho activation in cells where all three of these proteins are expressed (113). In addition, PDZ-RhoGEF and LARG are able to associate with the C-terminus of the LPA receptor, a GPCR that catalyzes the activation of $G\alpha_{12/13}$ subunits (114), and LARG is able to interact with the C-terminus of IGF1-R (115). Both of these interactions are mediated through the PDZ domain of these GEFs and the consequences of the interactions on the exchange potential of the GEFs have yet to be determined.

The GEFs in the p115-RhoGEF subfamily are also regulated by phosphorylation events. Signaling from the thrombin receptor leads to PKC activation, and activated PKC is able to phosphorylate and activate p115-RhoGEF (116). In addition, Tec, a non-

receptor tyrosine kinase that contains a PH domain, phosphorylates LARG and increases its exchange activity (117). In both of the above cases, Gα subunits are still required to unleash the full exchange potential of the phosphorylated GEF. In contrast, phosphorylation of the p115-RhoGEF subfamily GEFs by the p21-activated kinases (Paks) does not activate their exchange potential. Pak1 is able to phosphorylate p115-RhoGEF, and not PDZ-RhoGEF or LARG. This phosphorylation has no effect on the exchange activity of p115-RhoGEF (118). Pak4, in contrast, binds to the C-terminus of PDZ-RhoGEF, phosphorylates the GEF and decreases its exchange activity (119). In conclusion, members of the p115-RhoGEF subfamily can be activated by C-terminal truncation, not N-terminal truncation as has been described for many other Dbl-family members. Also, orthologs of p115-RhoGEFs are activated downstream of signaling from $G\alpha_{12/13}$-coupled receptors, and are inhibited by phosphorylation on serine or threonine residues.

Lbc subfamily:

The Lbc subfamily is made up of Lbc (**L**ymphoid **b**last **c**risis, also known as AKAP-Lbc, for **A**-**k**inase **a**nchoring **p**rotein, or Brx), GEF-H1 (also known as Lfc, for **L**bc's **f**irst **c**ousin), p190-RhoGEF, and p114-RhoGEF. Each of these proteins is composed of an extended N-terminus with no known domain architecture, a DH/PH cassette, and a C-terminal coiled-coil domain. All four proteins have been shown to be RhoA specific exchange factors. Of the four proteins in this subfamily, Lbc and GEF-H1 are the best studied (5).

p190-RhoGEF was identified in a yeast-two-hybrid screen for proteins that interact with c-**J**un amino-terminal kinase **i**nteracting **p**rotein 1 (JIP-1) (120). The full-

length protein is auto-inhibited with respect to the isolated DH/PH cassette. The protein is localized to the cytoplasm, distinct microdomains of the plasma membrane and microtubules. The C-terminus of p190-RhoGEF mediates the interaction with microtubules by directly binding to tubulin, although this interaction does not affect the exchange activity of p190-RhoGEF (38).

Stimulation of cells expressing p114-RhoGEF with thrombin, LPA or acetylcholine leads to Rho activation. Activation of Rho in this context is thought to be due to Gβγ binding to the DH/PH cassette of p114-RhoGEF and activating its exchange potential. Importantly, the isolated DH/PH cassette is more active than full-length p114-RhoGEF in catalyzing exchange of guanine nucleotides on RhoA (37).

Onco-Lbc was identified in a screen for oncogenes in a cDNA library isolated from a patient in the acute phase of chronic myelogenous leukemia (CML) (121). Onco-Lbc was shown to be transforming in NIH 3T3 cells and capable of inducing tumor formation in immunocompromised mice (122). Onco-Lbc is the result of a fusion event between the gene for proto-Lbc and an unrelated sequence, which led to the introduction of a nonsense mutation immediately following the PH domain (97). Proto-Lbc is auto-inhibited with respect to onco-Lbc in a variety of cellular assays, and both the DH and PH domains of onco-Lbc are necessary for its activity (34,123,124). Onco-Lbc localizes to actin stress fibers, and the PH domain is necessary for this localization pattern (34). Full-length Lbc, like its cousins, p115-RhoGEF, PDZ-RhoGEF, and LARG, is able to interact with $G\alpha_{12}$ and is able to form homo-dimers through its C-terminal coiled-coil domain. Homo-dimerization maintains the basal activity level of full-length Lbc (97,125).

A splice isoform of Lbc, known as Brx, is able to bind to and act as a transcriptional co-activator for various steroid hormone receptors, including both of the estrogen receptors, the retinoic acid receptor β and the glucocorticoid receptor (126,127). The consequences of these interactions on the exchange activity of Lbc have yet to be determined. Lbc is able to interact with the regulatory subunit of protein kinase A (PKA) (128). In turn, activated PKA phosphorylates Lbc on serine 1565. This phosphorylation event enables 14-3-3 to bind to Lbc, which inhibits the exchange activity of Lbc (129). Interestingly, binding of the metastasis suppressor, nucleoside diphosphate kinase nm23-H2 also inhibits the exchange activity of Lbc (130).

The oncogenic form of GEF-H1, which is N-terminally and C-terminally truncated with respect to the wild-type protein, was originally identified in a screen for oncogenes expressed in a leukemia cell line (31,131). GEF-H1 is unique among the members of the Lbc subfamily in that it contains a zinc finger motif in its N-terminus. Microtubules are able to interact with GEF-H1 directly by binding to the zinc finger motif. The interaction stabilizes the microtubules, but inhibits the exchange activity of GEF-H1 towards RhoA (132), potentially by stabilizing an auto-inhibitory interaction between the zinc finger motif and the PH domain (133). The interaction with microtubules, and thus the activity of GEF-H1, is regulated by the cell cycle. For example, GEF-H1 is cytosolic and active during interphase, but bound to the mitotic spindle during mitosis (85,134). Enteropathogenic *E. coli* is able to take advantage of this feature of GEF-H1 regulation in order to lead to an activation of RhoA in the cell. The type III effector Esp6/Orf3 is injected into cells, which triggers the destruction of microtubules, thus activating GEF-H1 and causing the formation of stress fibers (135).

GEF-H1 is also able to associate with tight junctions in epithelial cells and regulate paracellular permeability. The association with tight junctions is mediated by GEF-H1 binding through its PH domain to the F-actin binding protein, cingulin. This interaction, like the interaction with microtubules, decreases the RhoA exchange activity of GEF-H1 (133).

The exchange activity of GEF-H1 is also regulated by phosphorylation. Pak1 phosphorylates GEF-H1 on Ser 885, which has no direct effect on the exchange activity of GEF-H1. However, phosphorylation on Ser 885 creates a binding site for 14-3-3, which inhibits GEF-H1 exchange activity (9). The Class II Pak, Pak4, is also able to phosphorylate GEF-H1; in this case, Ser 810 is the target residue for phosphorylation. However, this phosphorylation causes a release of GEF-H1 from the microtubules into the cytoplasm (136). Finally, transcription of the GEF-H1 mRNA is regulated in several cases: mutant p53, which causes trans-activation of genes not induced by wild-type p53, up-regulates the transcription of GEF-H1 (137), while treatment of cells with Gleevac leads to a decrease in GEF-H1 expression (138). As a group, members of the Lbc subfamily are regulated similarly to the highly related p115-RhoGEF subfamily members. However, GEF-H1 is also uniquely down-regulated by interactions with microtubules as well as phosphorylation-dependent interactions with 14-3-3 proteins.

Vav subfamily:

The Vav subfamily is made up of three Dbl-family proteins, Vav1, Vav2 and Vav3. Each of these proteins is composed of eight structural domains: a calponin

GEF:	Kinase:	Sites of Phosphorylation:	Effect on Exchange Activity:	Upstream Signal:	Reference:
β-Pix	Pak1	S525, T526	Increased	bFGF, NGF	(139)
β-Pix	PKA	S516, T526	Unknown	Endothelin 1	(140)
β-Pix	Src/FAK	Y442	Increased (Rac)	EGF	(141)
Dbl	ACK1	ND (Y)	Increased	Unknown	(142)
Dbs	Src	ND (Y)	Increased	Epinephrine/ Norepinephrine	(143)
Dbs	Unknown	ND (Y)	Increased	Neurotrophin 3	(144)
Ect2	Cdk1	T814	None	G2 to M transition	(64)
Ect2	Plk	T412	Increased	G2 to M transition	(75)
Ephexin	Src	Y87	Increased (Rho)	Ephrin A	(78)
Ephexin	Cdk5	S139	Increased (Rho)	Ephrin A	(79)
FRG	Src	ND (Y)	Increased	Endothelin A; nectin	(46,47)
GEF-H1	Pak1	S885	Decreased (14-3-3)	Unknown	(9)
GEF-H1	Pak4	S810	Increased (release from microtubules)		(136)
Kalirin	Unknown	ND (Y)	None	Ephrin B	(145)
LARG	Tec	ND (Y)	Increased	Unknown	(117)
Lbc	PKA	S1565	Decreased (14-3-3)	Unknown	(129)
p115-RhoGEF	PKC	ND (S/T)	Increased	Thrombin	(116)
p115-RhoGEF	Pak1	ND (S/T)	Decreased	Unknown	(118)
PDZ-RhoGEF	Pak4	ND (S/T)	Decreased	Unknown	(119)
P-Rex1	PKA	ND (S/T)	Decreased	Epinephrine/ norepinephrine	(146)

GEF:	Kinase:	Sites of Phosphorylation:	Effect on Exchange Activity:	Upstream Signal:	Reference:
RasGRF	Src	ND (Y)	Increased	PDGF	(147)
Sos	Abl	ND (Y)	Increased	EGF; PDGF	(62)
Tiam1	CaMKII	ND (T)	Increased	LPA, PDGF, endothelin, bombesin, bradykinin	
Tiam1	ROCK	T1662	Decreased	Unknown	(148)
Tiam1	Src	ND (Y)	Increased	Unknown	(149)
Tiam1	TrkB	Y829	Increased	BNDF	(150)
Trio	Abl	ND (Y)	Unknown	Unknown	(151)
Vav	Multiple	Y142, Y160, Y172 (Vav1 numbering)	Increased	Multiple	(152)
Vsm-RhoGEF	Unknown	ND (Y)	Increased	Ephrin A	(80)

Table 4: Regulation of Dbl-family GEFs by phosphorylation.
ND denotes not determined; Y, S and T are tyrosine, serine and threonine, respectively.

homology (CH) domain, an acidic region, a DH domain, a PH domain, a cysteine-rich zinc-finger (CRD) domain, and an SH2 (Src homology 2) domain flanked by two SH3 domains. CH domains are potential actin-binding domains found in a variety of cytoskeletal and signal transduction proteins, while SH2 domains are known to bind phospho-tyrosine containing ligands (11). Vav1 is expressed primarily in hematopoetic cells, where it plays a role in B and T cell development, although it is ectopically expressed in some primary pancreatic adenocarcinomas (153). Vav2 and Vav3 have near ubiquitous expression patterns (152).

Regulation by intramolecular auto-inhibitory interactions has been studied extensively for Vav1. An NMR structure of the Vav1 DH domain and the C-terminal portion of the acidic region revealed that a helix N-terminal to the DH domain folds back to occlude the GTPase binding surface. Inhibition is relieved by phosphorylation of a tyrosine 174 within this helix, which disrupts the interactions of the helix with the DH domain. The DH domain is subsequently solvent exposed, able to bind GTPases and thus able to catalyze exchange (154).

While this auto-inhibitory helix functions to regulate Vav proteins *in vivo*, the complete mechanism of Vav regulation may be more complex. Vav is phosphorylated on two tyrosine residues in the acidic region, Y142 and Y160, in addition to Y174 highlighted above. Mutation of all three of these residues to phenylalanine activates the transformation potential and *in vitro* exchange potential of Vav1, but not to the same extent as truncating the CH domain (8). The CH domain, then, is required for the orientation of the auto-inhibitory helix on the surface of the DH domain in the context of full-length Vav1. In addition, the CH domain contributes to the auto-inhibition of Vav

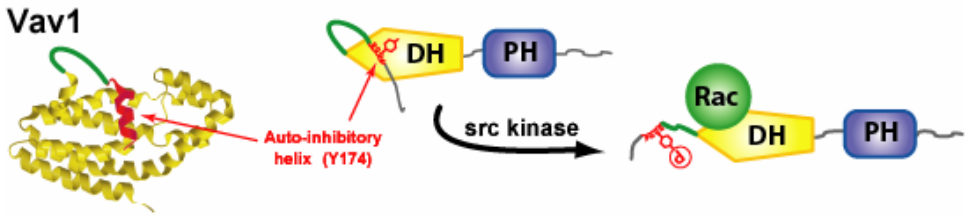

Figure 5: Vav1 is regulated by intramolecular interactions and phosphorylation.
A portion of the acidic region of Vav1, which has the consensus sequence ϕ Y x x ϕ (where ϕ denotes a hydrophobic amino acid residue and x denotes any amino acid residue), forms a helical structure that binds to the most conserved surface of the DH domain, preventing GTPase binding. Tyrosine phosphorylation, by the Src family kinase Lck, among others, disrupts the interaction of this auto-inhibitory helix with the DH domain. The DH domain is then able to bind and exchange guanine nucleotide on small GTPases such as Rac.

proteins by forming an intramolecular interaction with the CRD (45). Multiple diverse upstream signals lead to activation of Vav proteins. For example, cell surface receptors of the tyrosine kinase, cytokine, adhesion and G-protein coupled families are all able to induce downstream phosphorylation and activation of Vav proteins (152,155).

Vav proteins may also be regulated through binding of phospholipids to the PH domain. This mode of regulation is thought to be mediated by the PH domain binding to and occluding the GTPase binding site of the DH domain. Binding to the DH domain is enhanced by the PH domain binding to $PI(4,5)P_2$ and eliminated by the PH domain binding to $PI(3,4,5)P_3$ (156). However, a recent single particle electron microscopy study of full length Vav3 failed to provide any structural evidence for this mechanism, indicating that Vav proteins may be regulated primarily through phospholipid independent mechanisms (157).

The function of the C-terminal SH2-SH3-SH2 domain grouping of the Vav proteins appears to be cell-type specific. However, these domains have been shown to be important for the localization of Vav proteins, and their proper engagement of both upstream kinases and downstream effectors (45). The regulation of Vav proteins, then, is complex and is not facilitated simply by phosphorylation of Y174 (see Figure 5).

Pix subfamily:

The Pix subfamily consists of α-Pix (**P**ak **i**nteracting e**x**change factor, also known as Cool-2) and β-Pix (also known as p85-SPR or Cool-1) (5). Both of these proteins were identified by three independent laboratories based upon their ability to bind to p21-activated kinase (Pak) (158-160). Both α- and β-Pix are made up of an N-terminal SH3 domain, which binds to a non-canonical poly-proline region in either Pak or the E3

ubiquitin ligase, Cbl (**C**asistas **B-l**ymphoma); followed by the DH/PH cassette; a binding region for the ArfGAP, Git (**G**-protein coupled receptor kinase **in**t**e**ractor); and a leucine zipper domain (161). The N-terminus of α-Pix is longer than that of β-Pix, and contains a CH domain. Disruption of the CH domain in α-Pix is linked to the development of certain X-linked forms of mental retardation (162).

Initial studies into the regulation of the exchange activity of the Pix proteins gave conflicting results. First, it was shown that the leucine zipper domain of β-Pix mediated its homo-dimerization *in vitro* and *in vivo*. Over-expression of a β-Pix construct lacking this dimerization motif prevented PDGF from stimulating membrane ruffle formation in fibroblasts, indicating that dimerization was necessary for β-Pix exchange activity on Rac (95). However, it was also shown that the SH3-DH-PH domains of α- and β-Pix were able to stimulate exchange on Cdc42 *in vitro* (163). These seemingly paradoxical results were explained by the discovery that the specificity of the Pix proteins is coupled to the monomer-dimer equilibrium. As a dimer, α-Pix activates Rac specifically, and the DH domain of one molecule of α-Pix is assisted by the PH domain of its partner to catalyze exchange on Rac. However, as a monomer, α-Pix is able to activate either Rac or Cdc42, but only when either Pak or Cbl is bound to the SH3 domain (161). The binding of a complex of Pak and Gβγ to the SH3 domain of α-Pix leads to dissociation of the α-Pix dimer, and activation of the ability of α-Pix to stimulate exchange on Cdc42. In contrast, the binding of GTP-bound Cdc42 to the DH domain of one of the molecules in the α-Pix dimer activates the ability of its partner to stimulate exchange on Rac. The mechanisms by which Pak/Gβγ and activated Cdc42 affect the exchange potential of α-Pix are unknown, but are presumed to be allosteric (164).

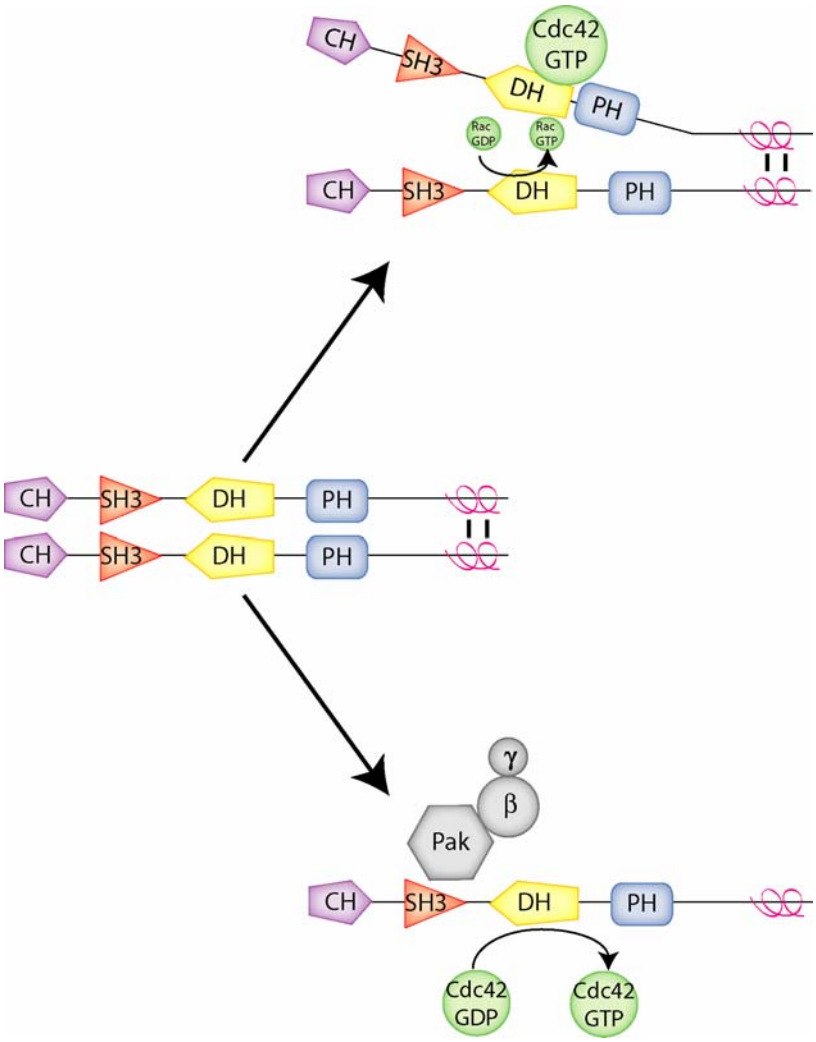

Figure 6: Pix proteins are regulated by protein-protein interactions.
In the basal state, α-Pix exists as a homodimer, capable of activating Rac1. The binding of activated Cdc42 to one DH domain of the homodimer increases the ability of the other DH domain to activate Rac1 (top). However, binding of a complex of Pak1 and Gβγ to the SH3 domain of α-Pix causes dissociation of the homodimer and enables α-Pix to activate Cdc42 (bottom).

In addition to being regulated by non-enzymatic protein-protein interactions as described above, Pix proteins are also regulated by phosphorylation. In PC12 cells, bFGF or NGF binding to their receptors leads to activation of the Ras-Raf-MEK-ERK MAP kinase signaling cascade. Activation of this signal transduction pathway stimulates Pak to phosphorylate β-Pix on S525 and T526, residues in the Git binding domain, and activates the exchange potential of β-Pix toward Rac (139). Interestingly, in human mesangial cells, endothelin 1 binding to its receptor leads to the activation of $G\alpha_s$, stimulation of adenylyl cyclase, and formation of cyclic AMP. The increase in cellular cyclic AMP stimulates protein kinase A to phosphorylate β-Pix on S516 and T526, although the effect of this phosphorylation on the exchange activity of β-Pix is unknown (140). Finally, β-Pix is tyrosine phosphorylated downstream of signals from the EGF receptor in a Src-and FAK- dependent manner. This phosphorylation, at Y442, in the Cbl and activated Cdc42 binding region, leads to an increase in the exchange potential of β-Pix towards Cdc42 but not Rac (141). The molecular mechanism by which phosphorylated Pix proteins have increased exchange potentials relative to their de-phosphorylated counterparts is currently unknown. Also unknown is whether or not phosphorylation impacts the dimerization or the specificity of the Pix proteins (see Figure 6).

Tiam subfamily:

The Tiam subfamily consists of Tiam1 (for **T**-cell **i**nvasion **a**nd **m**etastasis gene 1) and Tiam2 (also known as Stef, for **S**if and **T**iam1-like **e**xchange **f**actor) (5). Tiam1 was originally identified in a genetic screen based upon its ability to induce T-lymphoma cells to invade fibroblast monolayers (165), and was shown to be an exchange factor specific

GEF:	Ligand:	Effect on exchange activity:	Reference:
Asef	$PI(3,4,5)P_3$	Changes localization	(166)
Dbl	$PI(4,5)P_2$, $PI(3,4,5)P_3$	Decreases	(7)
Dbs	$PI(4,5)P_2$	None	(92)
Dbs	Rac1·GTP	Increases	(167)
GEF-H1	Cingulin	Decreases	(133)
Kalirin (N)	TrkA	Unknown	(168)
p115-RhoGEF	$G\alpha_{13}$	Increases	(111)
P-Rex	$PI(3,4,5)P_3$	Increases	(169)
Sos	$PI(4,5)P_2$	Decreases	(170)
Sos	$PI(3,4,5)P_3$	Increases	(170)
Tiam1	PI(3)P	None	(92)
Trio (N)	Filamin	None	(171)
Vav	$PI(4,5)P_2$	Decreases	(156)
Vav	$PI(3,4,5)P_3$	Increases	(156)

Table 5: Regulation of Dbl-family proteins through intramolecular interactions with the DH-associated PH domain.

for Rac1 (172). Both Tiam1 and Tiam2 are made up of an N-terminal PH domain, a coiled-coil region, a **R**as-**b**inding **d**omain (RBD) and a PDZ domain, followed by the catalytic DH/PH cassette (5). PDZ domains are homology regions named for **P**ost synaptic density 95, **D**iscs large, and **Z**o-1, the first proteins discovered to have this domain, and they function in mediating protein-protein interactions (11). The coiled-coil region is also known as the TSS (**T**iam1 and **S**tef **s**imilarity region) (43). In addition to its role in invasion and metastasis, Tiam1 has been found to be mutated in human renal cell carcinoma (173) and is significantly over-expressed in prostate carcinoma (174).

The presence of multiple PEST sequences in the extreme N-terminus of Tiam1 has led to the hypothesis that Tiam1 is regulated primarily at the level of protein stability. PEST sequences, which are motifs containing the primary sequence proline – glutamic acid – serine – threonine, target proteins to the proteasome for degradation. In fact, these PEST sequences do lead to increased turnover of Tiam1 protein upon Rac activation (175). For this reason, a mutant version of Tiam1 in which these sequences have been truncated, C1199, has historically been used to study Tiam1 activity in cells. This truncation, while affecting Tiam1 protein stability, does not otherwise affect Tiam1 exchange activity. In fact, Tiam1 is inhibited *in trans* by expression of the N-terminal PH domain and coiled-coil domain (43), indicating that the full-length protein, as well as the C1199 construct, is auto-inhibited. Tiam1 is cleaved by caspases during apoptosis, resulting in a protein product that is deficient in plasma membrane localization and Rac exchange activity (176). Tiam1 expression is also regulated at the transcriptional level, since transcription of the Tiam1 mRNA is up-regulated through the activity of the transcription factor, E1A (177).

The regulation of Tiam1 exchange activity by phosphoinositide binding is complex and incompletely understood, due in part to the fact that Tiam1 contains two PH domains, each of which could bind phosphoinositides. Tiam1 is known to translocate to the membrane upon treatment of cells with PDGF and LPA and this re-localization is dependent upon the N-terminal, non-DH-associated, PH domain (178). Membrane localization is essential for Tiam1 activity in cells, and the N-terminal PH domain can be functionally replaced by the myristoylated, membrane-localization domain of c-Src (179). Tiam1 activity in cells is also dependent upon PI3 kinase activity (180), an effect which is mediated by the N-terminal PH domain. The binding of the N-terminal PH domain to $PI(4,5)P_2$ mediates Tiam1 association with the plasma membrane of astrocytoma cells, while the binding of this domain to $PI(3,4,5)P_3$ stimulates the exchange activity of Tiam1 (181). The N-terminal PH domain may affect Tiam1 localization through binding to other proteins, as well as phospholipids, since this domain has been shown to interact with the protein scaffold, spinophilin (182).

Ascorbyl stearate, a PH-domain binding ligand, is able to stimulate the exchange activity of N-terminally truncated Tiam1 in cells. This effect that is due to ligand binding to the DH-associated PH domain, not the N-terminal PH domain (183). In contrast, the DH-associated PH domain was shown to bind specifically to PI(3)P with weak affinity, and this binding did not affect the exchange activity of Tiam1 *in vitro* (92). A mutation that rendered this PH domain unable to bind to PI(3)P impaired the ability of Tiam1 to activate Rac1 in cells, although the membrane targeting of this mutant Tiam1 was unaffected (184).

GEF:	G protein:	Effector domain:	Consequences on exchange activity:	Reference:
α-Pix	βγ	SH3	Increases (Cdc42)	(164)
Dbl	βγ	N-terminus	Unknown	(185)
LARG	βγ	RGS	Increases	(108)
p114-RhoGEF	βγ	Unknown	Increases	(37)
p115-RhoGEF	$\alpha_{12/13}$	RGS/PH	Increases	(107)
p63-RhoGEF	$\alpha_{q/11}$	C-terminus	Increases	(186)
PDZ-RhoGEF	$\alpha_{12/13}$	RGS	Increases	(106)
P-Rex	βγ	DH/PH	Increases	(169)
RasGRF	βγ	Unknown	Increases (Rac)	(51)

Table 6: Dbl-family GEFs that function as effectors for heterotrimeric G-protein subunits.

Multiple lines of evidence support the hypothesis that Tiam1 exchange activity is regulated by phosphorylation. Tiam1 was shown to be phosphorylated on multiple threonine residues upon stimulation of cells with LPA, PDGF, endothelin-1, bombesin and bradykinin, but not EGF (187). These phosphorylations were mediated by a signaling pathway involving $G\alpha_q$, phospholipase γ1 (PLCγ1), and protein kinase C (PKC), leading to activation of **ca**lcium- and cal**m**odulin-dependent protein **k**inase **II** (CaMKII), which is able to phosphorylate Tiam1 directly. Phosphorylation of Tiam1 by CaMKII led to a two-fold increase in the exchange activity of Tiam1 *in vitro* (188). In contrast, phosphorylation of Tiam2 by p160-Rho kinase on Thr 1662 leads to a decrease in its activity (148).

Tiam1 is also phosphorylated on multiple tyrosine residues in a Src-dependent manner, which increases the exchange activity of Tiam1 (149). Additionally, Tiam1 is able to interact with either the receptor tyrosine kinase, EphA2, or its ligand, ephrin B1, when the receptor and ligand are interacting. This interaction leads to an increase in Tiam1 exchange activity, although the phosphorylation state of Tiam1 in this case has yet to be examined (189). The EphB receptor tyrosine kinases have been shown to interact with both Tiam1 and the NMDA (N-methyl-D-aspartic acid) receptor in developing brain and regions of the adult brain undergoing synaptic remodeling. NMDA receptor stimulation induces Tiam1 phosphorylation and increases the exchange activity of Tiam1 in a CaMKII dependent manner, and this signaling pathway is required for NMDA receptor induced dendritic spine morphogenesis (190). Finally, stimulation of cells with BNDF leads to an association of Tiam1 with the receptor for BNDF (brain-derived neurotrophic factor, TrkB (neurotrophic tyrosine kinase receptor, type B). TrkB directly

phosphorylates Tiam1 at a tyrosine residue in the RBD, Y829, and this phosphorylation leads to an increase in Tiam1 exchange activity (150).

The presence of an RBD in the N-terminus of Tiam1 as well as the fact that Tiam1 is required for cellular transformation by activated versions of the Ras GTPases (191) has led to the hypothesis that Tiam1 is a Ras-effector protein. Ras effectors bind to Ras in a GTP-dependent manner and are activated by this binding event. Activated Ras has been shown to bind to the RBD of Tiam1, and Ras binding was shown to increase the exchange activity of Tiam1 in cells (192). However, the RBD of Tiam1 is unable to interact with H-Ras, Rap1B or M-Ras *in vitro* (193). Rap1A, though, has been shown to interact with the DH/PH cassette of Tiam1 (194). Several other PH domains are able to act as effector binding modules for small GTPases, including the PH domain of PLCβ (195), so the DH-associated PH domain, and not the RBD as originally thought, may be the binding site for activated Ras proteins in Tiam1.

Recently, Tiam1 and 2 have been shown to be part of the complex of Par3, Par6, atypical PKC and Cdc42 (Par refers to **par**titioning defective), which has been shown to be important for the development of epithelial and neuronal cell polarity. Par3 interacts directly with the proteins of the Tiam subfamily, through its PDZ array interacting with the RBD of the Tiam protein. This interaction serves to spatially restrict Tiam1 for activation of Rac in the proper location, rather than specifically activating the exchange potential of Tiam1 (87,196). Similarly, the N-terminal PH domain and coiled-coil region of Tiam1 interact with the p21-Arc subunit of the Arp2/3 complex, an interaction that serves to spatially restrict Tiam1 to actin rich regions of the plasma membrane (88).

GEF:	G protein:	Effector domain:	Consequences on exchange activity:	Reference:
α-Pix	Cdc42	DH	Increases	(164)
Dbs	Rac	PH	Increases	(167)
RasGRF	H-Ras	N-terminus	Unknown	(41)
Scambio	Rac	PH	Unknown	(197)
Sos	H-Ras	Ras exchanger motif (Rem)	Unknown (for Rac activity)	(198)
Tiam1	Rap1a	PH (DH-associated)	Unknown	(194)
Vav2	Rap1a	PH	Unknown	(194)

Table 7: **Dbl-family GEFs that function as effectors for small GTPases.**

Tiam proteins, then, are regulated by diverse signaling mechanisms, potentially due to the fact that they are composed of multiple signaling domains. They are repressed by proteolytic cleavage and activated by lipid binding, phosphorylation, and binding to activated forms of Ras family members.

Asef subfamily:

The Asef subfamily consists of Asef1 (**A**PC-**s**timulated **e**xchange **f**actor), Asef2, and Pem2 (**P**osterior **e**nd **m**ark, also known as collybistin). All three of these exchange factors are composed of an extended N-terminus with no known domain structure, followed by an SH3 domain and the DH/PH cassette (5). Additionally, all three of these exchange factors stimulate exchange of guanine nucleotide exclusively on Cdc42 (199,200).

Pem2 was originally cloned based upon its ability to interact with gephyrin, a protein scaffold that binds to and clusters inhibitory glycine receptors in the post-synaptic density of neurons (201). Pem2 is expressed predominantly in the brain, and two splice isoforms have been identified. The splice isoform that contains the SH3 domain is less active in an *in vitro* exchange assay than a splice isoform in which the SH3 domain is truncated, indicating that the exchange activity of Pem2 is negatively regulated by its SH3 domain (39). The interaction with gephyrin is mediated by the PH domain of Pem2, however, the crystal structure of the DH/PH cassette bound to Cdc42 revealed that the PH domain of Pem2 does not contact the GTPase during the exchange reaction (39). Therefore, the ability of gephyrin to modulate the exchange activity of Pem2 is unknown.

Asef was originally identified as a binding partner for the armadillo array of APC (**A**denomatous **P**olyposis **C**oli), the protein product of a tumor suppressor gene mutated

in many forms of colorectal cancers. Like that of Pem2, the exchange activity of Asef has been shown to be negatively regulated by a region N-terminal to the DH domain, a region that includes the APC binding site. APC binding to Asef allosterically activates the exchange factor (26). Although truncated forms of Asef are not transforming, over-expression of Asef decreases E-cadherin-mediated cell-cell adhesion and promotes cell migration in epithelial cells. Indeed, both Asef and truncated versions of APC are required for the migration, and presumably the subsequent invasion and metastasis, of colorectal tumor cells (202). The exchange activity of Asef2, which is expressed in a larger variety of tissues than Asef1, is also auto-inhibited by its N-terminus, and stimulated by APC binding (199). A crystal structure of an auto-inhibited form of Asef1 reveals that its SH3 domain binds to its DH domain in a manner different from that shown for SH3 domains binding to poly-proline containing ligands, and that this binding sterically occludes the GTPase binding surface of the DH domain, preventing Cdc42 binding and activation (203).

Most recently, the PH domain of Asef1 was shown to interact specifically with the product of PI3 kinase, PI(3,4,5)P_3. The PH domain of Asef1 is critical for its localization to sites of cell-cell contact at the plasma membrane of epithelial cells. The capacity of PI(3,4,5)P_3 to activate the exchange potential of Asef was not assessed (199). However, the members of the Asef family are regulated in two unique ways: they are repressed through a novel auto-inhibitory interaction between the SH3 and DH domains and activated through a novel interaction with the armadillo array of APC.

GEF:	Mechanism:	Signal:	Reference:
CDEP	Increased transcription	Parathyroid hormone	(27)
Dbl	Ubiquitin-mediated proteolysis	CHIP	(204)
Ect2	Increased transcription	Mitogens (KGF, EGF, PDGF)	(30)
Ect2	Decreased transcription	p53, Rb	(71)
Ect2	Ubiquitin-mediated proteolysis	UBE3A	(73)
Fgd1	Ubiquitin-mediated proteolysis	FWP1/βTrCP	(22)
Tiam1	Caspase-mediated cleavage	apoptosis	(176)
Tiam1	Increased transcription	E1A	(177)

Table 8: Regulation of Dbl-family GEFs by alteration of protein expression or mRNA transcription.

P-Rex subfamily:

The P-Rex subfamily consists of two highly related isozymes: P-Rex1 (for **P**I(3,4,5)P_3-dependent **R**ac **ex**changer) and P-Rex2 (5). P-Rex1 protein was originally purified from porcine neutrophils based upon its ability to stimulate Rac in response to PI(3,4,5)P_3, and its gene was subsequently cloned (169). The two isozymes have very similar domain architectures: they consist of a DH/PH cassette, two DEP domains (a homology region named for **D**isheveled, **E**GL-10 and **P**leckstrin, the first proteins shown to contain this domain), two PDZ domains, and a C-terminal **in**o**s**itol **p**hosphate – **4** – **p**hosphatase domain ($InsP_x$-4-P) (169,205,206). The $InsP_x$-4-P domain has not been shown to display phosphatase activity, and is truncated in an alternate splice isoform of P-Rex2, P-Rex2B. The expression profiles of the two P-Rex subfamily members are quite different, however. P-Rex1 is expressed exclusively in neutrophils and in the brain. P-Rex2A is expressed in skeletal muscle, heart, kidney, placenta, intestine and lung, while P-Rex2B expression is limited to cardiac tissues (205,206).

P-Rex subfamily members are exchange factors specific for Rac and this specificity is in part conferred by the β3-β4 loop of the PH domain making direct contacts with Rac that are not conserved in Rho or Cdc42 (207). The regulation of exchange activity of the P-Rex subfamily members, however, is complex and incompletely understood. The exchange activity of P-Rex proteins is stimulated by PI(3,4,5)P_3, which binds directly to the P-Rex PH domain (40,169). In addition, P-Rex proteins are stimulated through an interaction between Gβγ subunits and the DH domain (40,169). Neither Gα subunits, nor Gβγ dimers that contain $G\beta_5$, $G\gamma_1$ or $G\gamma_{11}$ are able to stimulate P-Rex exchange activity (146). The DEP, PDZ and PH domains, however, play

a role in the auto-inhibition of P-Rex activity, since their deletion stimulates exchange activity (40). The precise molecular mechanism behind this auto-inhibition has yet to be determined.

P-Rex has been identified as a component of several additional signaling pathways. First, P-Rex is localized to the leading process of migrating neurons in the intermediate zone of the developing cortex, where its exchange potential is activated downstream of NGF (nerve growth factor) binding to its receptor, TrkA. P-Rex is not phosphorylated in this signaling pathway, however. The pathway by which P-Rex is activated in this context depends on Ras activation of PI3 kinase, leading to production of $PI(3,4,5)P_3$. The activated Rac produced by P-Rex leads to an increase in neuronal motility (208). P-Rex has been shown to be phosphorylated by protein kinase A (PKA) downstream of signaling from the β_2-adrenergic receptor. PKA phosphorylation of P-Rex decreases both the basal activity of P-Rex and the ability of P-Rex to be stimulated by $G\beta\gamma$ (146). Finally, in migrating neutrophils, endogenous P-Rex translocates to the plasma membrane at the leading edge in response to GPCR stimulation with such ligands as fMLF and C5a. At the leading edge, P-Rex co-localizes with both Rac2 and F-actin, and interestingly, this translocation requires tyrosine kinase activity (209). Although a role for P-Rex regulation by tyrosine phosphorylation is emerging, P-Rex subfamily members represent the best characterized Dbl-family proteins regulated by $PI(3,4,5)P_3$ and $G\beta\gamma$.

Tuba subfamily:

The Tuba subfamily consists of Tuba, an uncharacterized protein (accession number XP376334), and Obscurin. The regulation of exchange activity of these proteins

is relatively unexplored. Tuba is ubiquitously expressed and is composed of four N-terminal SH3 domains, a DH domain, a BAR domain (named for **B**in, **A**mphiphysin and **R**VS, the first proteins shown to have this region of homology) and two C-terminal SH3 domains (5). BAR domains have been shown to bind and deform lipid bilayers and to mediate dimerization between proteins that contain this domain. In the case of Tuba, the BAR domain serves to functionally replace the PH domain, and binds specifically to $PI(4,5)P_2$ (210). Among the human Dbl-family proteins, Tuba, and its uncharacterized ortholog, are the only two that do not possess a PH domain immediately C-terminal to the catalytic DH domain. The isolated DH/BAR cassette of Tuba has been shown to specifically activate Cdc42 *in vitro* (211).

Tuba's N-terminal array of SH3 domains, like that of Intersectin, interacts with dynamin. The C-terminal SH3 domains bind to various regulators of the actin cytoskeleton, such as WAVE-1, Mena and N-WASP. In epithelial cells, Tuba is localized to the tight junction, where it interacts with ZO-1. Tuba may play a role in junctional organization in this context (89). In fibroblasts, over-expression of Tuba leads to actin-dependent membrane ruffling in the absence of growth factors (210).

Obscurin, like Tuba, is a very large protein, and is composed of multiple immunoglobulin-like domains, an SH3 domain, a DH/PH cassette and a C-terminal immunoglobulin-like domain (5,212). Obscurin was originally identified based upon its ability to interact with small ankyrin1, a protein that is an integral component of the sarcoplasmic reticulum (SR) membrane. Additionally, Obscurin interacts with the contractile apparatus of smooth muscle cells by binding both Titin and sarcomeric actin. Obscurin, then, may function to mediate the organization of smooth muscle myofibrils

and the SR (213). The exchange activity of Obscurin, like that of Tuba, however, has yet to be explored.

Dbl subfamily:

The Dbl subfamily is composed of the founding member of the Dbl family of proteins, Dbl (for **d**iffuse **B**-cell **l**ymphoma); a highly related protein, Dbs (for **D**bl's **b**ig **s**ister); two proteins with two DH/PH cassettes, Trio and Kalirin; and two relatively uncharacterized proteins, Scambio and p63-RhoGEF (also known as GEFT). Although these proteins are highly homologous with respect to the primary structure of their DH and PH domains (5), they are divergent in the regions outside of the DH/PH cassette, and therefore their domain architectures will be discussed individually below.

Onco-Dbl was originally isolated in a screen for oncogenes in a cDNA library derived from a B-cell lymphoma cell line (214). Proto-Dbl was later shown to be an N-terminally extended form of onco-Dbl, indicating that Dbl is regulated by auto-inhibition (215). In fact, Dbl is composed of an N-terminal spectrin domain (a structural motif found in proteins involved in cytoskeletal regulation), followed by the DH/PH cassette. The sequences N-terminal to the DH domain bind directly to the PH domain, and are inhibitory to the exchange activity of Dbl when expressed *in trans* (28). The N-terminal sequences are also important for proper localization of Dbl inside the cell: proto-Dbl is localized to the perinuclear region, while the isolated DH/PH cassette colocalizes with the actin cytoskeleton (28).

Like many of the other Dbl-proteins, Dbl itself is regulated through phosphoinositide binding. The PH domain of Dbl binds to both $PI(4,5)P_2$ and $PI(3,4,5)P_3$. Phosphoinositide binding impairs the ability of Dbl to activate Cdc42

(7,216). Mutation of the PH domain such that it is no longer able to bind phosphoinositides has no effect of the *in vitro* exchange activity of Dbl (7). However, a functional PH domain is required for localization of Dbl to both the actin cytoskeleton and the plasma membrane. This localization is essential for both the ability of Dbl to transform cells and to activate RhoA in cells (7,216,217). Whether the PH domain modulates the localization of Dbl through binding to phosphoinositides or to another protein is unknown.

The exchange activity of Dbl is modulated by signaling molecules in addition to phosphoinositides. The N-terminus of Dbl is able to interact directly with Gβγ subunits, although the capacity of Gβγ to modulate the exchange activity of Dbl has not been assessed (185). In addition, the non-receptor tyrosine kinase ACK1 (for **a**ctivated **C**dc42-associated **k**inase) induces the tyrosine phosphorylation of Dbl. This phosphorylation increases the exchange activity of Dbl towards Cdc42 and RhoA both *in vitro* and in cells (142). Finally, like the members of the RasGRF and Pix subfamilies, Dbl has been shown to form homodimers, mediated by the DH domain. Dimerization is required for the exchange and transformation activities of Dbl (96).

Interestingly, the exchange activity of Dbl is also regulated through modulation of the protein's stability in the cell. Early studies revealed that onco-Dbl was more stably expressed than proto-Dbl, and therefore that sequences in the N-terminus of the protein were important for rapid turnover of Dbl protein (218). Further work indicated that the **h**eat **s**hock **c**ognate protein **70** (Hsc70) is able to interact with both the PH and the spectrin domains of Dbl, serving to hold Dbl in its auto-inhibited conformation (219). Additional components of the Hsc70/Dbl complex include another chaperone, **h**eat **s**hock

protein **90** (Hsp90) and CHIP (**C**-terminus of **H**sc70 **i**nteracting **p**rotein), an E3 ubiquitin ligase. Proto-Dbl was shown to be a substrate for poly-ubiquitination by CHIP, and this ubiquitination targets proto-Dbl for degradation by the proteasome (see Figure 7). Since onco-Dbl lacks the spectrin domain, it is unable to interact with Hsc70 and CHIP, and is therefore stabilized in the cell (204).

Dbs, like Dbl, was isolated in a genetic screen for protein products that induce transformation of NIH 3T3 cells (220). Dbs is a larger protein than Dbl, in that it contains an N-terminal Sec14 domain (a lipid binding domain) in addition to the spectrin and DH/PH domains that the two proteins have in common (5). Although Dbs is able to activate RhoA and Cdc42 *in vitro* (5), its ability to transform cells depends only on its activation of RhoA (221). Originally, it was thought that Dbs is not regulated by auto-inhibition (220), however, subsequent studies have shown that the Sec14 domain inhibits Dbs-mediated cellular transformation by direct interaction with the PH domain (29).

The activity of Dbs is precisely regulated through binding to phospholipids. Initial studies showed that the PH domain of Dbs is critical for its transformation abilities, but that a membrane localization signal could functionally replace the PH domain (222). This hypothesis was called into question when it was discovered that the PH domain of Dbs binds to $PI(4,5)P_2$ when it is presented in a small unilamellar vesicle made up primarily of other anionic lipids, but with an affinity thought to be too low to drive translocation of Dbs to the plasma membrane (92). Interestingly, while the ability of the PH domain to bind phospholipids was critical for the proper subcellular localization of Dbs and the ability of Dbs to transform cells, phospholipid binding does not affect the *in vitro* exchange activity of Dbs (223). These seemingly disparate

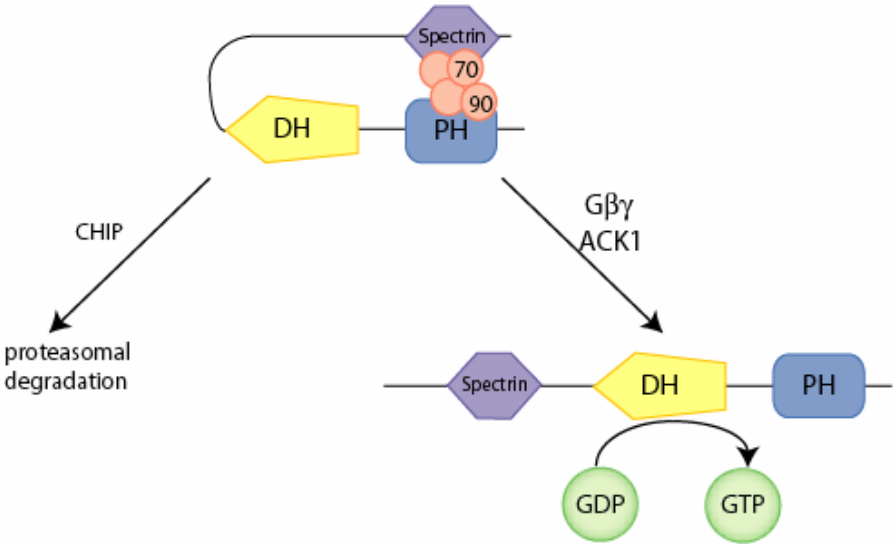

Figure 7: Regulation of Dbl by alterations in its cellular stability.
Heat shock cognate proteins (Hsc) 70 and 90 bind to both the spectrin and PH domains of Dbl, holding it in an auto-inhibited conformation. Binding of the E3 ubiquitin ligase, CHIP, to Hsc70 targets Dbl for proteasomal degradation (left). However, activation of various signal pathways leads to relief of Dbl auto-inhibition (right).

observations concerning the ability of the PH domain to dictate the subcellular localization of Dbs can be resolved by the observation that a version of the DH/PH cassette that is chemically modified to become a dimer is capable of being driven to the plasma membrane. Mutations in either PH domain of the engineered dimer prevent interaction with the membrane, but not nucleotide exchange *in vitro* (224). The PH domain in the full-length Dbs protein, then, is potentially able to drive Dbs to the plasma membrane in partnership with the Sec14 domain, which is able to bind the di-phosphorylated phosphoinositides (29).

The crystal structure of Dbs bound to its cognate GTPase, Cdc42, revealed a unique role for the PH domain. The PH domain of Dbs makes contacts with Cdc42 directly, assisting the DH domain in catalyzing guanine nucleotide exchange (225). The interactions between the PH domain in Dbs and Cdc42 were shown to be critical for Dbs-mediated cellular transformation (223).

Like that of Dbl, the exchange activity of Dbs is modulated downstream of several signaling pathways. For instance, signaling downstream of the α1B adrenergic receptor, a $G\alpha_q$ coupled receptor, activates the exchange potential of Dbs toward Cdc42, but not RhoA, in a Src-dependent manner (143). In addition, the PH domain of Dbs is able to serve as an effector binding domain for the activated form of the small GTPase, Rac1. This interaction increases the ability of Dbs to transform cells and activate RhoA in the context of the cellular milieu (167). Neurotrophin-3, acting through its receptor, TrkC, on the surface of Schwann cells leads to the phosphorylation of Dbs and activation of its exchange potential toward Cdc42, and a subsequent increase in the migratory capacity of these cells (144). Finally, the exchange potential of Dbs toward RhoA is

negatively regulated through an interaction between Dbs and the protein scaffold Ccpg1 (**c**ell **c**ycle **p**ro**g**ression protein 1) (226). Although Ccpg1 is able to interact with Dbs, Cdc42 and Src, the phosphorylation state of Dbs was not assessed in this study (see Figure 8).

Scambio, which gets its name from the Italian word for exchange, is made up of a DH/PH cassette with extended N- and C-termini that have limited homology to other Dbl-family proteins. Scambio is highly expressed in the heart and in skeletal muscle tissues, and is capable of stimulating exchange on both RhoA and RhoC. Its regulatory mechanisms are largely uncharacterized, but similar to Dbs, Scambio is able to interact with active Rac1 (197).

p63-RhoGEF is a relatively small Dbl-family member, consisting of a DH/PH cassette with N- and C-terminal extensions that show limited homology to other Dbl-family proteins (5). p63-RhoGEF was shown to have exchange activity for RhoA, and is expressed in excitable tissues, such as cardiac muscle, skeletal muscle and the brain (227). An alternate splice isoform of p63-RhoGEF, named GEFT, which lacks the N-terminal extension, was shown to promote dendritic outgrowth and spine morphogenesis in hippocampal neurons (228,229). GEFT was originally characterized as a Rac1 and Cdc42 specific exchange factor (228), but the most recent experimental evidence indicates that GEFT and p63-RhoGEF are encoded by the same gene and are both RhoA specific (230).

Recently, the exchange activity of p63-RhoGEF was shown to be activated downstream of signaling from $G\alpha_{q/11}$-coupled receptors. Additionally, $G\alpha_q$ was shown to interact with the C-terminal half of p63-RhoGEF. These results suggest that p63-

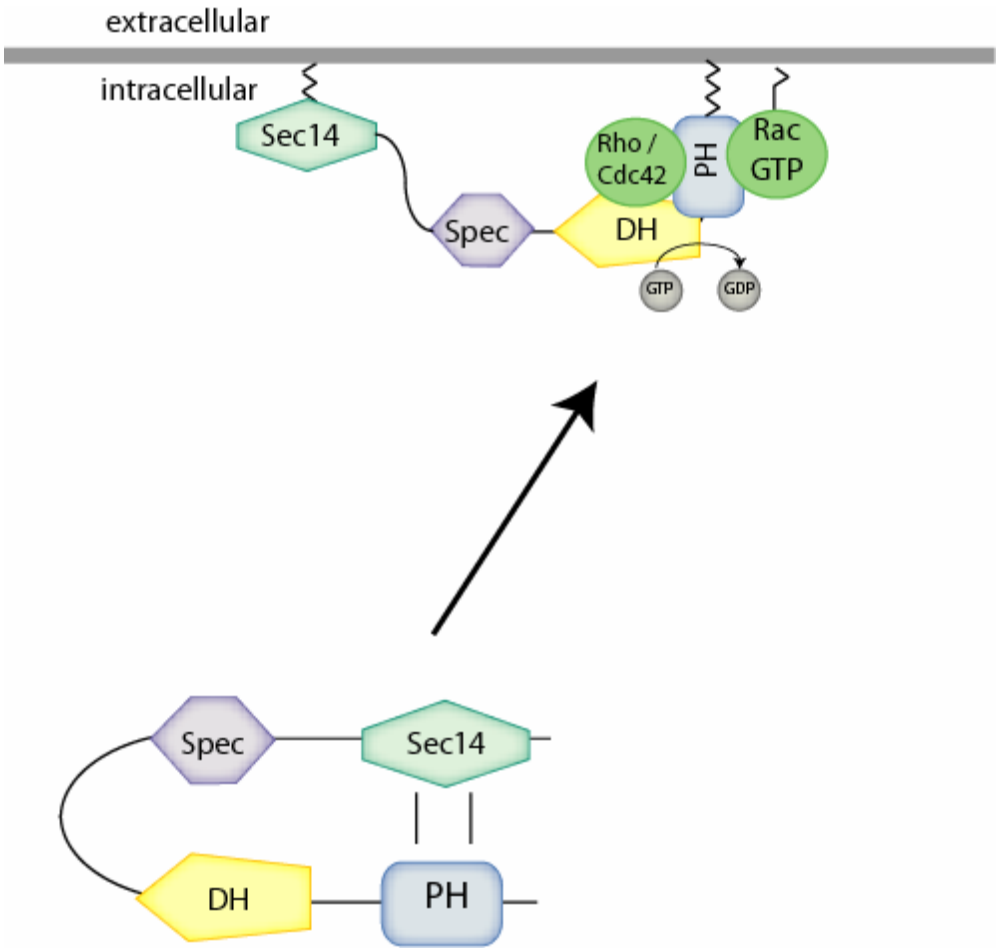

Figure 8: Targeting of Dbs to the plasma membrane requires two lipid binding domains.
In the cytoplasm, Dbs is held in an auto-inhibited conformation through an intramolecular interaction between the Sec14 domain and the PH domain. Auto-inhibition is relieved by an unknown mechanism. Activated Dbs, however, is targeted to the plasma membrane by interactions between both the Sec14 and the PH domains with membrane phosphoinositides. Activated Rac1 binding to the PH domain of Dbs helps to properly position this domain for contact with the cognate GTPases of Dbs, enabling efficient exchange.

RhoGEF may function as an effector protein for $G\alpha_{q/11}$, although the molecular mechanisms by which this occurs have yet to be uncovered (186). Finally, p63-RhoGEF expression is regulated at the transcriptional level during skeletal muscle regeneration. The transcription of p63-RhoGEF messenger RNA is increased during myogenesis and decreased during adipogenesis (231).

Trio is composed of an N-terminal Sec14 domain, an array of spectrin repeats, a DH/PH domain specific for Rac and RhoG, an SH3 domain, a DH/PH domain specific for RhoA, an additional SH3 domain, an immunoglobulin-like domain and a C-terminal serine/threonine kinase domain (5). Trio is so named because of the three functional enzymatic domains it possesses: two DH/PH cassettes and a kinase domain. While the genomes of invertebrates possess only one Trio isoform (dTrio in Drosophila melonogaster and UNC-73 in C. elegans), mammalian genomes possess two: Trio and the highly related Kalirin. Although both Trio and Kalirin are expressed in neurons, Trio is also expressed multiple other tissues (232).

Trio was identified by several independent labs simultaneously. One group identified Trio based upon its ability to interact with the cytoplasmic domain of the LAR transmembrane protein tyrosine phosphatase (232). The significance of that interaction remains unclear. Multiple groups, however, identified dTrio as in integral component of signaling pathways regulating photoreceptor axon guidance in the developing eye. In this context, Trio is localized to the plasma membrane of photoreceptor growth cones and the activity of its N-terminal DH/PH cassette is negatively regulated by the Sec14 and spectrin domains (233).

The expression of full-length Trio, but not the isolated DH/PH cassettes, has been shown to induce extension of neurites in an NGF-independent manner in the PC12 pheochromocytoma cell line. This effect is entirely mediated by the activation of RhoG by the N-terminal DH/PH cassette of Trio. In addition, the exchange activity of the N-terminal DH/PH cassette of Trio is required for induction of neurites by NGF in these cells (234). The function of the C-terminal DH/PH cassette remains unclear. However, the RhoA specific DH domain plus fifteen amino acid residues not found in Trio (termed Tgat, for **T**rio related **t**ransforming **g**ene in **A**TL tumor cells) was recently identified as an oncogene (6).

Multiple roles have been proposed for the PH domain associated with the Rac-specific DH domain of Trio. First, the N-terminal PH domain interacts with the actin filament cross-linking protein, filamin. This interaction is required for Trio to induce membrane ruffling, but does not modulate the Rac-specific exchange activity of Trio (171). Interestingly, the PH domain of the N-terminal DH/PH cassette is required for efficient exchange on Rac1, while the PH domain of the C-terminal DH/PH cassette inhibits exchange on RhoA (6,235).

Genetic and biochemical experiments in Drosophila show that both Trio and the non-receptor tyrosine kinase, Abl, interact with the cytoplasmic domain of Frazzled, which is the cell-surface receptor for Netrin (151,236). Although Trio was shown to be tyrosine phosphorylated in these experiments (151), the residues phosphorylated and the consequences of the phosphorylation event on the exchange activity of Trio were not determined. Finally, Trio, like Kalirin, as will be discussed below, is regulated by pre-mRNA splicing. An alternate splice isoform of Trio, termed Solo, is expressed in

Purkinje neurons. Solo is composed of the Sec14 domain, the spectrin domains, the first DH/PH cassette, and the SH3 domain of Trio followed by a short membrane anchoring domain, and is localized to early endosomes, where it mediates Rac activation (237).

The domain architecture of Kalirin is basically identical to that of Trio, however, the N- and C-terminal DH/PH cassettes of the human Kalirin protein were identified independently and named Duo and Duet, respectively. Kalirin was originally identified as a binding partner for the cytoplasmic domain of peptidyl-α-amidating-mono-oxygenase, a transmembrane enzyme essential for synthesis of neuropeptides. Kalirin was named for the Kali, a Hindu goddess with many hands, because of its multiple enzymatic domains (238).

Multiple splice isoforms of Kalirin are expressed at different points in the development of the rat nervous system. Kalirin7, which terminates in a PDZ-binding motif unique to this splice isoform immediately following the N-terminal, Rac-specific DH/PH cassette is localized to punctate structures along the shaft of developing neurites (239) and is the splice isoform of Kalirin that is expressed in the adult rat (240). The PDZ-binding motif interacts with multiple PDZ domain-containing proteins, including PSD-95, and serves to properly localize Kalirin7 (241).

The longer splice isoforms of Kalirin, Kalirin9 and Kalirin12, are expressed during embryonic development (240). Kalirin9 contains all of the domains of full-length Kalirin up to and including the second, RhoA specific DH/PH cassette, and is localized to both the cell bodies and the processes of neurons. Kalirin12, which also contains the kinase domain, is localized to only the cell bodies of neurons (239). Interestingly, over-expression of the first DH/PH cassette in primary cortical neurons led to shorter neurites,

both axons and dendrites, while over-expression of the second DH/PH cassette led to an increase in axon length (240). However, the first DH/PH cassette, by activating RhoG, induces superior cervical ganglion fiber outgrowth, indicating a possible cell-type specific difference in the effects of expression of the first DH/PH cassette (242).

Kalirin may play a role in signal transduction from several different receptor tyrosine kinases. First, EphB2 binding to its ligand ephrin B leads to the tyrosine phosphorylation of both over-expressed and endogenous Kalirin. While tyrosine phosphorylation doesn't alter the exchange activity of Kalirin, it does lead to the recruitment of Kalirin to EphB2 containing clusters on the plasma membrane (145). Additionally, Kalirin is required for NGF-induced neurite outgrowth in PC12 cells. Kalirin, through its N-terminal PH domain, binds to the cytoplasmic kinase domain of the NGF receptor, TrkA. Although Kalirin binding increases the kinase activity of TrkA, we do not yet know if Kalirin is phosphorylated or activated by TrkA (168).

The exchange activity of the first DH/PH cassette of Kalirin, however, is regulated by auto-inhibition. The SH3 domain, located between the two DH/PH cassettes, is able to form intramolecular interactions with multiple proline-containing sequences. Truncation of these poly-proline motifs leads to an increase in the Rac-specific exchange activity of the full-length protein. In addition, the SH3 domain is able to directly bind, and potentially sterically occlude, the N-terminal DH/PH cassette of Kalirin (243). In summary, the mechanisms of regulation for Dbl subfamily members is complex, but in most cases is related to the function of the DH-associated PH domain.

Concluding Remarks:

The mechanisms of regulation of Dbl-family proteins, as described in the preceding sections, are diverse. This situation is not surprising considering the disparity in the domain architectures of the various subfamilies of Dbl-family proteins. However, some generalizations can be drawn. First, many Dbl-family proteins are activated by truncation mutations (see Table 1). In fact, this mechanism of regulation is so common that the isolated DH/PH of many Dbl-family proteins has been used in functional assays as a constitutively active mutant. However, there are multiple mechanisms by which a truncation mutation is auto-activating. Most commonly, activation by truncation indicates that a particular Dbl-protein is regulated by intramolecular auto-inhibitory interactions. The Vav isozymes are the best understood examples of Dbl-family proteins that are regulated by auto-inhibition. In this case, an auto-inhibitory helix immediately N-terminal to the DH domain is able to sterically occlude the GTPase binding site on that catalytic domain. However, a review of Dbl-family protein regulation indicates that multiple different domains are able to bind to either the DH or the PH domain and sterically occlude the cognate GTPase from the catalytic interface. In many cases, the precise molecular interactions that lead to auto-inhibition of Dbl-family proteins remain to be discovered, and we do not yet know if other Dbl-family proteins are auto-inhibited by motifs that bear sequence homology to the auto-inhibitory helix of Vav.

Truncation of the N-terminus of the Dbl-family protein Net1, however, is activating in cellular assays because truncation removes Net1's nuclear localization signal, and prevents this GEF from being sequestered in the nucleus where it cannot activate its cognate GTPase. Dbl-family GEFs need to translocate from the cytoplasm to

the plasma membrane in order to be active, however, other Dbl-family proteins that are sequestered in a sub-cellular location where they are inactive or that are active in a particular domain of the plasma membrane are shown in Table 2. Prevention of intermolecular interactions, such as the formation of homo-dimers mediated by the C-terminal leucine zipper domain of p115-RhoGEF is yet another mechanism by which truncation can yield an activated GEF. The Dbl-family proteins known to form homo- and hetero-dimers are shown in Table 3.

The second most common mechanism by which Dbl-family proteins are regulated is phosphorylation. Multiple kinases, including tyrosine or serine/threonine kinases, as well as receptor or non-receptor kinases are able to phosphorylate Dbl-family proteins (see Table 4). These phosphorylation events can directly activate the exchange activity of the GEF, as in the case of the tyrosine phosphorylation of Vav proteins, or directly inactivate the GEF, as in the case of PKA phosphorylation of P-Rex. In addition, phosphorylation can lead to creation of a binding site for a phospho-specific protein-protein interaction. GEF-H1 phosphorylation by Pak1, followed by its inhibitory interaction with 14-3-3 can be characterized in this way.

Another mechanism by which Dbl-family proteins are regulated is through ligands binding to the DH-associated PH domain. These interactions are presumed to target the Dbl-family protein to the plasma membrane, where it is able to activate a prenylated GTPase. However, in many cases these interactions also mediate efficient exchange by properly orienting the DH-associated PH domain, which has significant conformational heterogeneity. In this scenario, the DH and PH domains of Dbl proteins function as a coincidence detector designed to integrate information regarding local

fluctuations in both GTPase concentrations and membrane composition. These interactions are summarized in Table 5.

Dbl-family proteins are able to be regulated by, and thus serve as effectors for both heterotrimeric G proteins (Table 6) and small GTPases (Table 7). The molecular details of these interactions and the ubiquity of this regulatory mechanism are currently unknown.

Although many mechanisms that increase the exchange activity of Dbl-family GEFs have been identified, very few mechanisms for returning the activity level to a basal state are known. One such mechanism is ubiquitin-mediated targeting of Dbl-family proteins to the proteasome. This mechanism has been shown to be important for the regulation of Dbl itself, as well as other GEFs in this family (Table 8). Interestingly, although many Dbl-proteins are activated by phosphorylation events, the phosphatases that might down-regulate Dbl-protein activity have yet to be identified.

This review of Dbl-family protein regulation strikingly highlights the fact that there are multiple mechanisms of regulation for each individual GEF. By requiring multiple inputs, the cell is able to achieve highly specific spatio- and temporal regulation of GEF activity, underlying the importance of proper regulation of these proteins for homeostasis.

CHAPTER 2: AUTO-INHIBITION OF THE DBL-FAMILY PROTEIN TIM BY AN N-TERMINAL HELICAL MOTIF

Introduction:

RhoA, Rac1, and Cdc42 are the best understood of the 22 human Rho-family GTPases, which comprise one of five branches of the Ras superfamily of small GTPases (1). Like Ras, Rho proteins function as binary switches that alternate between inactive, GDP-bound states and active, GTP-bound states. Once activated, Rho GTPases directly engage numerous downstream effectors to modulate their functions. Active Rho GTPases and their effectors orchestrate actin cytoskeleton rearrangement and gene transcription to coordinate diverse cellular processes including adhesion, migration, phagocytosis, cytokinesis, neurite extension and retraction, polarization, growth and survival (2). Not surprisingly, aberrant activation of Rho GTPases promotes various developmental, immunological and proliferative disorders (3).

The Dbl-family of guanine nucleotide exchange factors (GEFs) are the largest group of proteins directly responsible for the activation of Rho GTPases. Dbl-family proteins are characterized by a Dbl-homology (DH) domain, which contacts the Rho GTPase to catalyze nucleotide exchange, and an associated pleckstrin-homology (PH) domain, which fine-tunes the exchange process by a variety of mechanisms related to the binding of phosphoinositides. The 69 human Dbl-family proteins are divergent in

regions outside the DH/PH module, and contain additional domains that presumably dictate unique cellular functions (5).

The capacity of DH domains to activate Rho GTPases is tightly regulated through a multitude of diverse mechanisms ranging from alterations in transcript levels and protein expression (6) to subcellular re-distribution (7), post-translation modifications (8) and protein degradation (9). However, despite this large spectrum of regulatory mechanisms, in most cases, truncation of Dbl-family proteins often potently activates their exchange activities (10). Currently, there is no general understanding for why truncation promotes unregulated exchange.

In order to better understand potential mechanisms that regulate Dbl-family proteins, we have chosen to study the relatively small, human Dbl-member, Tim (Transforming Immortalized Mammary). Tim was originally identified based upon its capacity to induce transformation of NIH 3T3 cells upon truncation (83), and while there are multiple transcripts of TIM (44,83), endogenous Tim is expressed as a 60-kDa protein, consisting of a short N-terminal region (~70 residues) followed by a DH/PH cassette and an adjacent C-terminal SH3 domain. All conserved homologs of Tim preserve this domain architecture. mRNA transcripts encoding Tim are expressed in numerous tissues and cancer-derived cell lines; corresponding protein expression has been verified in various cell lines (44,83). The gene encoding human Tim has been localized to chromosomal region 7q33 -7q35, which has been implicated in rearrangements contributing to both acute myelogenous leukemia and breast carcinoma (84). Nonetheless, while Tim was originally identified as an oncogene, its *in vivo* functions and regulation are unknown. Indeed, although Tim was cloned from a cDNA

expression library derived from a human mammary epithelial cell line, Tim expression is down-regulated in breast carcinoma cell lines and aggressive primary breast carcinoma cells express versions of Tim in which the catalytic DH domain is either truncated or mutated, suggesting a possible tumor suppressor function for Tim (244).

Here we show that the exchange potential of Tim towards RhoA is inhibited by a short N-terminal region with high helical propensity that directly interacts with the DH domain to prevent access of Rho GTPases to the DH domain. Truncation, mutation or phosphorylation of this putative helix fully relieves this auto-inhibition. Addition of the putative helix *in trans* to truncated Tim restores auto-inhibition. Furthermore, a substitution within the DH domain designed to disrupt interactions with the N-terminal helix also relieves auto-inhibition. These results show that Tim, like the distantly related Vav isozymes, is activated by unintentional truncation and regulated phosphorylation.

Experimental Procedures:

Protein Expression and Purification:

Full-length and truncated versions of human Tim were PCR-amplified and ligated into pET-21a (Novagen) between NdeI and XhoI. The cDNA for Tim was a gift of Dr. David Siderovski (UNC).

Tim constructs were expressed in the *E. coli* strain Rosetta (DE3) (Novagen). Cell cultures were grown at 37ºC in LB/ampicillin (100 μg/mL), and induced with 1 mM isopropyl-β-D-thiogalactopyranoside (IPTG) for 5 h at 27ºC. Cell pellets were resuspended in 20 mM HEPES, pH 7, 1 mM EDTA, 2 mM DTT, 10 % glycerol (buffer A) containing 20 mM NaCl, lysed using an Emulsiflex C5 cell homogenizer (Avestin), and clarified by centrifugation at 40,000 *g* for 45 min at 4ºC. Clarified supernatant was

loaded on a Fast Flow S column (Pharmacia) equilibrated with buffer A and eluted with a linear gradient of 20-500 mM NaCl. Tim protein eluted at approximately 300 mM NaCl and was loaded onto an S-200 size exclusion column (Pharmacia) equilibrated with buffer A containing 300 mM NaCl. Fractions containing monomeric Tim were pooled, concentrated, and stored at -80ºC. Mutations were introduced into wild-type Tim using the Quikchange site-directed mutagenesis kit (Stratagene) as per the manufacturer's instructions, and these mutant proteins were expressed and purified as described above. DNA sequences of all expression constructs were verified by automated sequencing. RhoA was purified as described (94,225,245).

Baculoviruses encoding both the wild-type and kinase inactive (K297A) versions of the kinase domain of c-Src (*Mus musculus*) were generated from pFastBacHT vectors (gifts of Dr. David Siderovski, UNC) using the Bac-to-Bac method (Invitrogen). HighFive insect cells were infected with the baculovirus at a multiplicity of infection of 1.0. After 48 h of incubation at 27°C, cells were harvested by low speed centrifugation, resuspended and lysed in 20 mM HEPES, pH 7.5, 500 mM NaCl, 2 mM $MgCl_2$, 10% glycerol (buffer B) with 10 mM imidazole, and clarified by centrifugation at 100,000 *g* for 45 min. The clarified supernatants were diluted to a final volume of 150 ml and loaded onto a nickel-charged metal chelating column (Pharmacia) equilibrated with buffer B containing 10 mM imidazole, washed with buffer B containing 50 mM imidazole and eluted with buffer B containing 400 mM imidazole. Eluted Src was extensively dialyzed versus buffer B with 150 mM NaCl and 1 mM EGTA, concentrated, and stored at -80ºC.

The kinase domain of EphA4 was PCR-amplified from the full-length cDNA (gift of N. Mochizuki, National Cardiovascular Center Research Institute, Suita, Osaka, Japan), ligated into pGEX4T2 (Amersham Biosciences) in frame with an N-terminal GST tag, and expressed in BL21(DE3) *E. coli* as described above. Cell pellets were resuspended in 20 mM Tris pH 7.5, 150 mM NaCl, 1 mM EDTA, 2 mM DTT, 10% glycerol (buffer C), lysed and clarified as described above. Clarified lysate was loaded onto a glutathione-sepharose column (Pharmacia). EphA4 protein was washed and eluted in buffer C containing 10 mM glutathione. The GST tag was removed with TEV protease and protein was loaded on an S-200 column equilibrated with buffer C. Eluted EphA4 was concentrated and stored at -80ºC.

Guanine Nucleotide Exchange Assays:

Fluorescence spectroscopic analysis of N-methylanthraniloyl (mant)-GTP incorporation into RhoA was carried out as described (246). In brief, assay mixtures containing 20 mM Tris pH 7.5, 150 mM NaCl, 5 mM $MgCl_2$, 1 mM DTT and 100 μM mant-GTP (Molecular Probes) and 2 μM RhoA were allowed to equilibrate with continuous stirring. After equilibration, 50 nM Tim was added and nucleotide loading was monitored as the decrease in the tryptophan fluorescence (λ_{ex} = 295 nm, λ_{em} = 335 nm) of RhoA or the increase in the mant-GTP fluorescence (λ_{ex} = 360 nm, λ_{em} = 440 nm) as a function of time using a Perkin-Elmer LS 55 spectrophotometer. Rates of guanine nucleotide exchange were determined by fitting the data to a single exponential decay model with GraphPad Prizm. Data were normalized to yield percent GDP released and assays were performed in duplicate.

Cell Culture and Transformation Assays:

NIH 3T3 mouse fibroblasts were maintained in DMEM supplemented with penicillin/streptomycin and 10% calf serum (Hyclone). HEK 293T cells and SYF fibroblasts were maintained in DMEM supplemented with penicillin/streptomycin and 10% fetal bovine serum (Sigma). PCR-amplified Tim constructs were ligated into pcDNA 3.1 Hygro (Invitrogen) between *EcoRI* and *XhoI* such that an expressed HA-tag was encoded at the N-terminus of each construct. Mutations were introduced into wild type Tim as described above.

Cell lines stably expressing Tim were established by transfecting NIH 3T3 cells with 1 μg of each pcDNA construct using LipofectAMINE Plus (Invitrogen) according to the manufacturer's protocol. Three days post-transfection the cells were subcultured into growth medium supplemented with 300 μg/mL of hygromycin B. Mass populations of multiple, drug resistant colonies (>50) were pooled together for focus formation analyses. Western blot analysis with an anti-HA antibody (Covance) was performed to verify Tim expression in the cell lines.

For the secondary focus formation assays, equal numbers of cells from each cell line were seeded into 60 mm dishes. The growth medium of each dish was replaced with fresh hygromycin-supplemented medium every three days. 14 days after seeding, the dishes were stained with crystal violet and the foci were quantified by visual inspection. Individual experiments were performed in duplicate and independently carried out three times.

GTPase Activation Assays:

Affinity purifications of RhoA were carried out as described (66). In brief, the Rho binding domain (RBD) of Rhotekin (amino acids 7-89) was expressed as a GST fusion protein in BL21 (DE3) cells and immobilized on glutathione-coupled Sepharose 4B beads (Amersham Biosciences). HEK 293T cells were transiently transfected with 1 μg of various pcDNA-Tim constructs using LipofectAMINE 2000 (Invitrogen) according to the manufacturer's protocol. Immediately post-transfection, these cells were serum starved in DMEM supplemented with 0.1% FBS and incubated for 16 hours. Cells were washed in ice cold PBS and lysed in lysis buffer (50 mM Tris pH 7.5, 500 mM NaCl, 30 mM $MgCl_2$, 0.1% SDS, 0.5% sodium deoxycholate, 1.0% Triton X-100 and protease inhibitors). Lysates were clarified by centrifugation at 16,000 g for 10 min. Total protein concentration of the lysates was determined by a colorimetric assay (Bio-Rad). 1 mg of clarified HEK 293T lysate was incubated with 120 μg GST-Rhotekin-RBD beads for 1 hour at 4°C. The beads were washed three times in wash buffer (25 mM Tris pH 7.5, 30 mM $MgCl_2$, 40 mM NaCl and protease inhibitors). Total and affinity-purified lysates were subjected to SDS-PAGE and Western blot analysis using an anti-RhoA (Santa Cruz Biotechnology) monoclonal antibody. Each experiment was performed a minimum of three times. Precipitation of Tim with recombinant G17A RhoA was performed essentially as described (102).

In vitro kinase assay:

30 μg of purified Tim protein was incubated with 250 ng of recombinant Src or EphA4 kinase domain in kinase buffer (100 mM Tris, pH 7.5, 125 mM $MgCl_2$) supplemented with 100 μM ATP and 5 μCi [γ-^{32}P] ATP for 60 min at 30°C. Samples

were subjected to SDS-PAGE and autoradiography. Control substrate peptide was obtained from Upstate.

Immunoprecipitation:

The cDNAs for various Src constructs in pUSEamp were obtained from Upstate. SYF fibroblasts were transfected with 10 μg Src and 5 μg Tim using Superfect (Qiagen) according to the manufacturer's protocol. 24 hours post-transfection, the cells were serum starved in DMEM supplemented with 0.1% FBS and incubated for 16 hours. Cells were washed in ice-cold PBS and lysed in lysis buffer. Lysates were clarified by centrifugation at 16,000 g for 10 min. 1 mg of clarified SYF lysate was incubated with 25 μg anti-HA affinity matrix (Roche) for 1 hour at 4°C. The beads were washed three times in lysis buffer. Total and affinity purified lysates were subjected to SDS-PAGE and Western blot analysis using anti-phosphotyrosine (Transduction Laboratories), anti-Src (Upstate), anti-HA (Covance), and anti-β actin (Sigma) antibodies. The experiment was performed three times.

Results:

Specificity of the Guanine Nucleotide Exchange Activity of Tim:

Previous studies by our lab have shown that Tim catalyzes exchange of guanine nucleotides on RhoA, but not on Rac1 or Cdc42 (94). This specificity of exchange activity is due to the fact that Tim possesses a basic residue in helix α5 of the DH domain, which is able to form an energetically favorable salt-bridge interaction with glutamate 54 of RhoA. Rac1 and Cdc42 do not have an acidic residue in the position analogous to E54 of RhoA, and thus cannot make this contact with Tim (94). However,

recent work in which Tim is over-expressed in various mammalian cell types suggests that Tim may catalyze exchange on more than one Rho family GTPase. For example, expression of Tim in COS-7 or NIH 3T3 cells leads to a loss of actin stress fibers and the formation of membrane ruffles, dorsal ruffles, and filopodia, suggesting that Tim may activate Rac1, RhoG or Cdc42 but not RhoA in these cell types (244). However, expression of Tim in COS-7 cells leads to activation of RhoA, and not Rac1 or Cdc42, in pulldown experiments using GST-tagged versions of the Rho binding domains of the Rho effector, Rhotekin, and the Rac1 and Cdc42 effector, Pak (44). In the same study, Tim expression in NIH 3T3 cells led to activation of JNK, SRF and AP-1 regulated transcription, suggesting that Tim activates multiple GTPases in this cell type. However, in the same work, Tim expression in Swiss 3T3 cells led to cell rounding, while Tim expression in HeLa cells led to an increase in vinculin-enriched focal adhesions, suggesting that Tim activates RhoA in these cell types.

In an attempt to resolve these conflicting data, and to test the hypothesis that Tim activates multiple GTPases, we performed a fluorescence-based guanine nucleotide exchange assay on a library of Rho-family GTPases (Figure 9). In this assay, Tim robustly activated each of the members of the RhoA subfamily of Rho GTPases, RhoA, RhoB, and RhoC. However, Tim failed to activate the members of the Rac1 (Rac1, Rac2, Rac3 and RhoG) or Cdc42 (Cdc42, TCL and TC10) subfamilies. These data suggest that Tim directly activates members of the RhoA subfamily of GTPases, but may activate indirectly additional GTPases when over-expressed in various cell types.

Regulation of Tim by regions preceding its DH domain:

Tim was originally identified by its capacity to transform NIH 3T3 cells upon N-terminal truncation (83). Since many Dbl-family proteins are activated by similar truncations, we undertook a detailed analysis of the structural determinants within the N-

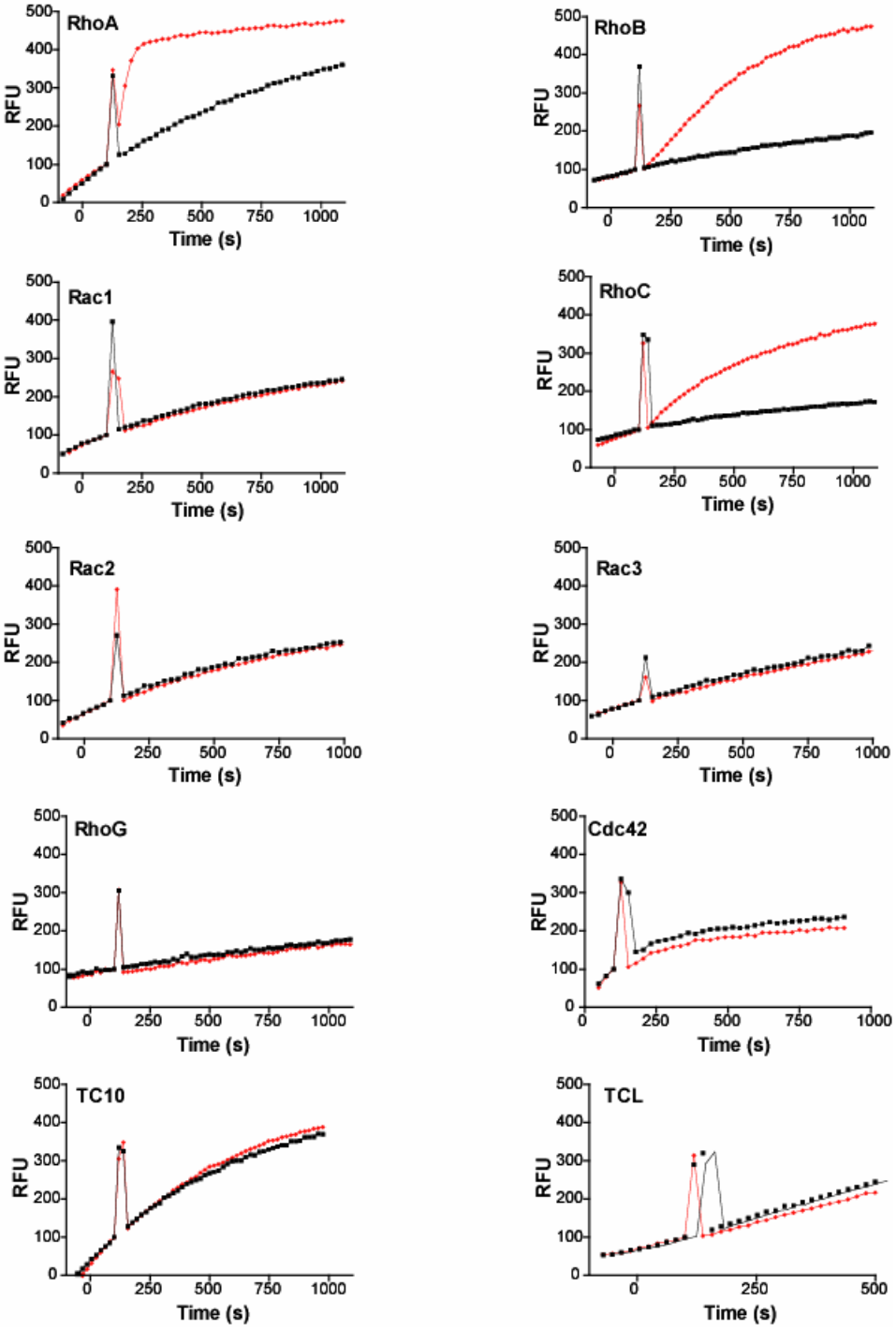

Figure 9: Tim is specific for RhoA, RhoB and RhoC.
The exchange of GDP bound to various Rho GTPases and catalyzed by Tim was measured using a standard fluorescence-based assay (245,246). The relative fluorescence units (RFU) resulting from mant-GTP loading onto each GTPase are shown for Tim catalyzed (red curves) and intrinsic (black curves) exchange reactions. The GTPases were purified and assessed for GTP-loading stimulated by EDTA as previously described (195).

terminal region of Tim required for its auto-inhibition. Using purified proteins, full-length Tim (wt, Figure 10A) enhanced the rate of exchange of guanine nucleotide bound to RhoA by a modest five-fold relative to the equivalent, spontaneous reaction (-). In contrast, truncation of the first 22 residues of Tim (Δ22) greatly enhanced the normalized loading of nucleotide by more than thirty-fold.

Constitutive RhoA activation promotes cellular transformation, and consistent with the *in vitro* exchange data, stable expression in NIH 3T3 cells of Tim (Δ22) promoted robust formation of foci relative to background (vector) and full-length Tim (wt) (Figure 10B). The combined results from the *in vitro* exchange assays and cellular transformation assays indicate that Tim is auto-inhibited by its N-terminus and that deletion of the first 22 residues of Tim relieves this auto-inhibition to promote robust guanine nucleotide exchange on RhoA *in vitro* as well as significant transformation of NIH 3T3 cells.

To produce a high-resolution map of the residues within the N-terminal portion of Tim necessary for auto-inhibition, this region was subjected to alanine-scanning mutagenesis and the resulting purified mutant proteins were tested for their capacity to activate RhoA *in vitro* (Figure 11A). This analysis identified residues 15 through 22 of Tim as necessary for its auto-inhibition *in vitro*. Stable expression of these substituted forms of Tim in NIH 3T3 cells indicated an approximate direct correlation between the capacity of Tim to activate RhoA *in vitro* and the transformation potential of the mutated forms of Tim (Figure 11B). One exception to this rule, Y22A, significantly relieved the auto-inhibition of Tim *in vitro*, but failed to activate Tim's transforming potential. It was reasoned that in the cellular environment secondary intermolecular interactions might

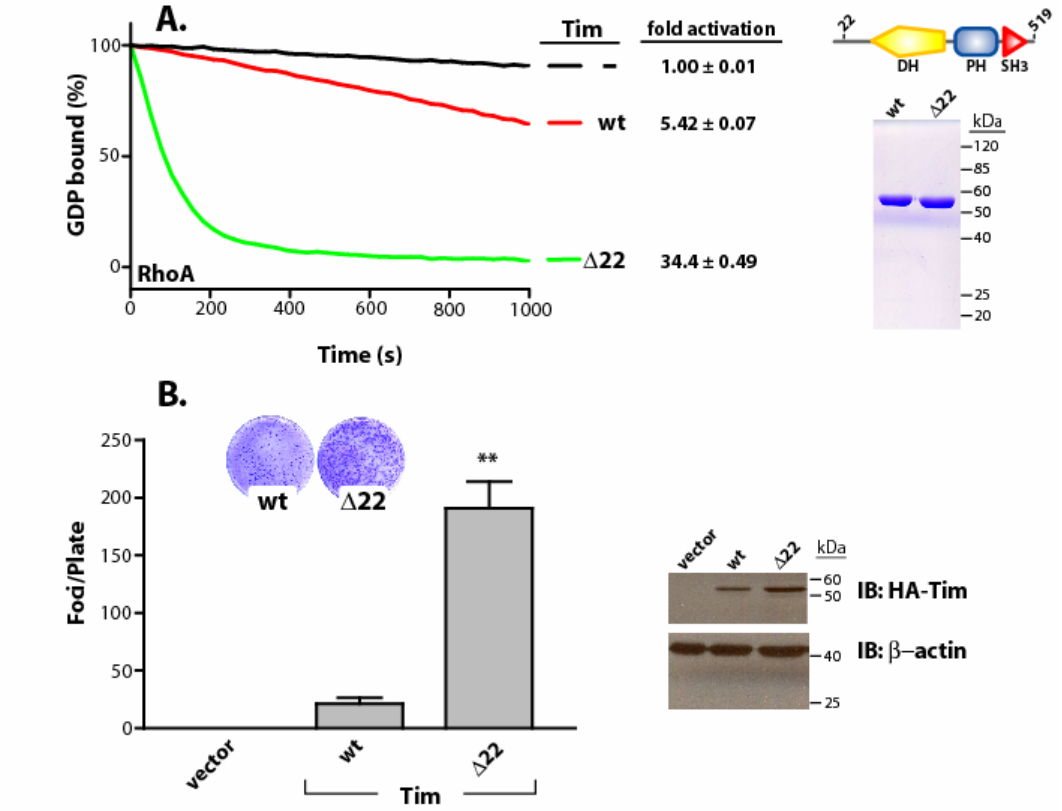

Figure 10: Full-length Tim is auto-inhibited by its N-terminal region.
(A) The exchange of GDP bound to RhoA and catalyzed by Tim was measured using a standard fluorescence-based assay (245,246). Fold-activation is relative to the spontaneous loading of guanine nucleotide and represents the average of two independent reactions for each trace. Equal amounts (2 μg) of purified proteins used in the exchange assays are shown at right following SDS-PAGE and staining with Coomassie brilliant blue. Also shown is a schematic of the domain architecture of Tim with the site of N-terminal truncation indicated. **(B)** N-terminally truncated Tim potentiates transformation of NIH 3T3 cells. Data represent the averages of three independent experiments carried out in duplicate. ** denotes $p < 0.01$, as determined by a pairwise t-test assuming equal variances. Inset illustrates representative plates of foci. Right panel verifies approximately equal expression of Tim variants used in the focus formation assays.

serve to stabilize the auto-inhibited state. These secondary stabilizing interactions would be lacking in the *in vitro* exchange assays using purified components such that even modest perturbation to the auto-inhibition of Tim (*e.g.* Y22A) would appear relatively enhanced. To explore this possibility, Tyr 22 was subsequently mutated to Glu (Y22E) with the anticipation that the added negative charge would further perturb auto-inhibitory interactions. The identical substitution was separately created at Tyr 19, and the resulting mutant proteins were analyzed as above. Both potentially phosphomimetic substitutions led to robust *in vitro* activation of RhoA and correspondingly large increases in the transformation potential of Tim. To the best of our knowledge, these data represent the first report of a full-length Dbl-family protein that is activated by single substitutions to the same extent as activation by N-terminal truncation.

To determine if residues 15 through 22 of Tim are sufficient for its auto-inhibition, we created a peptide comprising this region and performed an *in vitro* guanine nucleotide exchange assay in which this peptide (WT, Figure 12A) was added to Tim (Δ22) in *trans*. The exchange activity of Tim (Δ22) alone was greatly enhanced with respect to full-length Tim, as was also shown in Figure 9A. However, the exchange activity of Tim (Δ22) in the presence of the wild type peptide was reduced to that of full-length, auto-inhibited Tim. To determine if the observed inhibition was specific for this peptide, we also created a peptide in which the tyrosine residue corresponding to Tyr 19 in full-length Tim was converted to glutamic acid (MT, Figure 12A). Substitution of Tyr 19 with glutamic acid in the context of full-length Tim led to Tim activation in both the *in vitro* exchange assay and the cellular transformation assay (Figure 11). We therefore expected that a peptide incorporating this substitution would have no effect on the

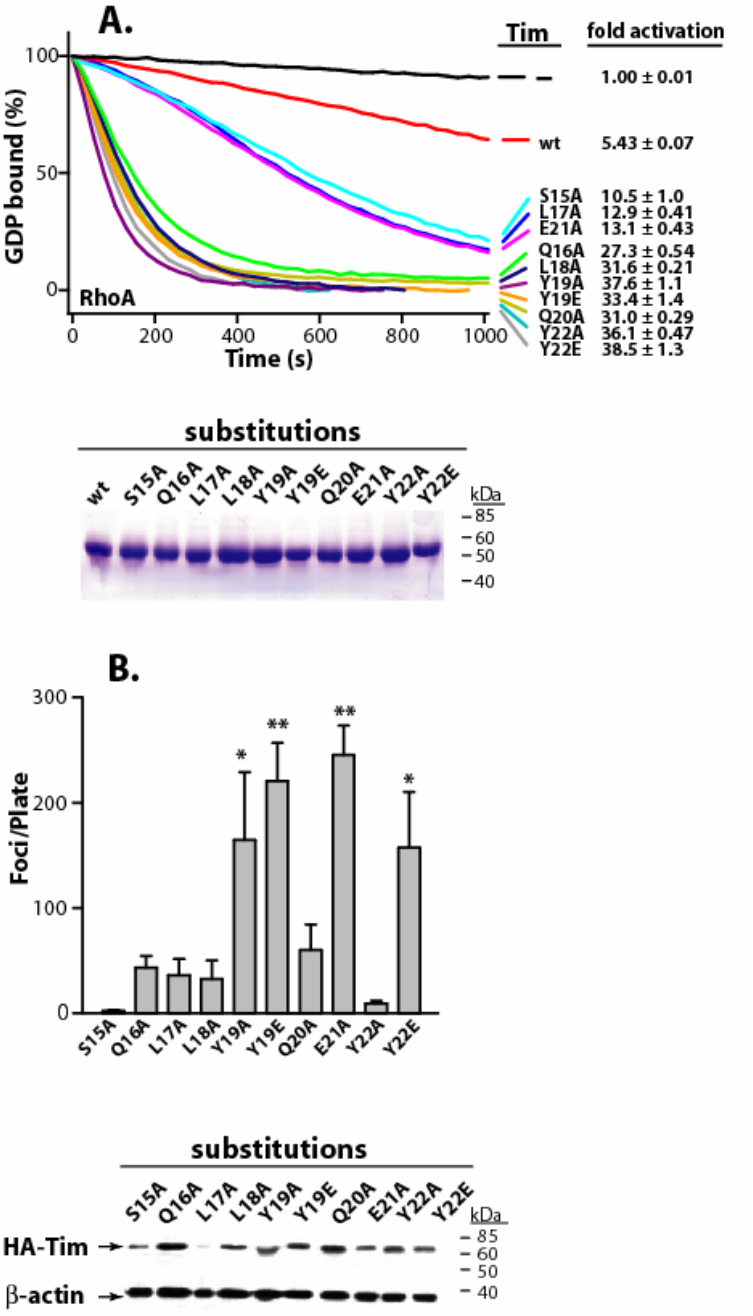

Figure 11: A short region within Tim is responsible for auto-inhibition.
(A) The N-terminal portion of Tim was subjected to scanning mutagenesis and the purified proteins were assayed for their capacity to catalyze the exchange of guanine nucleotides on RhoA. Fold-activation is relative to the spontaneous loading of nucleotide onto RhoA (-) and represents the average of two independent assays for each mutant. Equal amounts (2 µg) of purified proteins used in the exchange assays are shown in the lower panel following SDS-PAGE and staining with Coomassie brilliant blue (a composite of several gels is shown). **(B)** Equivalent forms of Tim were stably expressed in NIH 3T3 cells (lower panel, composite western blot) and assayed for foci formation (upper panel). Data represent the averages of three independent experiments carried out in duplicate. * denotes $p < 0.05$, ** denotes $p < 0.01$, as determined by a pairwise t-test assuming equal variances.

exchange potential of Tim (Δ22). This hypothesis was borne out experimentally, since the exchange potential of Tim (Δ22) in the presence of the mutant peptide was identical to that of Tim (Δ22) alone. Importantly, neither peptide had an effect on the intrinsic rate of exchange on RhoA. These data strongly suggest that residues 15 through 22 are both necessary and sufficient for Tim auto-inhibition.

To confirm that the N-terminal region is necessary for Tim inhibition in the context of an intact cell, we performed affinity purifications of active Tim using a GST-tagged version of nucleotide-free RhoA (RhoA G17A, Figure 12B). Since Dbl-family proteins bind preferentially to nucleotide-free Rho family GTPases, this construct is expected to affinity purify any active, RhoA-specific GEF present in a cell lysate. Wild type, HA-tagged Tim, when expressed in serum-starved HEK 293T cells, did not appreciably interact with RhoA G17A. In contrast, both truncated Tim (Δ22) and full-length Tim possessing the double substitution, Y19E + Y22E were robustly affinity purified by the RhoA G17A matrix, suggesting that the immediate N-terminal region of Tim, and tyrosines 19 and 22 in particular, lead to Tim auto-inhibition by preventing its interaction with RhoA.

Affinity purifications of active RhoA (Figure 12C) confirmed the direct correlation between the capacity of Tim to activate RhoA *in vitro* and Tim's transforming potential. For example, while wild-type Tim did not significantly activate RhoA relative to empty vector upon transfection into HEK 293T cells, both truncated Tim (Δ22) and full-length Tim possessing the double substitution, Y19E + Y22E, dramatically stimulated the loading of GTP onto RhoA. These data strongly suggest that the increased

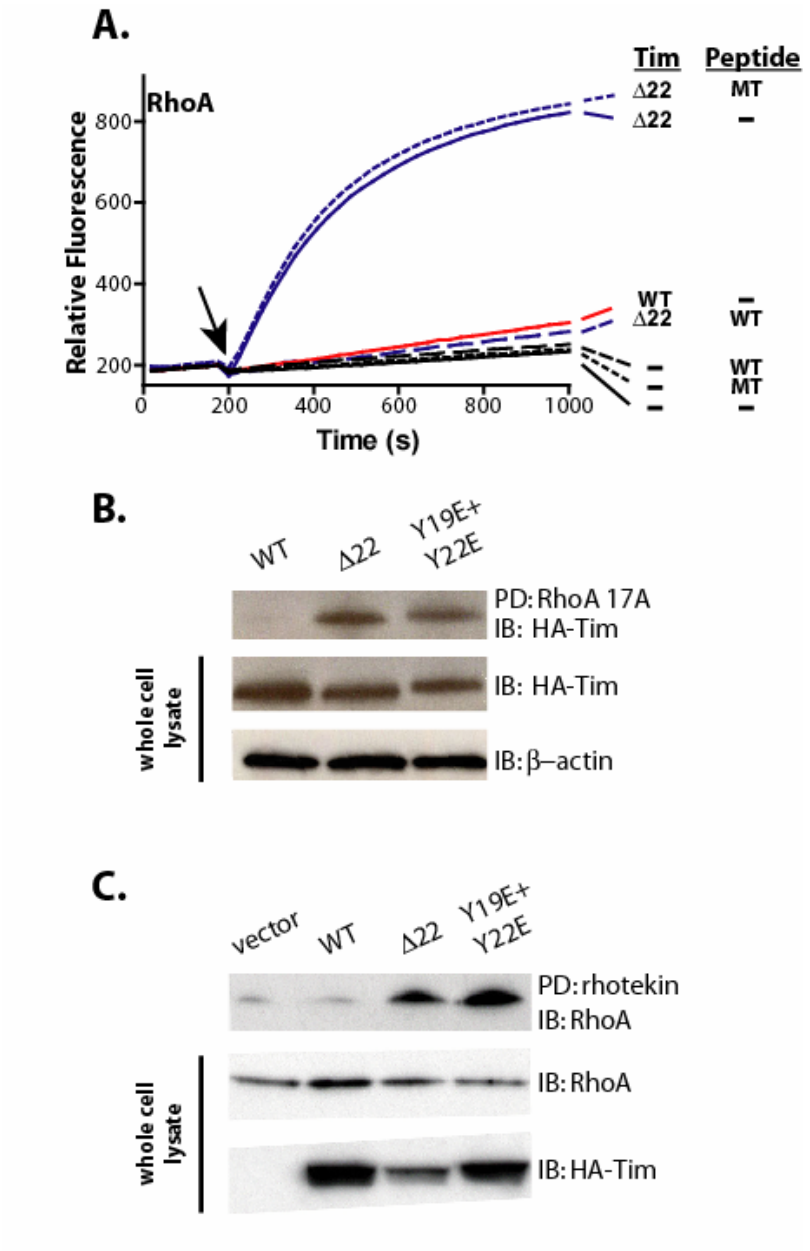

Figure 12: The N-terminal region is necessary and sufficient for Tim auto-inhibition.
(A) Tim (Δ22) was incubated with either a peptide corresponding to the N-terminal auto-inhibitory region (WT, biotin-SQLLYQEYSDV-amide) or a mutant peptide (MT, biotin-SQLLEQEYSDV-amide) at room temperature for 20 minutes. The resulting complexes were assayed for their ability to stimulate loading of mant-GTP onto RhoA. The peptide concentrations were 100 μM. **(B)** The activity of Tim constructs transiently expressed in quiescent HEK 293T cells was assessed by a pulldown assay using GST-tagged nucleotide-free RhoA as the affinity purification matrix. Levels of active Tim were determined by immunoblotting the pulldown samples. Immunoblots of the total cell lysate (2.5% input shown) show approximately equal expression of the Tim constructs. **(C)** The ability of Tim constructs to stimulate GTP-loading on RhoA in HEK 293T cells was assessed by affinity precipitation of active RhoA with rhotekin. Levels of RhoA-GTP were determined by immunoblotting the affinity-precipitated samples and were compared to RhoA pools in the total cell lysate (1% input shown). In the same experiment, HA-tagged Tim variants were checked for approximately equal expression by immunoblotting.

transformation potential of mutant forms of Tim is directly caused by their increased *in vivo* exchange activities.

Regulation of Tim by Tyrosine Phosphorylation:

Based upon primary and secondary amino acid sequence analyses, the auto-inhibitory region within Tim is strongly predicted to be helical (residues 16 – 26; (247)) and tyrosines 19 and 22 within this region are predicted to be excellent substrates for phosphorylation by Src-family non-receptor tyrosine kinases (248). Since the activation of many Dbl-family GEFs is associated with phosphorylation (155), the potential regulation of Tim by phosphorylation was tested both *in vitro* and *in vivo* (Figure 13). First, it was confirmed that indeed, full-length, purified Tim was an excellent substrate for purified Src, with kinetics and extent of phosphorylation resembling control reactions with a standard, control peptide (Figure 13A and data not shown). Furthermore, phosphorylation was confined to the N-terminal region of Tim, since Src was incapable of phosphorylating Tim (Δ22). Residues 19 and 22 are the only tyrosines encompassed within this deletion, and both residues are phosphorylated by Src since substitution at both sites (Y19A + Y22A) is required to prevent the phosphorylation of full-length Tim. Intriguingly, single substitution at either Tyr 19 or 22 enhances phosphorylation at the other tyrosine, indicating that the two sites might be functionally linked. One simple interpretation for these data posits that substitution at either tyrosine significantly disrupts intramolecular interactions associated with auto-inhibition such that the remaining tyrosine is more accessible for phosphorylation by Src.

A logical extension of this scenario is that phosphorylation at tyrosines 19 and 22 might be physiologically relevant for relieving the auto-inhibition of Tim *in vivo*.

Consequently, it was shown that constitutively active (CA) but not kinase dead (KD) Src was capable of phosphorylating Tim *in vivo* upon co-expression in SYF fibroblasts designed to lack endogenous Src-family kinases (Figure 13B). In the same vein, Src robustly activated Tim *in vitro* using purified components (Figure 13C). In this setting, maximal activation required ATP consistent with the idea that phosphorylation of Tim by Src relieves auto-inhibition of Tim to promote activation of RhoA. Taken together, these data strongly suggest that the *in vivo* phosphorylation of Tim within its auto-inhibitory region by Src might be a physiologically relevant means of activating the exchange potential of Tim and linking as yet unidentified upstream cellular events with the activation of RhoA.

Src without ATP also activated Tim (Figure 13C), suggesting that the binding of Src to Tim partially disrupted the auto-inhibition of Tim. However, the possibility exists that Src remained bound to ATP during the purification of the kinase domain, and that additional ATP is not required for this kinase domain to phosphorylate Tim. To test this hypothesis, we incubated Tim with increasing amounts of purified Src kinase domain and performed a phosphotyrosine blot (Figure 14A). Auto-phosphorylation of the kinase domain, and phosphorylation of Tim, only occurred when ATP was included in the reaction, suggesting that the purified Src kinase domain is not bound to ATP. To confirm that Src binding to Tim, in the absence of phosphorylation, activates Tim, we also performed an exchange assay in which Tim was incubated with a kinase inactive (K297A) version of Src (Figure 14B). Kinase inactive Src was also able to activate Tim, indicating that formation of a complex between Src and Tim, decoupled from phosphorylation, is sufficient to partially activate the exchange capacity of Tim. We

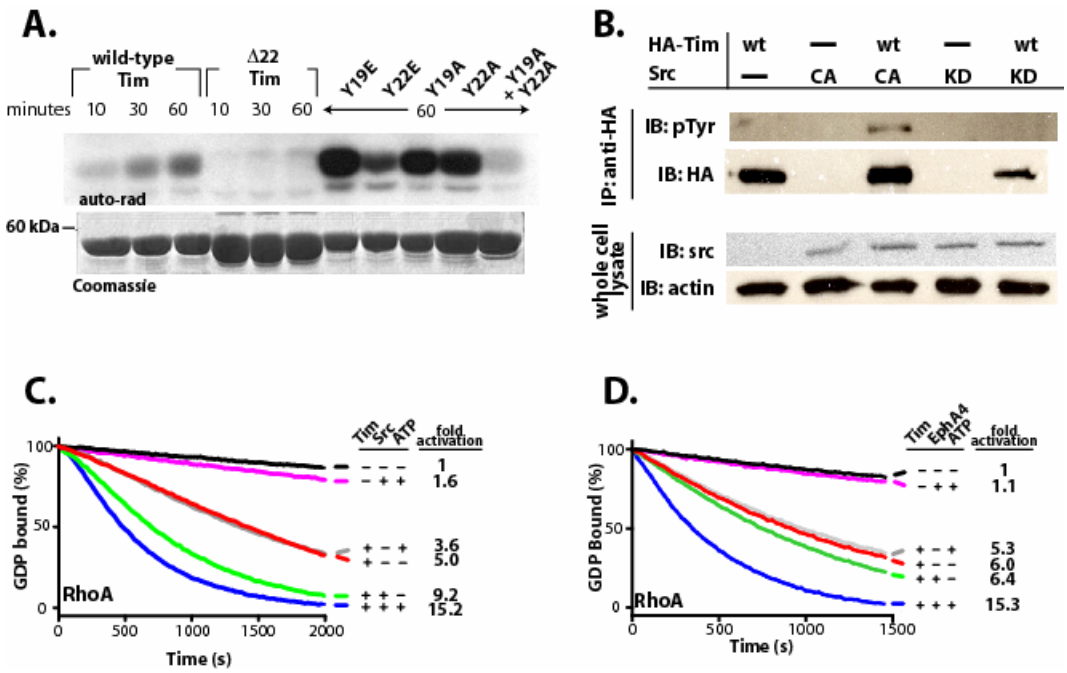

Figure 13: Src phosphorylates Tim and activates its exchange activity.
(A) Src specifically phosphorylates two tyrosines (19 and 22) within the auto-inhibitory helix of Tim. Purified forms of Tim (lower panel) were incubated with recombinant Src and radioactive ATP for various times prior to SDS-PAGE and auto-radiography was used to assess levels of phosphorylation (upper panel). Deletion of the entire inhibitory region (Δ22), or tandem substitution of Tyr 19 and 22 abrogates phosphorylation. **(B)** Src phosphorylates Tim *in vivo*. SYF fibroblasts were transiently cotransfected with HA-Tim and constitutively active (CA) or kinase-dead (KD) Src constructs. HA-Tim was immunoprecipitated from cell lysates, and immunoblotted to determine the extent of phosphorylated Tim. The experiment was performed three times and a representative example is shown. Phosphorylation of Tim by Src **(C)** or EphA4 **(D)** promotes the capacity of Tim to catalyze nucleotide exchange on RhoA. Full-length Tim was incubated with combinations of kinase and ATP as indicated for thirty minutes prior to addition of the mixtures to exchange reactions. Fold-activation is relative to the spontaneous loading of nucleotide onto RhoA (black trace) and represents the average of two independent runs for each condition.

have been unable to isolate a complex of Tim and Src by co-immunoprecipitation experiments from cells over-expressing both of the proteins (data not shown), suggesting that their interaction is transient *in vivo* where endogenous concentrations of ATP favor completion of the phosphorylation reaction.

The Tim homologs, ephexin and Vsm-RhoGEF, interact with and are tyrosine phosphorylated downstream of the EphA4 receptor tyrosine kinase (77,80). To test the hypothesis that Tim is directly phosphorylated by EphA4, we performed *in vitro* kinase assays with recombinant kinase domain of EphA4. Tim was robustly phosphorylated by the kinase domain of EphA4 (data not shown), indicating that Tim is phosphorylated by EphA4 directly. Additionally, EphA4 activated Tim *in vitro* (Figure 13D). In this case, the kinase in the absence of ATP did not activate Tim, suggesting that the interaction between EphA4 and Tim is transient compared to the interaction between Tim and Src. These data suggest that binding of ligand to the EphA4 receptor may lead to the phosphorylation and activation of Tim.

Disrupting auto-inhibition by mutating the DH domain:

The above experiments have shown that Tim is auto-inhibited by a small, conserved region with high helical propensity and that this auto-inhibition can be relieved by truncation, mutation, or phosphorylation of the auto-inhibitory region. This situation is reminiscent of regulation of the Vav isozymes whereby a short helix immediately preceding the DH domain lies down on the most conserved surface of the DH domain to prevent Rho GTPases from engaging this same surface for effective nucleotide exchange (154). Phosphorylation of the inhibitory helix in the Vav isozymes by Src and related non-receptor tyrosine kinases stimulates exchange *in vitro* and *in vivo* (249-253) and is

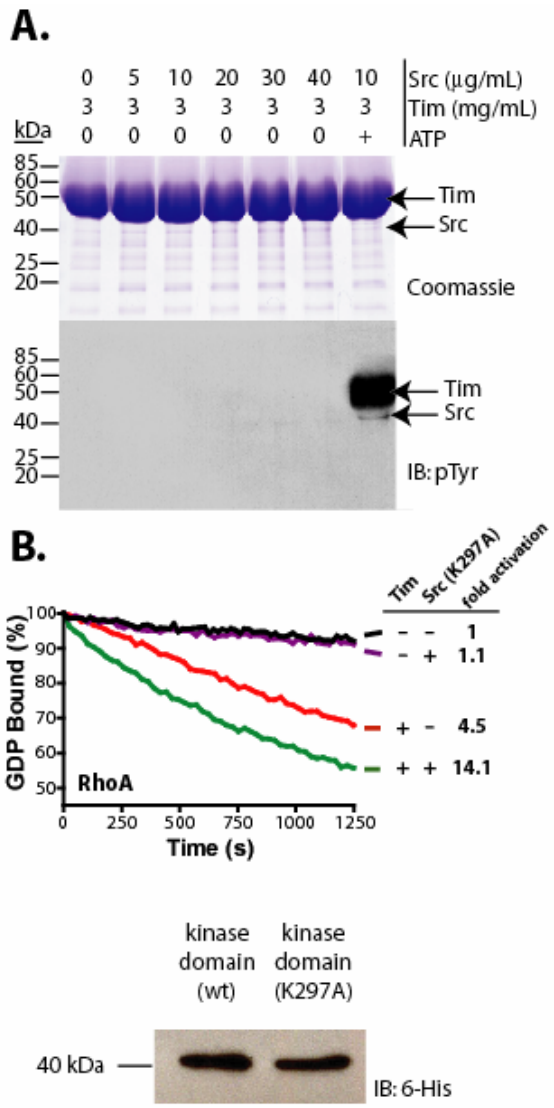

Figure 14: The Src kinase domain activates Tim in the absence of phosphorylation.
(A) ATP is required for the phosphorylation of Tim by recombinant Src produced in baculovirus-infected HighFive cells. Various combinations of Tim and Src were incubated for 30 minutes at 37 ºC prior to SDS-PAGE and immunoblot analysis. **(B)** Kinase-inactive Src activates Tim. Full-length Tim was incubated with combinations of kinase-inactive Src as indicated for thirty minutes prior to addition of the mixtures to exchange reactions. Fold-activation is relative to the spontaneous loading of nucleotide onto RhoA (black trace) and represents the average of two independent runs for each condition. Equal amounts of the purified Src proteins are shown in the lower panel following immunoblot analysis.

required for some physiological functions of Vav (254). If a similar mechanism is operative for Tim, then it might be possible to mutate specific residues within the DH domain to disrupt interactions with the auto-inhibitory helix without affecting GTPase binding, and in this way constitutively activate Tim. Such residues within the DH domain would be expected to be conserved, equivalent to sites that contact the auto-inhibitory helix of Vav1, and yet not critical for the interaction of the DH domain with GTPases. Appropriate analyses of the available sequence and structure data (Figure 15A and references within) identified several sites that fit these criteria, and Tim was mutated with individual substitutions (Y111L and S114A) to test this hypothesis. Tim (Y111L) was destabilized, insoluble and inactive *in vitro* (data not shown). In contrast, Tim (S114A) is stable, soluble, and able to activate RhoA *in vitro* (Figure 15B) approximately four-fold more efficiently than wild-type Tim. Importantly, under identical conditions, S114A is relatively silent within the context of Tim lacking the auto-inhibitory helix (Δ22), indicating that the intrinsic exchange mechanism of Tim is unaffected by S114A. The ability of this mutant (Δ22 + S114A) to catalyze exchange, however, is inhibited by addition of 100 μM of the peptide corresponding to the N-terminal putative helical motif (residues 15-25) of Tim used in Figure 12A (data not shown). This result indicates that the S114A substitution does not completely abolish the interaction between the N-terminal auto-inhibitory motif of Tim and the DH domain pocket and is consistent with the partial relief of inhibition of exchange caused by the S114A substitution within the context of full-length Tim (Figure 15A).

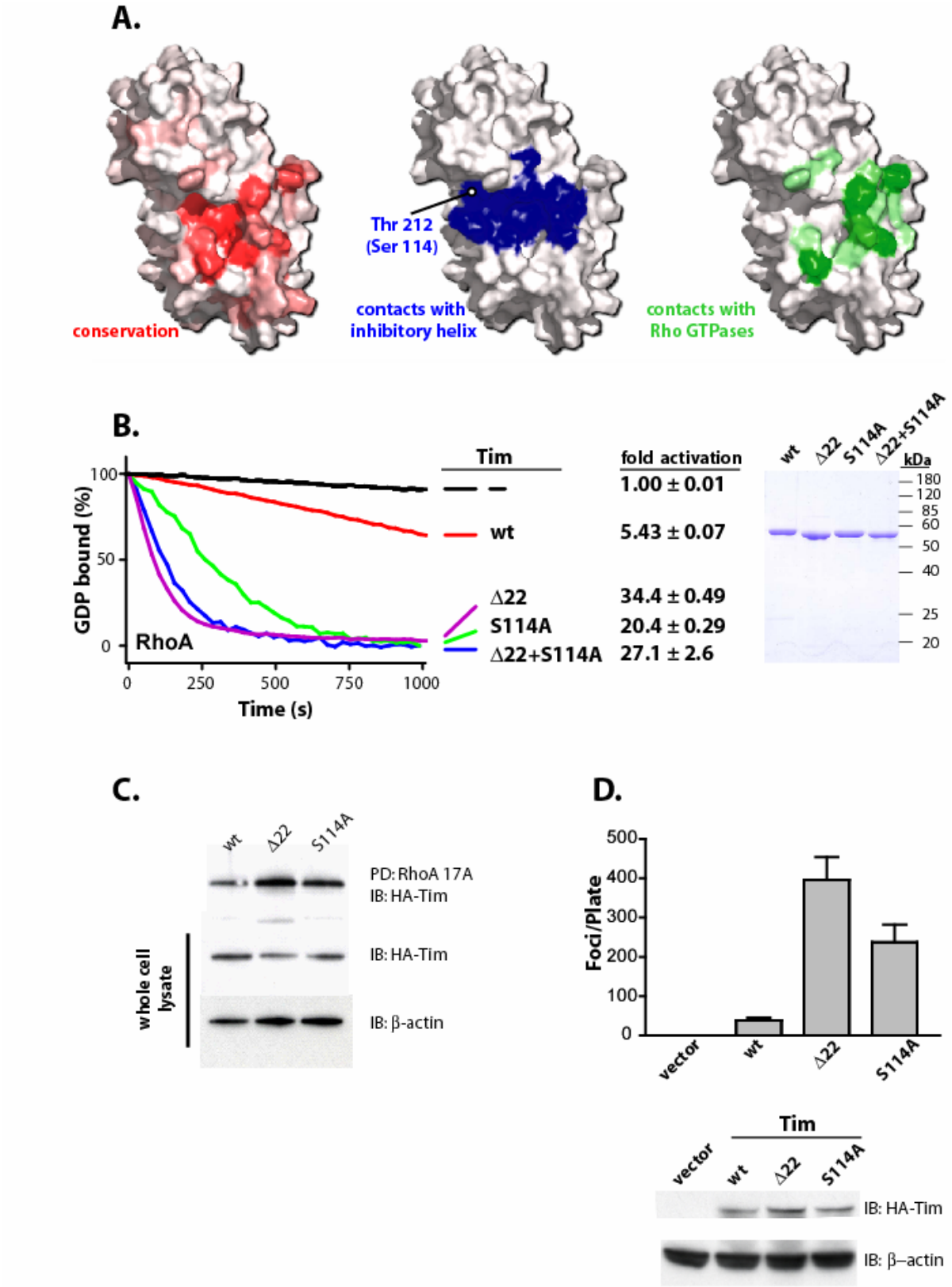
A.
conservation
Thr 212
(Ser 114)
contacts with
inhibitory helix
contacts with
Rho GTPases
B.
GDP bound (%)
100
50
0
RhoA
0
250
500
750
1000
Time (s)
Tim
fold activation
wt
1.00 ± 0.01
wt
5.43 ± 0.07
Δ22
34.4 ± 0.49
S114A
20.4 ± 0.29
Δ22+S114A
27.1 ± 2.6
wt
Δ22
S114A
Δ22+S114A
kDa
180
120
85
60
50
40
25
20
C.
wt
Δ22
S114A
PD: RhoA 17A
IB: HA-Tim
IB: HA-Tim
IB: β-actin
whole cell
lysate
D.
Foci/Plate
500
400
300
200
100
0
vector
wt
Δ22
S114A
Tim
vector
wt
Δ22
S114A
IB: HA-Tim
IB: β–actin

Figure 15: Mutations within the DH domain designed to disrupt the interaction with the auto-inhibitory helix lead to auto-activation.
(A) Surface representations of the Vav1 DH domain (PDB accession 1F5X, murine Vav1 residues 198-372) that illustrate (left) the positions of highly conserved residues among DH domains from 70 human Dbl-family sequences as determined by ClustalX (bright red is most conserved); (center) the sites of contact (≤ 5 Å; blue) between the Vav1 DH domain and the Vav1 auto-inhibitory helix (residues 170-179); and (right) the sites and degree of conservation of interactions observed within the structures of Tiam1•Rac1, Intersectin•Cdc42, Dbs•RhoA and Larg•RhoA that occur between Rho GTPases and DH domains (≤ 3.5 Å between residues, bright green is fully conserved) mapped onto the surface of the DH domain of Vav1. Surface representations were produced using the programs ProtSkin (255) and PyMOL (256) and reveal a region of high sequence conservation in a pocket that contacts the auto-inhibitory helix but does not contact Rho GTPases. Thr 212 of Vav1 is indicated and the equivalent residue (Ser 114) in Tim has been mutated to disrupt auto-inhibition as shown below. **(B)** Relative to the spontaneous loading of guanine nucleotide onto RhoA (- , black trace) auto-inhibition of full-length Tim (wt, red trace) is relieved by mutation within its DH domain (S114A, green trace) while the exchange activity of truncated, constitutively active Tim (Δ22, magenta trace) is relatively unaffected by the equivalent mutation (Δ22 + S114A, blue trace). The traces corresponding to spontaneous loading, full-length Tim and Tim (Δ22) are reproduced from Figure 10 for reference. Proteins used in the exchange assays are shown at right. **(C)** The S114A mutation increases the ability of Tim transiently expressed in quiescent HEK 293T cells to associate with nucleotide-free RhoA. The activity level of Tim constructs was assessed as described in Figure 12. Levels of active Tim were determined by immunoblotting the pulldown samples. Immunoblots of the total cell lysate (2.5% input shown) show approximately equal expression of the Tim constructs. **(D)** Mutation in the DH domain (S114A) increases the ability of Tim to induce foci when expressed in NIH 3T3 cells. Data represent the averages of three independent experiments carried out in duplicate. The lower panel shows approximately equal expression of the Tim constructs.

Consistent with the *in vitro* exchange data, though, Tim (S114A) behaved similarly to truncated Tim (Δ22) in its ability to interact with nucleotide free RhoA (Figure 15C) and its ability to induce formation of foci (Figure 15D). Consequently, it is possible to decouple the auto-inhibitory and exchange functions of Tim through mutation of its DH domain.

Discussion:

Figure 16 presents a model for the relief of auto-inhibition of Tim. In this model, an auto-inhibitory helix packs against the conserved pocket of the DH domain in the basal, inactive state to prevent Rho GTPases from accessing the surface of the DH domain necessary for guanine nucleotide exchange. Activation of Src leads to phosphorylation of the auto-inhibitory helix, which disrupts the interactions between the auto-inhibitory helix and the DH domain, thereby freeing the DH domain to interact with cognate GTPases and activate them by nucleotide exchange. If the auto-inhibitory helix is truncated, or otherwise mutated such that it can no longer bind to the DH domain, Tim will be constitutively activated. Likewise, if residues within the conserved binding patch of the DH domain are mutated such that it is no longer able to bind the auto-inhibitory helix, Tim will be constitutively activated.

Tim clusters with five other human Dbl-family proteins: neuroblastoma, Sgef, Wgef, Ngef, and Vsm-RhoGEF, based on high sequence identity among DH domains and overall domain architecture that includes an SH3 domain carboxyl-terminal to the canonical DH/PH module. While not readily evident using standard sequence alignment algorithms such as PSI-BLAST, all members of this sub-group possess a putative auto-inhibitory region N-terminal to the DH domain with high sequence identity to the short

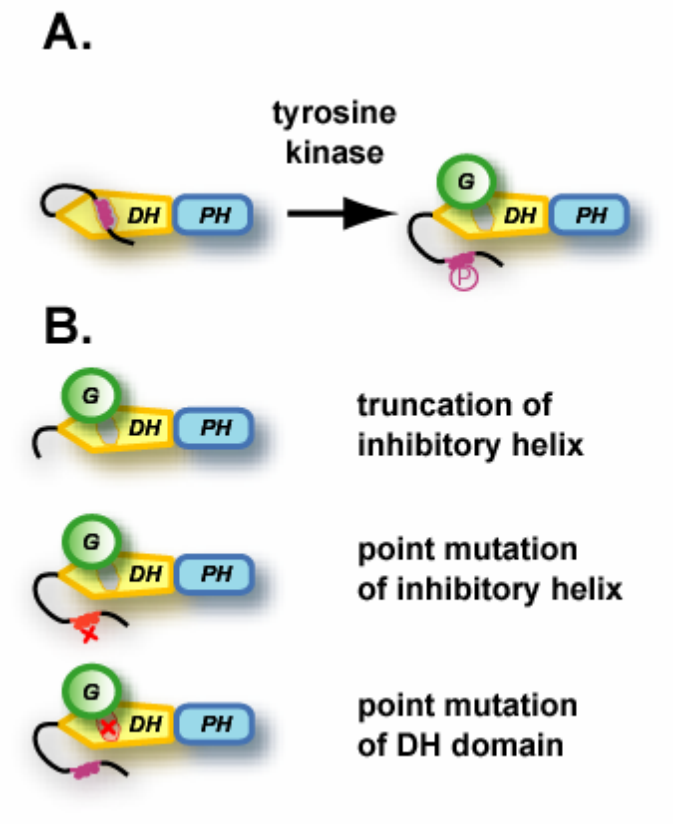

Figure 16: Model of Tim auto-inhibition.
(A) Regulation of Tim exchange activity by sequences N-terminal to the DH domain. The auto-inhibitory helix packs against the conserved pocket of the DH domain, preventing the binding and consequent activation of the cognate Rho GTPase. Tyrosine phosphorylation leads to the removal of the auto-inhibitory helix from the DH domain. Tim can now bind Rho to catalyze the exchange of guanine nucleotide. **(B)** Mechanisms of constitutive activation of Tim proteins. The auto-inhibitory helix is truncated, or otherwise mutated such that it can no longer bind to the DH domain. Alternatively, residues within the conserved binding patch of the DH domain are mutated such that it is no longer able to bind the auto-inhibitory helix, leading to a constitutively active GEF. In each of these scenarios, the end result is loss of auto-inhibition leading to constitutive activation of Tim.

auto-inhibitory region mapped in Tim (data not shown). Consequently, it is likely that other members of this subgroup are regulated in a manner similar to Tim. In fact, the mouse homolog of Ngef, ephexin, is tyrosine phosphorylated in an N-terminal motif with significant sequence identity to the auto-inhibitory helix within the Tim subgroup of Dbl proteins. However, phosphorylation of ephexin alters its exchange profile. Specifically, unphosphorylated ephexin activates RhoA, Rac1 and Cdc42; but when tyrosine phosphorylated, ephexin exclusively activates RhoA (78). The mechanism by which this specificity switch occurs is currently unknown and not encompassed within the model presented here for the activation of Tim.

The mechanism of auto-inhibition of Tim presented above is reminiscent of the mechanism of auto-inhibition of the Vav isozymes. In fact, the auto-inhibitory helix of Tim shows high sequence homology to the auto-inhibitory helix of Vav1 (data not shown). The structure of an extended fragment of the DH domain of Vav1 highlights the steric occlusion of the DH domain through interaction with an N-terminal helix to prevent GTPase binding and guanine nucleotide exchange (154). This inhibition is relieved upon phosphorylation of Tyr 174 within the inhibitory helix, which disrupts the interaction of the inhibitory helix with the DH domain and allows Rho GTPases to access the catalytic surface of the DH domain for effective guanine nucleotide exchange. While this regulatory mechanism is operative *in vivo* for the three Vav isozymes, complete regulation of Vav isozymes is more complex. For example, Vav1 is additionally phosphorylated at Tyr 142 and 160 within a highly acidic region, and substitution of all three tyrosines to phenylalanine greatly enhances the transformation potential of full-length Vav1 relative to any single substitution. However, a mutant of Vav1 truncated to

remove its N-terminal calponin homology (CH) domain, but not the phosphorylated tyrosines, is also transforming, suggesting that the CH domain stabilizes interactions of the auto-inhibitory helix with the DH domain within the context of full-length Vav1 (8). In addition, the CH domain contributes to the auto-inhibition of Vav proteins by interacting with a cysteine-rich domain C-terminal to the DH/PH cassette (45,157). Furthermore, Vav proteins may also be regulated allosterically through the binding of phospholipids to the PH domain, although this concept remains controversial (156,170). Thus, the regulated activation of the Vav isozymes is more complex than what we have shown above for Tim since the activation of the Vav isozymes cannot be attributed solely to the phosphorylation of tyrosine residues N-terminal to the DH domain.

The human genome encodes 58 receptor tyrosine kinases (RTKs), and more than half of the RTKs are known to activate at least one of the Rho family members. At least 16 of the 69 human Dbl-family proteins are known to interact with and/or be phosphorylated by RTKs, thus serving as a link between ligation of RTKs and Rho activation (155). For instance, FRG, a Dbl-family protein specific for Cdc42, is activated upon phosphorylation by Src downstream of signals arising from both the endothelin A receptor (46) and nectins (47). Similarly, the exchange activity of Dbs for Cdc42 is enhanced upon the phosphorylation of Dbs by Src downstream of the α1B adrenergic receptor (143). Activated TrkB directly binds to and activates Tiam1 (150), which is also known to be phosphorylated and activated by Src (149). In each case mentioned above, the mechanisms by which phosphorylation increases exchange activity have yet to be determined. Clearly, one fruitful avenue of research will be to assess mechanistically

how these phosphorylations enhance exchange; one likely mechanism is that phosphorylation perturbs auto-inhibition as described here.

The Rho GTPases have long been thought to play a role in tumorigenesis. However, in contrast to Ras GTPases, animal studies and studies of human tumors have yet to further our understanding of the role of Rho GTPases in promoting tumorigenesis. In fact, constitutively active, GTPase-deficient mutants of Rho GTPases have yet to be found in human tumors. However, several Rho GTPases, including RhoA, RhoC and Rac1, are over-expressed in human tumors, leading to the hypothesis that Rho GTPases, unlike Ras GTPases, must undergo cycling of GTP loading to be oncogenic (3,257). Consistent with this idea, Dbl-family Rho GEFs are more potent oncogenes than their substrate GTPases. Although many Dbl-family proteins, including Tim, were identified as proto-oncogenes in expression library screens using DNA or RNA derived from human cancer cells, these activation events have proven to be experimental artifacts. Of the 69 human Dbl-family proteins, only Tiam1 has been shown to be mutated in human tumors (5), although Vav1 is ectopically expressed in some primary pancreatic adenocarcinomas (153) and neuroblastomas (258). The mutations characterized in this study, both in the auto-inhibitory helix and in the DH domain, represent potential mechanisms by which Tim and other Dbl-family proteins might be activated in human tumors. Identification of such mutations in human tumors would further define the role of Rho GTPases in tumorigenesis.

If versions of Tim mutated in either the auto-inhibitory helix or in the region of the DH domain thought to interact with the auto-inhibitory helix should be isolated from human tumors, then Tim would represent an attractive target for rational drug design.

The peptide inhibitor shown in Figure 11A could serve as the basis for design of peptidomimetic inhibitors of aberrant Tim activation of Rho. Several inhibitors of small GTPase activation have been previously identified. TRIPα was isolated as a random peptide aptamer that selectively binds to the second DHPH cassette of the RhoGEF Trio and inhibits the exchange activity of Trio *in vitro* and in PC12 cells through an unknown mechanism (259). Additionally, the small molecule NCS23766 was identified in structure-based virtual screen for compounds that might fit into a pocket on the surface of Rac1. Residues in this pocket contact Tiam1 during the exchange reaction. This compound selectively inhibits Rac1 binding to Rac1-specific GEFs *in vitro* and prevents PDGF induced Rac activation in cells (260,261). Finally, brefeldin A inhibits the activation of the small GTPase Arf1 by its exchange factors by binding to and stabilizing a complex of Arf1-GDP and the catalytic Sec7 domain (262). The Tim peptide, then, is a unique GEF inhibitor in that its mechanism of action is identical to that of the auto-inhibitory helix of the wild-type protein.

In summary, we have shown that the Dbl-family protein, Tim, is a RhoA, RhoB and RhoC-specific GEF that is auto-inhibited by a putative helix N-terminal to the DH domain, which directly binds the DH domain to sterically exclude Rho GTPases and prevent their activation. This auto-inhibition is relieved by truncation, mutation, or phosphorylation of the auto-inhibitory helix, or by mutation of the conserved surface of the DH domain to disrupt interactions with the auto-inhibitory helix. Since inhibition of Tim can be restored by addition of the auto-inhibitory helix in *trans*, the auto-inhibitory helix is necessary and sufficient for maintenance of a basal state of Tim activation.

CHAPTER 3: REGULATION OF NEURONAL-SPECIFIC GEF BY AUTO-INHIBITION AND PHOSPHORYLATION

Introduction:

In the development of the nervous system, Rho GTPases integrate extracellular signals to direct outgrowth of both axons and dendrites; and the formation and dynamics of dendritic spines. Active RhoA leads to a decrease in growth cone motility, a decrease in neurite elongation, and an increase in actomyosin-dependent contraction of the developing neuron. Active Rac1, in contrast, leads to an increase in lamellae formation, and an increase in the initiation, elongation, branching complexity and dynamics of dendrites. Like Rac1, active Cdc42 leads to an increase in dendritic branch formation, as well as an increase in filopodia and neurite formation. In addition, conditional *in vivo* deletion of Cdc42 has revealed that this GTPase is required for establishment of apical-basal polarity and maintenance of ventricular zone neuronal progenitor cells (263,264). Deletion or mutation of crucial components of the Rho signaling pathway, then, renders neurons less responsive to environmental cues, leading to compromised neuronal connectivity and plasticity (4).

Many Dbl-family proteins, which activate Rho GTPases by catalyzing the exchange of GDP for GTP, are associated with neurological disorders. Fgd1 was originally identified as a gene that is deleted in patients with faciogenital dysplasia, a developmental disorder characterized by skeletal defects as well as mental retardation

(12). In addition, a truncation mutation of αPix/COOL2 has been identified in forms of X-linked mental retardation (162), while intersectin is associated with certain forms of Downs syndrome (265). Finally, a loss of function of Alsin is associated with juvenile onset amyotrophic lateral sclerosis (ALS) (266).

Other Dbl-family proteins are known to play a role in neuronal development, although a link between these GEFs and a neurological disorder has yet to be discovered. For example, Kalirin has been shown to affect neurite outgrowth, and neuronal and dendritic spine morphogenesis (145). In addition, P-rex was shown to be involved in neurotrophin-derived signaling and neuronal migration (208). FRG (also known as FARP2 or FIR) is expressed in the ventricular zone during mouse brain development and may play a role in neurogenesis, asymmetric cell division, neuronal migration and neurite remodeling (267). Plexin A1 binds to the N-terminal FERM domain of FRG, and activation of plexin A1 by its ligand, semaphorin 3A leads to an increase in the exchange activity of FRG and subsequent growth cone collapse (268). Finally, Tiam1 binding to the polarity protein, Par3, spatially restricts this Dbl-family GEF to dendritic spines. This restricted localization is required for dendritic spine morphogenesis (87).

Although many Dbl-family proteins are known to be involved in many different facets of neuronal development, the mechanisms by which these proteins are regulated in this context are largely unknown. We have recently shown that Tim, a small Dbl-family protein, is also auto-inhibited by a putative helix N-terminal to the DH domain, which directly binds the DH domain to sterically exclude Rho GTPases and prevent their activation. This auto-inhibition is relieved by truncation or mutation of the auto-inhibitory helix, or by a mutation in the conserved surface of the DH domain that disrupts

interactions with the auto-inhibitory helix. Src and EphA4 phosphorylate Tim on two tyrosines in the auto-inhibitory helix, Tyr 19 and Tyr 22, which activates the exchange potential of Tim. Finally, a peptide comprising the auto-inhibitory helix is able to inhibit a truncated version of Tim in *trans* (269).

Tim consists of an SH3 domain C-terminal to the DH and PH domains and this domain architecture is shared with a small group of Dbl-family members including: Wgef, Sgef, Vsm-RhoGEF, neuroblastoma and Ngef. In contrast to Vav and other Dbl-family members, relatively little is known about the physiological importance and molecular regulation of this sub-group. For example, Ngef is expressed primarily in the brain, is localized to chromosomal region 2q37, and is transforming in cell culture (36,76). The mouse ortholog of Ngef, ephexin, is expressed in the central nervous system during development and was originally cloned based upon its ability to interact with the EphA4 receptor tyrosine kinase. Ephexin activates RhoA, Rac1 and Cdc42 in cell-based assays; mediates ephrinA-induced growth cone collapse (77); and is phosphorylated by Src family kinases downstream of EphA4 receptor activation (76). When ephexin is not tyrosine phosphorylated, it activates RhoA, Rac1 and Cdc42; but when ephexin is tyrosine phosphorylated; it activates RhoA exclusively (78). Most recently, ephexin has been shown to be phosphorylated in its N-terminus by Cdk5 downstream of EphA4 receptor activation (79). The precise mechanism by which ephexin undergoes its specificity switch and the mechanisms by which Cdk5 and Src coordinate to modulate ephexin activity are poorly understood.

Here we show that Ngef is also regulated by phosphorylation of the auto-inhibitory helix. Truncation, mutation or phosphorylation of the auto-inhibitory helix

activates the exchange potential of Ngef toward RhoA, Rac1 and Cdc42 *in vitro* and *in vivo*. However, in contrast to Tim, Ngef is phosphorylated by Src on only one of the tyrosines in the auto-inhibitory helix, and Ngef is not phosphorylated by EphA4. Additionally, a subset of cortical progenitor cells expressing a phosphomimetic mutant of Ngef are able to differentiate into neurons but do not extend neurites. This phenotype is effectively reversed by inhibition of the Rho effector, p160-Rho kinase. These results extend our knowledge of the regulation of Dbl-family proteins as a whole, and Ngef in particular.

Materials and Methods:

Protein Expression and Purification:

Full-length and truncated versions of human Ngef were PCR-amplified and ligated into pET-21a (Novagen) between *NdeI* and *XhoI* in frame with a C-terminal, non-cleavable hexahistidine tag. The cDNA for Ngef was obtained as I.M.A.G.E. clones (ATCC) (Accession number: Q8N5V2).

Ngef constructs were expressed in the *E. coli* strain BL21 (DE3) (Novagen). Cell cultures were grown at 37ºC in LB/ampicillin (100 μg/mL), and induced with 1 mM isopropyl-β-D-thiogalactopyranoside (IPTG) for 5 h at 27ºC. Cell pellets were resuspended in 20 mM Tris, pH 8, 300 mM NaCl, 10% glycerol (buffer A) with 10 mM imidazole, lysed using an Emulsiflex C5 cell homogenizer (Avestin), and clarified by centrifugation at 40,000 *g* for 45 min at 4ºC. Clarified supernatants were loaded on a nickel-charged metal chelating column (Pharmacia) equilibrated with buffer A containing 10 mM imidazole, washed with buffer A containing 50 mM imidazole and eluted with buffer B containing 400 mM imidazole. Eluted proteins were subsequently loaded onto

an S-200 size exclusion column equilibrated with 20 mM Tris pH 7.5, 150 mM NaCl, 2 mM DTT, 1 mM EDTA and 5 % glycerol. Fractions containing monomeric Ngef were pooled, concentrated and stored at -80ºC. Mutations were introduced into wild-type Ngef using the Quikchange site-directed mutagenesis kit (Stratagene) as per the manufacturer's instructions, and these mutant proteins were expressed and purified as described above. DNA sequences of all expression constructs were verified by automated sequencing. RhoA, Cdc42 and Rac1 were purified as described (94,225,245). The kinase domains of Src and EphA4 were also purified as described (269).

Guanine Nucleotide Exchange Assays:

Fluorescence spectroscopic analysis of N-methylanthraniloyl (mant)-GTP incorporation into RhoA was carried out as described (246). In brief, assay mixtures containing 20 mM Tris pH 7.5, 150 mM NaCl, 5 mM $MgCl_2$, 1 mM DTT and 100 μM mant-GTP (Molecular Probes) and 2 μM RhoA were allowed to equilibrate with continuous stirring. After equilibration, 400 nM Ngef was added and nucleotide loading was monitored as the decrease in the tryptophan fluorescence (λ_{ex} = 295 nm, λ_{em} = 335 nm) of RhoA as a function of time using a Perkin-Elmer LS 55 spectrophotometer. Rates of guanine nucleotide exchange were determined by fitting the data to a single exponential decay model with GraphPad Prizm. Data were normalized to yield percent GDP released and assays were performed in duplicate.

Fluorescence spectroscopic analyses of mant-GTP release from Cdc42 and Rac1 were also carried out as described (246). In brief, assay mixtures containing 20 mM Tris pH 7.5, 150 mM NaCl, 5 mM $MgCl_2$, 1 mM DTT, 20 μM GTP and 250 nM Rac1 or Cdc42 preloaded with mant-GTP were allowed to equilibrate with continuous stirring.

After equilibration, 400 nM Ngef was added and mant-GDP release was monitored as the decrease in mant-GTP fluorescence (λ_{ex} = 360 nm, λ_{em} = 440 nm) as a function of time. Rates of guanine nucleotide exchange were determined as described above.

Cell Culture and Mammalian Expression Constructs:

NIH 3T3 mouse fibroblasts were maintained in DMEM supplemented with penicillin/streptomycin and 10% calf serum (Hyclone). COS-7 cells were maintained in DMEM supplemented with penicillin/streptomycin and 10% fetal bovine serum (Sigma). PCR-amplified Ngef constructs were ligated into pcDNA 3.1 Hygro (Invitrogen) between *EcoRI* and *XhoI* such that an expressed HA-tag was encoded at the N-terminus of each construct. In addition, PCR-amplified HA-tagged Ngef constructs were also ligated into the pCIG vector (270), which contains (cDNA) – IRES – eGFP under the control of a CMV promoter and a chicken β-actin promoter, between *EcoRI* and *XhoI*. Mutations were introduced into wild type Ngef as described above.

Transformation Assays:

Cell lines stably expressing Ngef were established by transfecting NIH 3T3 cells with 1 μg of each pcDNA construct using LipofectAMINE Plus (Invitrogen) according to the manufacturer's protocol. Three days post-transfection the cells were subcultured into growth medium supplemented with 300 μg/mL of hygromycin B. Mass populations of multiple, drug resistant colonies (>50) were pooled together for focus formation analyses. Western blot analysis with an anti-HA antibody (Covance) was performed to verify Ngef expression in the cell lines. The secondary focus formation assay was performed essentially as described (269).

GTPase Activation Assays:

Affinity purifications of Rho A, Rac1 and Cdc42 were carried out as described (66,271). In brief, the Rho binding domains (RBD) of Pak (amino acids 70-132) and Rhotekin (amino acids 7-89) were expressed as a GST fusion proteins in BL21 (DE3) cells and immobilized on glutathione-coupled Sepharose 4B beads (Amersham Biosciences). COS-7 cells were transiently transfected in 100 mm dishes with 12 μg of various pCIG-Ngef constructs using LipofectAMINE 2000 (Invitrogen) according to the manufacturer's protocol. Immediately post-transfection, these cells were serum starved in DMEM supplemented with 0.1% FBS and incubated for 16 hours. Cells were washed in ice cold PBS and lysed in lysis buffer (50 mM Tris pH 7.5, 150 mM NaCl, 30 mM $MgCl_2$, 1.0% Triton X-100 and protease inhibitors). Lysates were clarified by centrifugation at 16,000 rpm for 10 min. Total protein concentration of the lysates was determined by a colorimetric assay (Bio-Rad). 1 mg of clarified COS-7 lysate was incubated with 120 μg GST-Pak-RBD beads for 1 hour at 4°C. The beads were washed three times in lysis buffer. Total and affinity-purified lysates were subjected to SDS-PAGE and Western blot analysis using anti-Cdc42 (Transduction Laboratories) monoclonal antibodies. Each experiment was performed two or three times.

Activated GEF assays:

The activated GEF assays were performed essentially as described (102). In brief, nucleotide-free mutants of RhoA (G17A), Rac1 (G15A) and Cdc42 (G15A) were expressed as GST-fusion proteins in BL21 (DE3) cells and immobilized on glutathione-coupled Sepharose 4B beads (Amersham Biosciences). COS-7 cells were transiently transfected in 100 mm dishes with 12 μg of various pCIG-Ngef constructs using

LipofectAMINE 2000 (Invitrogen) according to the manufacturer's protocol. Immediately post-transfection, these cells were serum starved in DMEM supplemented with 0.1% FBS and incubated for 16 hours. Cells were washed in ice cold PBS and lysed in lysis buffer (20 mM Hepes pH 7.5, 150 mM NaCl, 2 mM $MgCl_2$, 1.0% Triton X-100 and protease inhibitors). Lysates were clarified by centrifugation at 16,000 rpm for 10 min. Total protein concentration of the lysates was determined by a colorimetric assay (Bio-Rad). 0.5 mg of clarified COS-7 lysate was incubated with 120 μg GST-GTPase beads for 1 hour at 4°C. The beads were washed three times in lysis buffer. Total and affinity-purified lysates were subjected to SDS-PAGE and Western blot analysis using anti-HA (Covance) monoclonal antibodies. Each experiment was performed two or three times.

In vitro kinase assay:

30 μg of purified Ngef protein was incubated with 250 ng of recombinant Src or EphA4 kinase domain in kinase buffer (100 mM Tris, pH 7.5, 125 mM $MgCl_2$) supplemented with 100 μM ATP 30 min at 37°C. Samples were subjected to SDS-PAGE and Western blot analysis using anti-phosphotyrosine monoclonal antibodies (BD Transduction laboratories).

Animals:

Mice (BalbC) were used according to a protocol approved by the Institutional Animal Care and Use Committee at the University of North Carolina at Chapel Hill and in accordance with guidelines put forth by the National Institutes of Health. Time-

pregnant females were maintained by overnight breeding with males of the same strain, and noon following breeding was considered to be the E0.5 time-point.

Dissociated Cortical Cultures:

Electroporation of dorsal telencephalic progenitors was performed essentially as described (270). In brief, various pCIG2 constructs were injected into the lateral ventricles of isolated E15.5 embryonic mouse heads using a Picospritzer III (General Valve) microinjector. The whole head was electroporated using an EXM 830 electroporator and gold-coated electrodes (BTX). After removal of the skin, skull, pia, thalamus, hippocampus and basal ganglia, the resulting cortices were dissociated using a papain-based method as previously described (272). 5×10^4 of these cells were plated onto glass coverslips coated with poly-L-lysine and laminin, and the cultures were maintained in serum free media (neurobasal media with B27, N2, L-glutamine and penicillin/streptomycin supplements) for 4 days prior to being fixed in 4% paraformaldehyde.

Confocal Microscopy:

Cultured cortical progenitor cells were immunostained as previously described. The primary antibodies used include: mouse anti-Tuj1 (βIII tubulin) (Sigma), mouse anti-HA (Covance) and mouse anti-nestin (BD Biosciences). Direct fluorescence (GFP, Alexa-546 conjugated phalloidin, Molecular Probes) and indirect fluorescent immunostaining (Alexa-546 conjugated secondary antibodies, Molecular Probes)was observed using a LEICA TCS-SL laser scanning confocal microscope mounted on a DM-IRE2 inverted microscope stand and equipped with an argon laser (488 nm), green helium-neon laser (546 nm), red helium-neon laser line (633 nm) and X-Y motorized

Märzhäuser stage. For quantification of axonal length, the tile scan function was used to assemble multiple 20X fields. Axon length was then measured using ImageJ (rsb.info.nih.gov). In the time-lapse studies, dissociated cortical progenitor cells were imaged at a frequency of one picture every five minutes for 40 minutes before and an hour and 40 minutes after the addition of 20 μM Y-27632 (Calbiochem).

Results:

The exchange activity of Ngef toward its cognate GTPases is regulated by auto-inhibition and tyrosine phosphorylation.

We have previously shown that the Dbl-family protein, Tim, is auto-inhibited by a short, putative helix N-terminal to its DH domain. Tim shares domain architecture and high sequence identity with five other human Dbl-family proteins: neuroblastoma, Sgef, Wgef, and Vsm-RhoGEF and Ngef. All members of this sub-group possess a putative auto-inhibitory region N-terminal to the DH domain with high sequence identity to the short auto-inhibitory region mapped in Tim (Figure 17A). Consequently, it is likely that other members of this subgroup are regulated in a manner similar to Tim, and this hypothesis was tested for Ngef.

The mouse homolog of Ngef, ephexin, has been shown to activate RhoA, Rac1 and Cdc42 in cell-based activity assays (77), and similarly, Ngef activated these GTPases *in vitro* (Figure 17B). However, this activation required deletion of the putative auto-inhibitory helix, since a construct lacking this helix showed robust activity (Δ185), while the shorter N-terminally truncated form of Ngef (Δ166) and the full-length version (wt) were essentially inert in RhoA, Rac1, and Cdc42 exchange assays. Furthermore, substitution of Tyr 179 to Glu (Y179E) within the putative auto-inhibitory helix activated

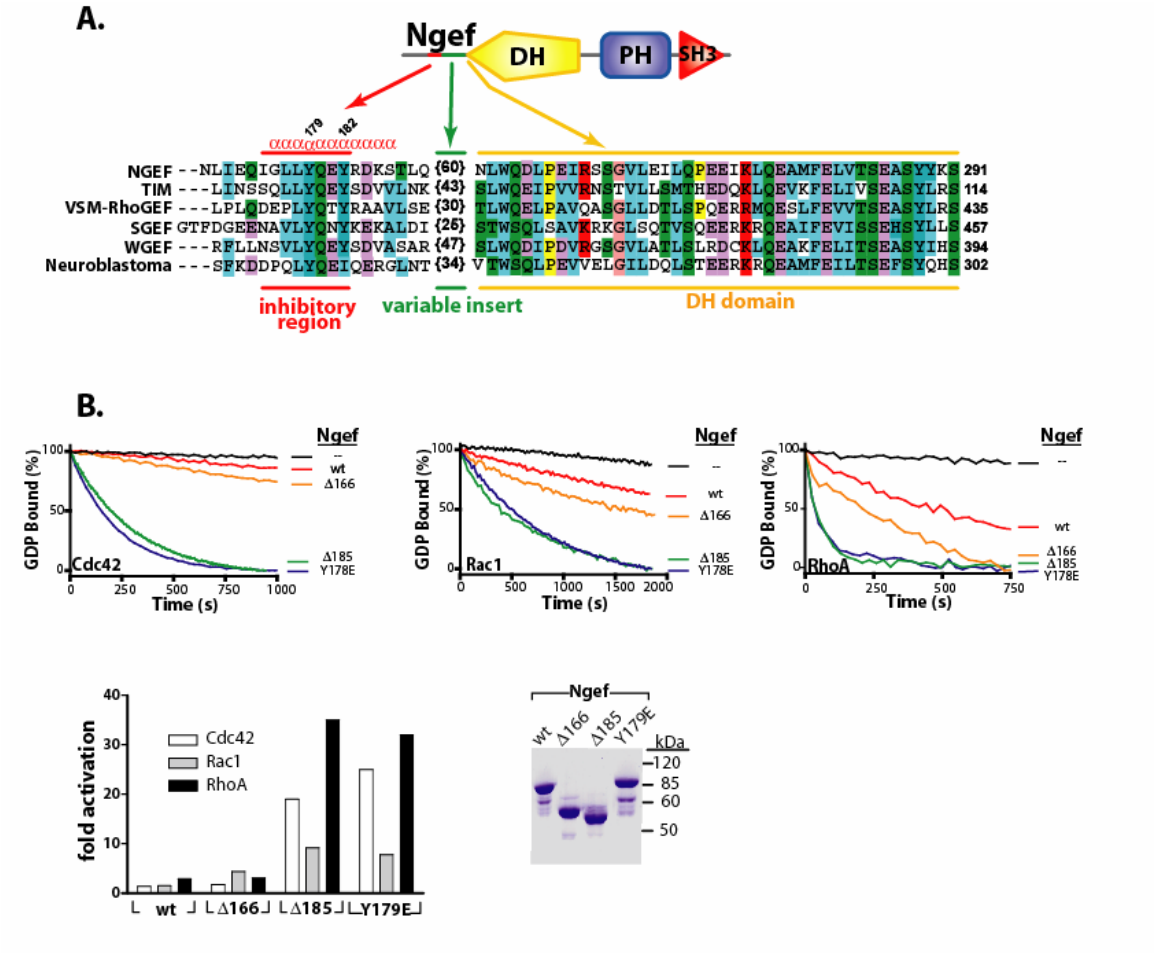

Figure 17: Ngef is regulated by auto-inhibition.
(A) The N-terminal portions of Ngef and its closest homologs are highlighted in the multiple sequence alignment. Colored bars underneath the alignment demark regions in Ngef corresponding to the auto-inhibitory helix (red), an intervening region (green), and the start of the DH domain (yellow). Tyrosines 179 and 182 of Ngef are numbered. The region in Ngef and its close homologs that is strongly predicted to be helical using standard algorithms is indicated (α). The domain architecture of Tim and its closest homologs is shown above the alignment. **(B)** Full-length (wt) and truncated (Δ166) forms of Ngef that retain the conserved auto-inhibitory helix modestly activate RhoA, Rac1 and Cdc42. In contrast, Ngef in which the auto-inhibitory helix is truncated (Δ185) or mutated (Y179E) have dramatically enhanced capacities to catalyze nucleotide exchange on all three GTPases. Fold-activation (lower panel) is relative to the spontaneous loading of guanine nucleotide and represents the average of two independent reactions for each condition. Equal amounts (5 μg) of purified proteins used in the exchange assays are shown at lower right following SDS-PAGE and staining with Coomassie brilliant blue.

Ngef to the same extent as removing this region by truncation. Therefore, like Tim, Ngef is activated toward its full repertoire of Rho GTPase substrates by removal or substitution of a small, conserved segment with high helical propensity located N-terminal to its DH domain.

Similar to the correlation seen with Tim, the *in vitro* guanine nucleotide exchange activity of Ngef tracked with its capacity to transform NIH 3T3 cells (Figure 18). For instance, stably expressing Ngef lacking the auto-inhibitory helix (Δ185) or mutated within this region (Y179E) led to an approximately two-fold increase in foci relative to either expression of full-length Ngef or the N-terminally truncated version (Δ166) that retains the auto-inhibitory region. The Ngef constructs consistently expressed to varying degrees and the results are even more striking if the numbers of foci are normalized for Ngef expression. In this case, Ngef (Y179E) was 4- and 16-fold more efficient at promoting foci than Δ166 and full-length Ngef, respectively.

To confirm that the N-terminal region is necessary for Ngef inhibition in the context of an intact cell, we performed affinity purifications of active Ngef using GST-tagged versions of nucleotide-free RhoA, Rac1 and Cdc42 (RhoA G17A, Rac1 G15A and Cdc42 G15A, Figure 19A). Since Dbl-family proteins bind preferentially to nucleotide-free Rho family GTPases, these constructs are expected to affinity purify any active GEF specific for these GTPases present in a cell lysate. HA-tagged Ngef (Δ166), when expressed in serum-starved COS7 cells, did not appreciably interact with RhoA G17A, Rac1 G15A or Cdc42 G15A. In contrast, Ngef (Δ166+Y179E), in which a key tyrosine in the auto-inhibitory helix is mutated was affinity purified by all three of the nucleotide-free GTPases, suggesting that the region of Ngef immediately N-terminal to its DH

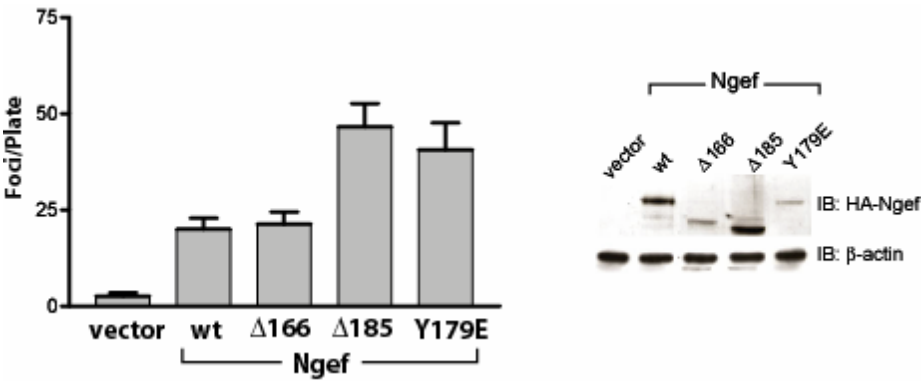

Figure 18: Ngef in which the auto-inhibitory helix is truncated (Δ185) or mutated (Y179E) potentiates transformation of NIH 3T3 cells.
Data represents the averages of three independent experiments carried out in duplicate. An immunoblot showing expression levels of the various Ngef constructs is shown at right. Δ166 and Y179E Ngef consistently express less robustly than either wt or Ngef (Δ185).

domain, and Y179 in particular, leads to Ngef auto-inhibition by preventing its interaction with its cognate GTPases.

Affinity purifications of active RhoA and Rac1 from the lysates of COS7 cells (Figure 19B) confirmed the direct correlation between the capacity of Ngef to activate RhoA and Rac1 *in vitro* and in cells. Transfection of Ngef (Δ166+Y179E) significantly stimulated loading of GTP onto RhoA and Rac1 upon its transfection into COS7 cells relative to empty vector. We were unable to detect an increase in levels of Cdc42·GTP due to Ngef (Δ166+Y179E) expression (Figure 19B), indicating that either Ngef expression does not lead to Cdc42 activation in COS7 cells, or Ngef expression is associated with a transient activation of Cdc42 that we are unable to detect by affinity precipitation of steady-state levels of activated Cdc42. Another Dbl-family protein, Dbs, has been shown to be a RhoA and Cdc42 specific exchange factor *in vitro* but its expression in NIH 3T3 cells does not lead to an increase in Cdc42·GTP as determined by affinity purification assays (221). Interestingly, a peptide corresponding to the auto-inhibitory helix of Tim (269) effectively inhibits both the RhoA and Cdc42-specific exchange activity of Ngef in vitro (Figure 19C), confirming that these two proteins are regulated similarly.

Also like Tim, Ngef containing the auto-inhibitory region (Δ166) was robustly phosphorylated by Src *in vitro,* while further truncation (Δ185) to remove the auto-inhibitory region led to loss of phosphorylation by Src (data not shown). Since Tyr 179 and 182 are the only tyrosines removed by the larger truncation, these data indicate that Δ166 Ngef is phosphorylated by Src exclusively within the auto-inhibitory region at either one or both of these tyrosines. Interestingly, mutation of Y179 led to a loss of

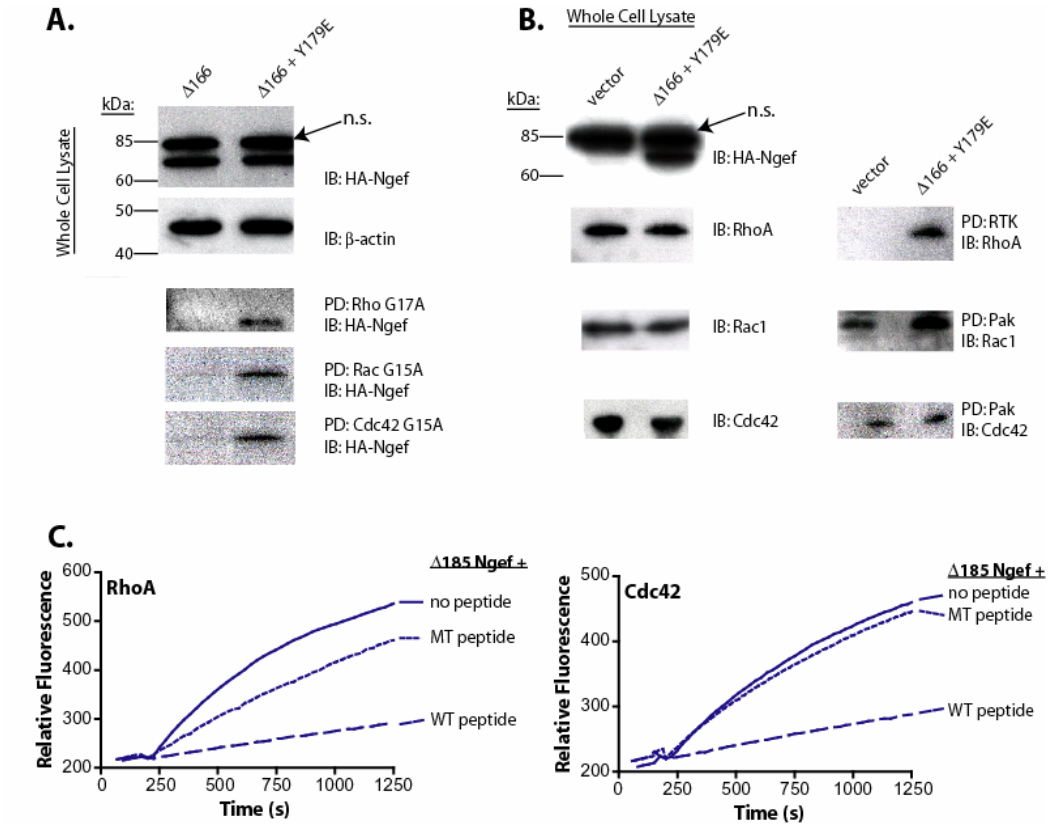

Figure 19: Ngef in which the auto-inhibitory helix is mutated activates endogenous RhoA and Rac1 in COS7 cells.

(A) The activity of Ngef constructs transiently expressed in quiescent COS7 cells was assessed by a pulldown assay using GST-tagged nucleotide-free RhoA, Rac1 or Cdc42 as the affinity purification matrix. Levels of active Ngef were determined by immunoblotting the pulldown samples. Immunoblots of the total cell lysate (2.5% input shown) show approximately equal expression of the Ngef constructs (n.s. denotes non-specific). The experiments were performed three times and representative examples are shown. **(B)** Expression constructs for the phosphomimetic form of Ngef or vector alone were transfected into COS7 cells, which were subsequently serum starved in DMEM supplemented with 0.1% FCS for 16 hours prior to affinity purification of the active forms for RhoA, Rac1 and Cdc42. The levels of active and total GTPases were determined by immunoblotting. In the same experiment, expression of the HA-tagged Ngef variant was verified by immunoblot (n.s. denotes non-specific). The experiments were performed three times and representative examples are shown. **(C)** Ngef (Δ185) was incubated with a peptide corresponding to the N-terminal auto-inhibitory region of Tim (WT, biotin-SQLLYQEYSDV-amide) or a mutant peptide (MT, biotin-SQLLEQEYSDV-amide) at room temperature for 20 minutes. The resulting complexes were assayed for their ability to stimulate loading of mant-GTP onto RhoA or Cdc42. The peptide concentrations were 100 μM.

Ngef phosphorylation by Src (Figure 20A), while mutation of Y182 led to a substantial increase in the phosphorylation of Ngef by Src. These data indicate that both Y179 and Y182 are important for the maintenance of Ngef in the auto-inhibited state, but in contrast to the situation described for Tim, only Y179 is a substrate for direct phosphorylation by Src.

Relative to its unphosphorylated form, phosphorylation of Ngef (Δ166) by Src led to an 8-fold increase in the rate of catalyzed guanine nucleotide exchange using RhoA as substrate *in vitro* (Figure 20B). Using Cdc42 as substrate, the equivalent enhancement was 3-fold (Figure 20C). Reminiscent of the situation with Tim, Src most likely also forms a metastable complex with Ngef, since Src in the absence of ATP was able to stimulate guanine nucleotide exchange catalyzed by Ngef (Δ166) approximately 3- and 1.5-fold for RhoA and Cdc42 substrates, respectively. These rate enhancements required both Ngef and Src since the kinase alone is incapable of stimulating exchange with either RhoA or Cdc42 (Figure 20B and C). Interestingly, and in contrast to Tim, Ngef is neither directly phosphorylated nor activated by the kinase domain of EphA4 *in vitro* (data not shown).

Expression of activated Ngef causes defects in axon extension.

Previous studies have shown that the unphosphorylated form of the Ngef ortholog, ephexin, activates RhoA, Rac1 and Cdc42; but ephexin that is phosphorylated at Tyr 87 activates RhoA exclusively (78). The results that we present above suggest that phosphorylated Ngef activates RhoA and Rac1, both *in vitro* and in fibroblasts, more efficiently than unphosphorylated, auto-inhibited Ngef. Since RhoA and Rac1 are known

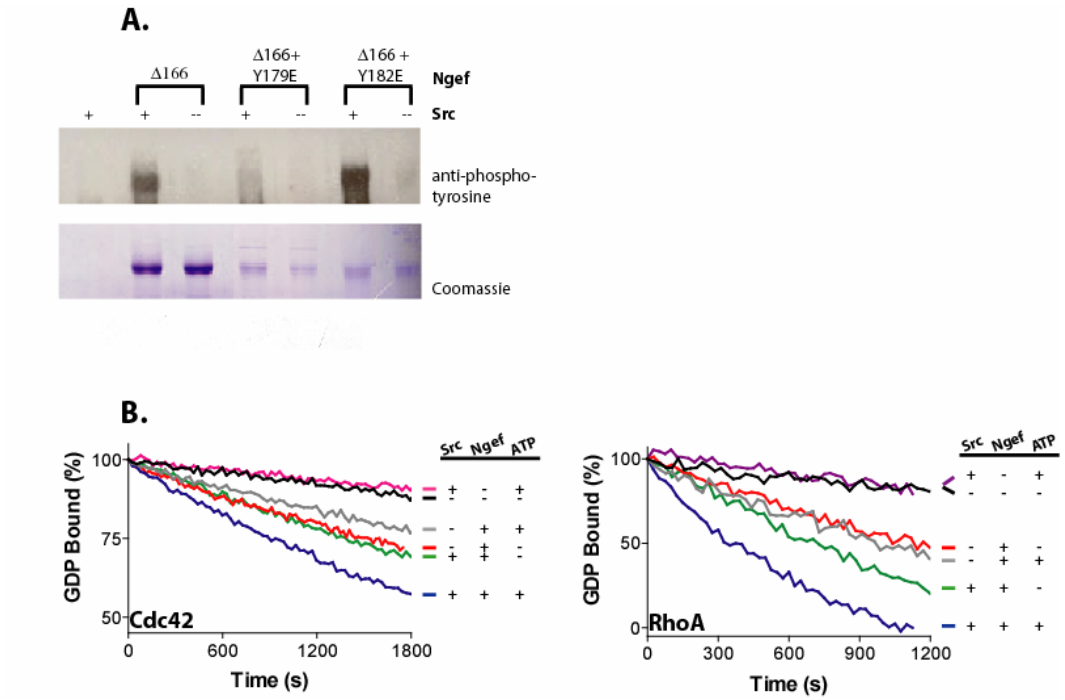

Figure 20: Phosphorylation by Src directly activates Ngef.
(A) Src specifically phosphorylates tyrosine 179 within the auto-inhibitory helix of Ngef. Purified forms of Ngef (lower panel) were incubated with recombinant Src and ATP for thirty minutes prior to SDS-PAGE and immunoblotting was used to assess levels of phosphorylation (upper panel). Substitution of Tyr 179 abrogates phosphorylation. **(B)** Phosphorylation of Ngef by Src promotes the capacity of Ngef to catalyze nucleotide exchange on Cdc42 (left) and RhoA (right). Δ166 Ngef was incubated with combinations of kinase and ATP as indicated for thirty minutes prior to addition of the mixtures to exchange reactions.

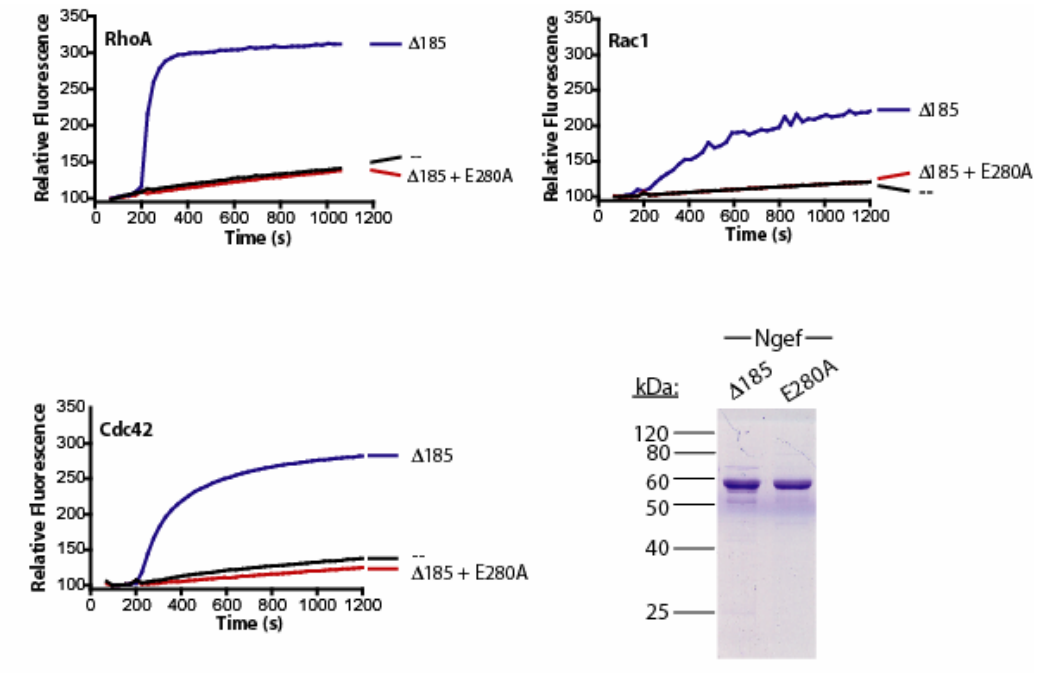

Figure 21: E280A Ngef is catalytically inactive.
The E280A substitution renders Δ185 Ngef inactive on RhoA, Rac1 and Cdc42. Equal amounts (5 µg) of purified proteins used in the exchange assays are shown at lower right following SDS-PAGE and staining with Coomassie brilliant blue.

to play opposing roles in axon extension (273), we asked if cultured neuronal progenitor cells over-expressing the active form of Ngef showed defects in axon extension.

We measured the length of the presumptive axon in mouse cortical neuronal progenitor cells cultured for 4 days in vitro (DIV) and over-expressing either GFP alone (pCIG2) or GFP in conjunction with one of three forms of Ngef: auto-inhibited (Δ166), constitutively active (Δ166 + Y179E) or exchange inactive (Δ166 + Y179E +E280A). The exchange inactive mutation renders Δ185 Ngef, a version of Ngef in which the auto-inhibitory helix is truncated, completely inactive on RhoA, Rac1 and Cdc42 *in vitro*, although the purified protein is soluble and monomeric (Figure 21). The E280A mutation removes a hydrogen bonding interaction between the catalytic DH domain and switch I of the cognate GTPase that has been shown to be critical for GTPase binding in other Dbl-family proteins (245).

Cells expressing either GFP alone or GFP in conjunction with Δ166 Ngef had elaborated both an axon and dendritic arbors on the fourth DIV (Figure 22). Interestingly, cells expressing GFP and Δ166 + Y179E Ngef displayed two phenotypes. The majority of the cells expressing Δ166 + Y179E extended single axons that were slightly shorter than the axons extended from cells expressing Δ166 Ngef or GFP alone. However, a minority of cells expressing Δ166 + Y179E did not extend an axon and displayed a rounded, ruffling phenotype. These cells are differentiated neurons, based on their expression of a neuronal-specific tubulin isoform, βIII. The cause of the development of two phenotypes for cells expressing Δ166 +Y179E Ngef is currently unknown. During the developmental time frame of this experiment, the neuronal progenitor cells that incorporate plasmid DNA as a result of the electroporation, are a mixed population of

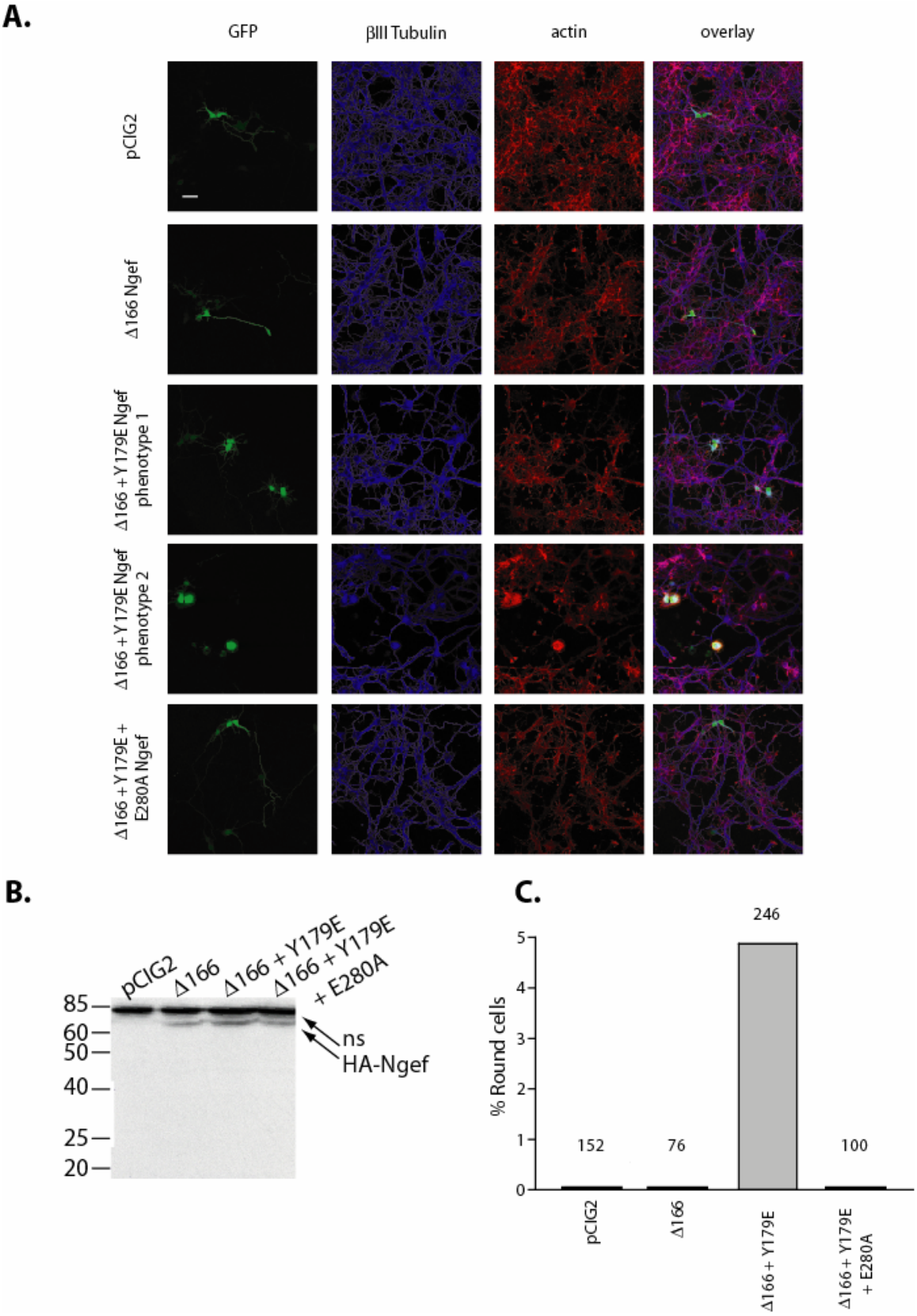
A.
GFP
βIII Tubulin
actin
overlay
pCIG2
Δ166 Ngef
Δ166 + Y179E Ngef phenotype 1
Δ166 + Y179E Ngef phenotype 2
Δ166 + Y179E + E280A Ngef
B.
pCIG2
Δ166
Δ166 + Y179E
Δ166 + Y179E + E280A
85
60
50
40
25
20
ns
HA-Ngef
C.
% Round cells
246
152
76
100
pCIG2
Δ166
Δ166 + Y179E
Δ166 + Y179E + E280A

Figure 22: Over-expression of an activated form of Ngef affects axonogenesis.
(A) Cortical neurons (DIV 4) expressing GFP (green) and various forms of HA-Ngef were immunostained for βIII tubulin (blue), a neuron-specific marker, and simultaneously stained with phalloidin (red). The scale bar (upper left) indicates 37 μm. (B) Expression of HA-Ngef constructs. COS7 cells were transfected with the indicated HA-Ngef constructs and lysed. The lysates were analyzed by SDS-PAGE and immunoblotting. The symbol ns indicates a non-specific band that serves as a loading control for this experiment. (C) Quantification of cells displaying a rounded phenotype. The total number of cells counted for each condition is displayed above the bar corresponding to that condition.

cells destined to become a part of both layer 4 and layer 5 of the adult cortex. Perhaps the heterogeneity of the population of cells expressing Δ166 + Y179E Ngef can account for the formation of two phenotypes. Alternatively, the two phenotypes represent populations of cells responding differently to an extracellular signal.

Cells expressing the exchange inactive version of Ngef extended single axons that were slightly longer than the axons extended from cells expressing GFP alone, suggesting that this mutant form of Ngef forms a non-productive complex with upstream activators, such as EphA4 of wild type ephexin, which is present in these cells. These results are consistent with a role for Ngef activity in inhibition of axon outgrowth.

In order to determine if the only the Rho-specific exchange activity of Ngef inhibits axon outgrowth, we attempted to create a mutant of Ngef that is only able to activate Rac1. An interaction between a basic residue in the loop between helices α4 and α5 of the DH domain and glutamate 54 of RhoA has been shown to be critical for recognition of RhoA (94). Primary sequence alignment experiments indicated that Ngef possesses two basic residues in this loop (K399 and R401), however, mutation of both of these residues crippled Ngef exchange activity on RhoA, Rac1 and Cdc42 (data not shown).

Since we were unable to create a mutant of Ngef that did not activate RhoA, we attempted to uncouple the effects of activated Ngef and activated RhoA by pharmacologically inhibiting a key downstream effector of RhoA, p160-Rho kinase (ROCK). ROCK has been shown to be necessary and sufficient for agonist induced neurite retraction and cell rounding, and it can be effectively inhibited in neurons and neuronal cell lines with the small molecule Y-27632 (274,275). Prior to treatment, cells

expressing activated Ngef that displayed the rounded phenotype were identified and imaged. These cells were treated with Y-27632 (20 μM) and time-lapse imaged to document the elaboration of multiple neurites (Figure 23), indicating that the rounded cells are indeed viable and that the RhoA/ROCK signaling pathway is critical for the maintenance of the rounded phenotype.

Discussion:

For proper nervous system development, nascent neurons must migrate to their characteristic locations, extend axons and dendrites in the appropriate directions and form synapses with the appropriate partners. Rho GTPases are an integral part of the signaling pathways required for each of the above processes, but their role in the guidance of the axonal growth cone to its appropriate partner has not been extensively characterized. The axonal growth cone is a specialized structure present at the distal end of the growing axon, which acts as a pathfinder to sense extracellular cues. This is accomplished by the production of a single lamellipodium from the leading edge of the growth cone, which is capped by multiple filopodia. Filopodia play a sensory role, allowing the growth cone to search for attractive and repulsive extracellular cues. Most of the filopodia, which are extruded in a constant, stochastic manner, are retracted through myosin-dependent contraction of the cortical actin network. However, should a filopodium become fixed to an extracellular ligand and should transmembrane receptors in that filopodium become activated, the growth cone is able to use both myosin-dependent traction and the extension of a lamellipodium to advance its body toward that ligand (276,277).

It is currently accepted that active Rac1 and Cdc42 positively influence axonal outgrowth, by inducing the formation of lamellipodia and filopodia, respectively. Active

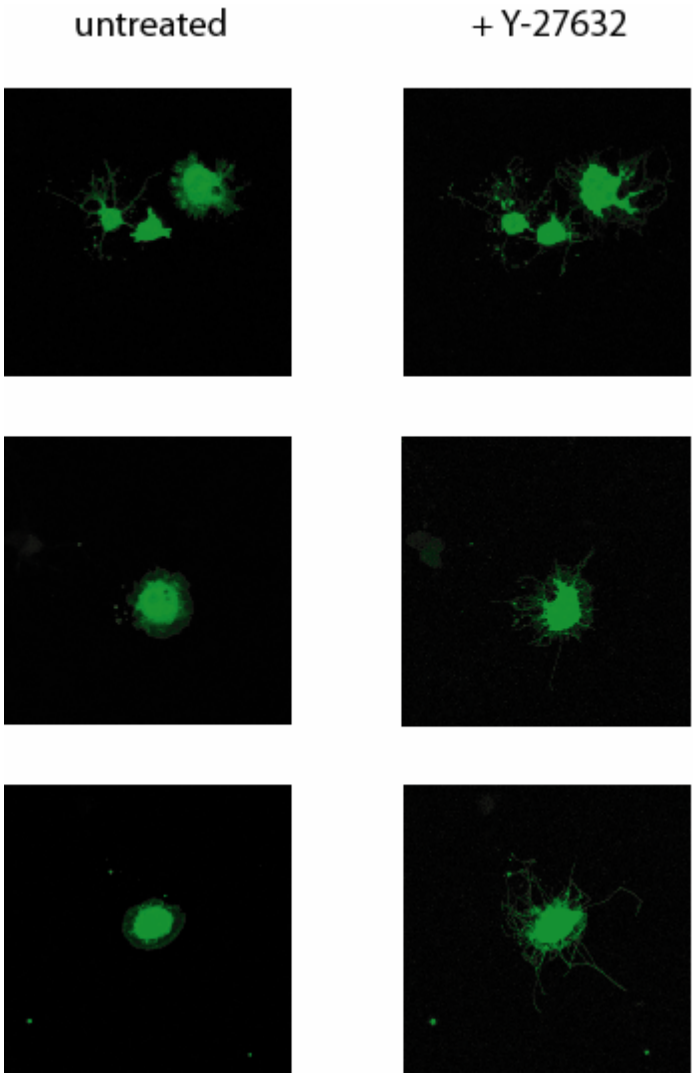

Figure 23: Treatment of Δ166 + Y179E Ngef-expressing cortical progenitors that display the rounded phenotype with the ROCK inhibitor, Y-27632, leads to the elaboration of multiple neurites.
Images of three individual cortical progenitor cells before and after treatment are displayed.

RhoA is currently thought to mediate growth cone retraction, through activation of downstream effectors that lead to increased myosin-dependent contractility (273,278). However, recent evidence suggests that this hypothesis represents an over-simplification of the role of Rho GTPases in axon guidance. For example, active RhoA has been shown to be critical for the formation of point contacts, the neuronal equivalent of focal adhesions in the fibroblast, that allow the extending growth cone to adhere to the extracellular matrix (279). Rac1 has also been shown to play an important role in growth cone collapse (280). Clearly, the roles of RhoA, Rac1 and Cdc42 in axon pathfinding are complex and context-dependent.

One group of repulsive cues a sensory filopodium from a migrating growth cone might encounter, particularly at the midline of the nervous system, is the ephrins. The six GPI-linked ephrin As and three transmembrane ephrin Bs are the ligands for the largest family of receptor tyrosine kinases, the EphAs and EphBs, respectively. The binding of ephrins by the Eph receptors induces receptor clustering, auto-phosphorylation and activation. Since the ephrins are themselves transmembrane proteins, signaling is bi-directional as a result of the ephrin/Eph interaction. After the initial adhesive interaction between a cell expressing an ephrin and a growth cone expressing an Eph receptor, downstream signaling pathways that mediate repulsive responses are activated. The ephrin/Eph interaction ultimately results in weakened growth cone attachment to the extracellular matrix and retraction of cellular processes such as lamellipodia and filopodia. These repulsive responses are achieved through activation of a metalloprotease, which cleaves the ephrin, severing the adhesive interaction; through

internalization of membrane patches containing the ephrin/Eph complex; and through the actions of Rho GTPases (281).

Activation of Rho GTPases downstream of transmembrane receptors such as Ephs occurs through either inactivation of GAPs or activation of GEFs. While EphB receptors are able to interact with Intersectin (98), Kalirin (145) and Vav2 (282), the best characterized interaction between an Eph receptor and a Dbl protein is that of EphA4 and ephexin. Ephexin is tyrosine phosphorylated in an N-terminal motif with significant sequence identity to the auto-inhibitory helix described here for Tim. Phosphorylation of ephexin in this motif changes the specificity of this GEF for cognate GTPases. Specifically, when ephexin is not tyrosine phosphorylated, it activates RhoA, Rac1 and Cdc42; but when ephexin is tyrosine phosphorylated; ephexin activates RhoA exclusively (78). These results, based largely upon examining the cellular morphology of fibroblasts transiently transfected with mutants of ephexin and EphA4, are in contrast to those shown here.

We have used *in vitro* guanine nucleotide exchange assays and cell-based GTPase activity assays to show mechanistically that phosphorylation or phospho-mimetic mutation of Ngef leads to an activation of the exchange potential for this GEF on all three GTPases studied: RhoA, Rac1 and Cdc42. This discrepancy could be explained in several different ways. First, phosphorylated Ngef may be differentially localized in the growth cone to activate Rac1 and Cdc42 in restricted microdomains. High-resolution microscopy studies examining the intracellular localization of phosphorylated Ngef and the activated cognate GTPases need to be carried out to examine this idea. Second, ephrinA binding to EphA4 could independently activate an as yet unidentified GAP for

Rac1 and Cdc42, such that the net result of this signaling pathway is a preferential activation of RhoA. Finally, activation of Rac1 and Cdc42 by Ngef could play a role in growth cone collapse. Rac1 activity has been shown to be required for growth cone collapse since it promotes internalization of the Eph/ephrin complex from the plasma membrane (282,283). Additionally, active Rac1 and Cdc42 are critical for axon retraction, branching and defasiculation following growth cone collapse (284). The role of Ngef in these processes has yet to be determined.

In conclusion, we have demonstrated that Ngef is activated towards its full repertoire of cognate GTPases, namely RhoA, Rac1 and Cdc42, by removal, substitution or Src-dependent tyrosine phosphorylation of a small, conserved sequence N-terminal to its DH domain. Ngef exchange activity is inhibited by a peptide derived from the auto-inhibitory sequence of the related protein, Tim, indicating that these two proteins are regulated in a near identical manner. Importantly, we have also shown that the exchange activity of Ngef, and its Rho-specific exchange activity in particular, functions to inhibit axon outgrowth in developing neurons.

CHAPTER 4: REGULATION OF THE EXCHANGE ACTIVITY OF TIM BY INTRAMOLECULAR INTERACTIONS

Introduction:

Src homology 3 (SH3) domains are independently folding modules of approximately 60 amino acid residues found in many signaling molecules such as non-receptor tyrosine kinases and Dbl-family GEFs. These domains have largely been characterized as protein-protein interaction domains, and bind preferentially to proteins containing multiple proline residues. Structural studies of SH3 domains have revealed that these domains consist of two three-stranded anti-parallel β-sheets, oriented perpendicular to each other. Two variable regions, the RT- and n-Src loops, contribute aromatic residues, which form pockets on the surface of the SH3 domain that are capable of accepting a proline residue from the ligand protein, and an acidic residue, which typically forms a salt bridge with a basic residue in the ligand protein. The ligand of SH3 domains is a left-handed poly-proline type II helix, from which proline containing di-peptides contact the binding pockets on the surface of the SH3 domain directly (285).

In addition to their role in intermolecular protein-protein interactions, SH3 domains also function in intramolecular, auto-inhibitory interactions in a variety of signaling proteins. The SH3 domain was originally identified in the Src family kinases, which include Src, Lck, Hck, Blk, Fyn, Lyn, Fgr, Yes and Yrk. These non-receptor tyrosine kinases are composed of an N-terminal region of 9-12 amino acid residues

important for membrane localization, a variable region, an SH3 domain, an SH2 domain, a kinase domain, and a short C-terminal tail. Src family kinases are held in a basal, inactive state by intramolecular interactions that are interrupted downstream of signaling from various cell surface receptors such as the EGFR (286).

Originally it was thought that auto-inhibition of Src family kinases was mediated by the SH2 domain of the Src family kinase binding to a phosphorylated tyrosine in its own C-terminal tail. However, structural characterization of Src family kinases in the auto-inhibited state have revealed that while the SH2 domain of these proteins does indeed bind to the C-terminal tail, auto-inhibition is primarily achieved through the SH3 domain binding to a poly-proline type II helix found in the poly-peptide that links the SH2 domain to the kinase domain. The interaction between the SH3 domain and the SH2-kinase linker region locks the kinase domain in a conformation incapable of binding to ATP, and thus incapable of catalyzing the tyrosine phosphorylation of substrate molecules (286). The binding proteins containing poly-proline regions with a higher affinity for the SH3 domain of Src family kinases than the internal SH2-kinase linker binding site relieves this auto-inhibition. Poly-proline containing proteins are able to relieve Src family kinase auto-inhibition even if the SH2 domain remains bound to the C-terminal tail. The function of the interaction between the SH2 domain and the C-terminal tail, then, is largely to properly position the SH2-kinase linker region such that it is able to bind to the SH3 domain (287,288).

Auto-inhibition mediated by an intramolecular interaction between an SH3 domain and a proline-rich region has also been shown for non-receptor tyrosine kinases of other families. For example, the Tec family kinases, Tec, Txk, Bmx, Itk and Btk, are

composed of an N-terminal PH and Tec homology (TH) domains, followed by SH3, SH2 and kinase domains. Tec family kinases lack the regulatory C-terminal tail found in Src family kinases, but do contain two poly-proline regions (289). The first of these poly-proline regions, located immediately N-terminal to the SH3 domain, is involved in an intramolecular, auto-inhibitory interaction with the SH3 domain (290). The second poly-proline region, located in the TH domain, mediates an intermolecular homo-dimerization interaction (291,292). It is thought that formation of Tec family kinase dimers disrupts the intramolecular, auto-inhibitory SH3 domain interaction and enables these kinases to phosphorylate and activate each other *in trans* (293). In addition, the non-receptor tyrosine kinase Abl, which contains a variable N-terminal region, an SH3 domain, an SH2 domain and a long C-terminal domain without a phospho-tyrosine, is regulated by an intramolecular interaction between its SH3 domain and a poly-proline region in the kinase domain. In this case, the auto-inhibitory interaction is stabilized by the N-terminal region binding to the SH2 and SH3 domains in a manner similar to the SH2 domain binding to the C-terminal tail of Src (294,295).

The Dbl-family of guanine nucleotide exchange factors (GEFs) are the largest group of proteins directly responsible for the activation of Rho GTPases. Dbl-family proteins are characterized by a Dbl-homology (DH) domain, which contacts the Rho GTPase to catalyze nucleotide exchange, and an associated pleckstrin-homology (PH) domain, which fine-tunes the exchange process by a variety of mechanisms related to the binding of phosphoinositides. The 69 human Dbl-family proteins are divergent in regions outside the DH/PH module, and contain additional domains that presumably

dictate unique cellular functions. The additional domains also mediate Dbl-family protein auto-inhibition (5).

Of the 69 human Dbl-family proteins, approximately one third contain an SH3 domain in addition to the DH/PH module. Several of these SH3 domain-containing Dbl-family proteins also contain a proline rich region, indicating that intramolecular interactions between an SH3 domain and a poly-proline region may be one mechanism by which Dbl-family proteins are auto-inhibited. In fact, the Rac-specific exchange activity of the Dbl-family protein, Kalirin, which contains an SH3 domain between its two DH/PH cassettes, is negatively regulated by an intramolecular interaction between that SH3 domain and three different poly-proline containing regions in the GEF (243). However, the Dbl-family proteins Asef and Intersectin-L, which contain SH3 domains N-terminal to their DH/PH cassettes, are negatively regulated by SH3 domains directly binding to the DH domain in a manner independent of the poly-proline binding site of the SH3 domain (203,296). Dbl-family GEFs, then, are able to be regulated by intramolecular interactions involving SH3 domains in both poly-proline dependent and independent manners.

Recently, we have shown that the Dbl-family protein Tim is auto-inhibited by an N-terminal helical region that directly occludes the catalytic interface of the DH domain to prevent GTPase activation. Here we show that intramolecular interactions between the C-terminal SH3 domain of Tim and a poly-proline region immediately N-terminal to the DH domain are similarly auto-inhibitory. The exchange potential of Tim, then, is negatively regulated by two distinct intramolecular interactions, and each of these interactions must be disrupted in order to fully activate this Dbl-family protein.

Experimental Procedures:

Protein Purification:

Mutations were introduced into a pET-21a (Novagen) construct encoding full-length length or Δ22 Tim using the Quikchange site-directed mutatgenesis kit (Stratagene) as per the manufacturer's instructions. The PCR-amplified product for Δ57 Tim was ligated into pET-21a between *NdeI* and *XhoI*. These mutant proteins were expressed and purified as described previously (269). In brief, Tim constructs were expressed in the *E. coli* strain Rosetta(DE3) (Novagen). Cell cultures were grown at 37ºC in LB/ampicillin (100 μg/mL), and induced with 1 mM isopropyl-β-D-thiogalactopyranoside (IPTG) for 5 hours at 27ºC. Cell pellets were resuspended in 20 mM HEPES, pH 7, 1 mM EDTA, 2 mM DTT, 10 % glycerol (buffer A) with 20 mM NaCl, lysed using an Emulsiflex homogenizer (Avestin), and clarified by centrifugation at 40 000 *g* for 45 min at 4ºC. Clarified supernatant was loaded on a Fast Flow S column (Pharmacia) equilibrated with buffer A and eluted with a linear gradient of 20-500 mM NaCl. Tim protein was next loaded on an S-200 size exclusion column equilibrated with buffer A containing 300 mM NaCl. Fractions containing monomeric Tim were pooled, concentrated, and stored at -80ºC. RhoA was purified as previously described (94).

Guanine Nucleotide Exchange Assays:

Fluorescence spectroscopic analysis of N-methylanthraniloyl (mant)-GTP incorporation into RhoA was carried out as described (246). In brief, assay mixtures containing 20 mM Tris pH 7.5, 150 mM NaCl, 5 mM $MgCl_2$, 1 mM DTT and 100 μM mant-GTP (Molecular Probes) and 2 μM RhoA were allowed to equilibrate with

continuous stirring. After equilibration, 50 nM Tim was added and nucleotide loading was monitored as the decrease in the tryptophan fluorescence (λ_{ex} = 295 nm, λ_{em} = 335 nm) of RhoA as a function of time using a Perkin-Elmer LS 55 spectrophotometer. Rates of guanine nucleotide exchange were determined by fitting the data to a single exponential decay model with GraphPad Prizm. Data were normalized to yield percent GDP released and assays were performed in duplicate.

Cell Culture and Transformation Assays:

NIH 3T3 mouse fibroblasts were maintained in DMEM supplemented with penicillin/streptomycin and 10% calf serum (Hyclone). HEK 293T cells were maintained in DMEM supplemented with penicillin/streptomycin and 10% fetal bovine serum (Sigma). PCR-amplified Tim constructs were ligated into pcDNA 3.1 Hygro (Invitrogen) between *EcoRI* and *XhoI* such that an expressed HA-tag was encoded at the N-terminus of each construct. Mutations were introduced into wild type Tim as described above.

Cell lines stably expressing Tim were established by transfecting NIH 3T3 cells with 1 μg of each pcDNA construct using LipofectAMINE Plus (Invitrogen) according to the manufacturer's protocol. Three days post-transfection the cells were subcultured into growth medium supplemented with 300 μg/mL of hygromycin B. Mass populations of multiple, drug resistant colonies (>50) were pooled together for focus formation analyses. Western blot analysis with an anti-HA antibody (Covance) was performed to verify Tim expression in the cell lines.

For the secondary focus formation assays, equal numbers of cells from each cell line were seeded into 60 mm dishes. The growth medium of each dish was replaced with fresh hygromycin-supplemented medium every three days. 14 days after seeding, the

dishes were stained with crystal violet and the foci were quantified by visual inspection. Individual experiments were performed in duplicate and independently carried out three times.

HEK 293T cells were transiently transfected with 1 μg of each pcDNA construct using LipofectAMINE Plus (Invitrogen) according to the manufacturer's protocol. The cells were lysed 18 hours post-transfection in 50 mM Tris, pH 7.6, 500 mM NaCl, 0.1 % SDS, 0.5 % sodium deoxycholate, 1 % Triton-X 100, 0.5 mM $MgCl_2$ and protease inhibitors (Roche) prior to being used in the affinity purification assays described below.

Affinity Purification Assays:

GST and a GST-tagged version of the Tim SH3 domain (residues 434-519) were expressed in BL21 (DE3) E. coli and batch purified on glutathione sepharose beads (Amersham). 100 μg of immobilized protein was incubated with either 100 μg of purified Δ22 or Δ57 Tim or 1 mg of HEK 293T whole cell lysate for 1 hour at 4 ºC. The beads were washed extensively in lysis buffer and analyzed by either SDS-PAGE or SDS-PAGE in combination with immunoblotting.

Analytical Gel Filtration Chromatography and Ultracentrifugation:

1 mg of purified full-length Tim was loaded onto a calibrated Superdex S-75 column (Amersham) in buffer A containing 300 mM NaCl, and eluted at a flow rate of 0.5 mL/min. In addition, purified full-length Tim in the above buffer at several different concentrations (OD_{280} of 1.0. 0.8 and 0.6 at 1 cm pathlength) was analyzed by analytical ultracentrifugation (297) in a Beckman Optima XL-I ultracentrifuge equipped with a Ti60 rotor and a 6-sector cell (1.2 cm pathlength). The samples were centrifuged at

11,000 rpm for 26 hours at 20 ºC. The offset was determined by meniscus depletion, which was achieved by centrifugation at 45,000 rpm for 6 hours at 20 ºC. The data were fit to a one-state model using the XL-A/XL-I Data Analysis Software package version 4.0 (Beckman).

Surface Plasmon Resonance (SPR) experiments:

N-terminally biotinylated peptides corresponding to the poly-proline region of Tim (residues 39-54), a proline-rich region of Ngef (residues 223-233) and mNotch (298) were diluted to 0.1 μg/mL in BIA running buffer (10 mM Hepes, 150 mM NaCl, 10 mM MgCl2 and 0.005% NP-40). These peptides were coupled to separate flow cells of a streptavadin-coated biosensor chip to a surface density of 1000 response units using the MANUAL INJECT command on a BIAcore 3000 (Biacore). The resulting chip was used in surface plasmon resonance experiments as previously described (299). In brief, 30 μL of Tim SH3, diluted to various concentrations in BIA running buffer, were simultaneously injected over all flow cells using the KINJECT command at a flow rate of 10 μL/min, followed by 300 s of dissociation. The surfaces were regenerated between titrations using a 10 μL pulse of 500 mM NaCl and 25 mM NaOH at a flow rate of 20 μL/min. Thermodynamic constants were calculated by normalizing the resulting sensorgrams using the BIAevaluation software package (Biacore), and plotting the response units at binding equilibrium versus the Tim SH3 concentration for that sensorgram using GraphPad Prizm (GraphPad) and these constants represent the results of two independent experiments.

Confocal Microscopy:

NIH 3T3 cells transiently transfected with pcDNA-Tim constructs were plated onto glass coverslips and serum starved for 48 hours prior to being fixed in 3.8% paraformaldehyde and stained with anti-HA (Covance) and Alexa-488 conjugated anti-mouse antibodies as well as Alexa-546 conjugated phalloidin. Images were taken on a LEICA TCS-SL laser scanning confocal microscope.

Results:

Tim is auto-inhibited by a proline-containing region in its N-terminus.

The N terminus of Tim consists of an extended region of low complexity and no known domain structure. Truncation of the N-terminal 22 amino acids of Tim leads to a robust increase in its exchange activity *in vitro* (269). To determine if additional regions of the Tim N terminus play a role in its regulation, we tested the exchange activity of Tim mutants in which the N-terminus had been further truncated. A shorter version of Tim (Δ57, see Figure 24A) was able to catalyze exchange of guanine nucleotide bound to RhoA 45% more efficiently than the previously characterized Δ22 Tim. Further N-terminal truncations destabilized Tim upon over-expression in *E.coli* (data not shown), most likely reflecting the loss of important secondary structural elements necessary for the integrity of the extended DH domain, which begins at residue 70 in full-length Tim.

Primary sequence analysis indicated that the region of Tim between residues 23 and 57 contains a Type 1A poly-proline containing SH3 domain binding ligand. To test if the integrity of this region was important for maintenance of Tim auto-inhibition, we mutated a key proline residue to alanine in the context of both full-length and Δ22 Tim

(P49A, Figure 24A, upper and lower panel). Δ22 + P49A Tim, similar to Δ57 Tim, was approximately 45% more efficient at catalyzing nucleotide exchange than Δ22 Tim. Importantly, P49A Tim was itself 3-fold more efficient at catalyzing nucleotide exchange. These data indicate that the poly-proline region of Tim, proline 49 in particular, is involved in the regulation of Tim by auto-inhibition.

We have previously shown that stable expression of active forms of Tim promotes the transformation of NIH 3T3 cells (269). Here, we show that expression of Δ22 and Δ57 Tim robustly induces the formation of foci relative to background levels (vector and wt, Figure 24B). While Δ57 Tim expression does induce the formation of more foci then Δ22 expression, this difference is not statistically significant.

The SH3 domain of Tim is involved in intramolecular auto-inhibitory interactions.

Tim is a member of a subfamily of Dbl-family members that contain an SH3 domain C-terminal to the DH and PH domains, which also includes Ngef, Sgef, Vsm-RhoGEF, neuroblastoma and Wgef (269). Because the poly-proline region in the N-terminus was determined to be required for Tim auto-inhibition, we wanted to test the hypothesis that the C-terminal SH3 domain and the N-terminal poly-proline region are involved in an intramolecular SH3 domain/ligand interaction.

First, we used affinity purification assays to test if the isolated SH3 domain of Tim was able to bind to portions of Tim. The SH3 domain of Tim was able to interact with purified, recombinant Δ22 Tim, while GST alone was unable to interact with Δ22 Tim in this assay. Unexpectedly, Δ57 Tim, in which the poly-proline region has been truncated, was also affinity purified by the isolated SH3 domain of Tim, albeit to a lesser

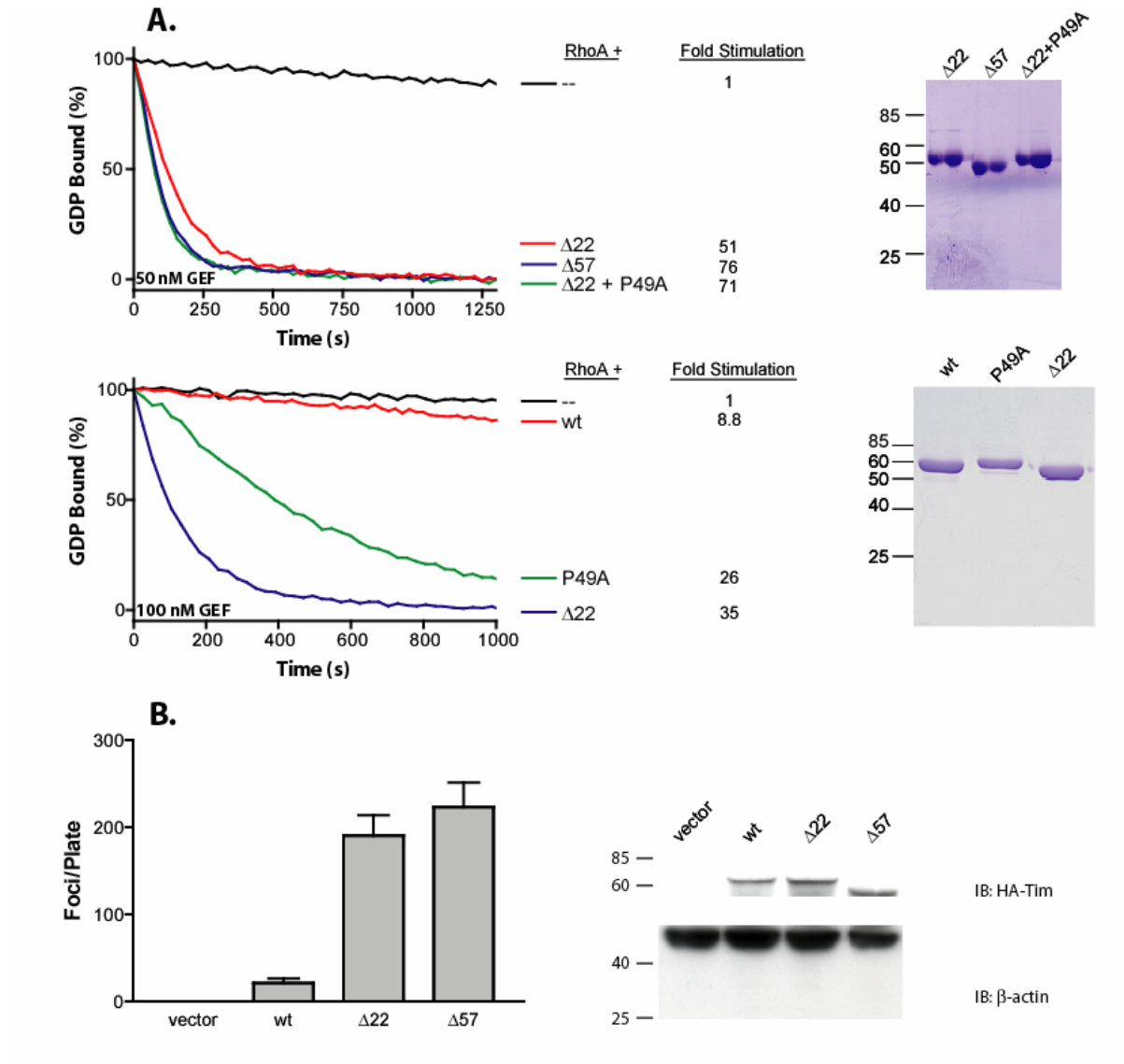

Figure 24: An intramolecular interaction between the SH3 domain of Tim and its N-terminal poly-proline region negatively regulates the exchange potential of Tim.
(A) Upper panel: The region of Tim between the auto-inhibitory motif and the DH domain contains a stretch of proline residues that conform to the consensus sequence of a Type 1A SH3 domain binding ligand. Truncation of these residues (Δ57) or mutation of proline 49 to alanine in the context of a version of Tim lacking the auto-inhibitory helix (Δ22) is slightly activating with respect to Δ22 Tim. The proteins used in the exchange assay are shown at right. **Lower panel:** Mutation of proline 49 to alanine in the context of full length Tim is also activating. Again, the proteins used in the exchange assay are shown at right. **(B)** N-terminally truncated forms of Tim potentiate transformation of NIH 3T3 cells. Data represent the averages of three independent experiments carried out in duplicate. Right panel verifies approximately equal expression of Tim variants used in the focus formation assays.

extent than Δ22 Tim (Figure 25A). These data suggest that the SH3 domain of Tim is able to bind to portions of Tim in both a poly-proline region dependent and independent manner.

To confirm that the isolated SH3 domain interacts with Tim, we performed affinity purification assays from HEK 293 T cell lysates. GST-tagged SH3 Tim, but not GST itself, was able to affinity purify full-length Tim (Figure 25B). Importantly, pre-incubation of the GST-SH3 matrix with a peptide comprising the Tim poly-proline region did not abrogate the interaction between Tim and the SH3 domain, confirming that there are additional binding determinants for the SH3 domain in Tim besides the poly-proline region.

In order to show that the SH3 domain of Tim is able to bind to the N-terminal poly-proline region, we performed surface plasmon resonance experiments (Figure 25C). The purified SH3 domain of Tim was able to interact with a surface composed of the Tim poly-proline region, but not a surface composed of the poly-proline region of its paralog, Ngef, or an unrelated peptide. The interaction between the SH3 domain and the poly-proline region was determined to be of modest affinity (35 μM), although this is a biologically relevant affinity for an intramolecular interaction in which the relative concentrations of the SH3 domain and its ligand would be very high. In addition, GST alone was unable to interact with the surface composed of the Tim poly-proline region at a concentration of 100 μM (data not shown).

To assess whether or not the interactions between the SH3 domain and various other regions of Tim were intramolecular, we attempted to determine if purified Tim is oligomeric in solution. First, we performed sedimentation equilibrium experiments on

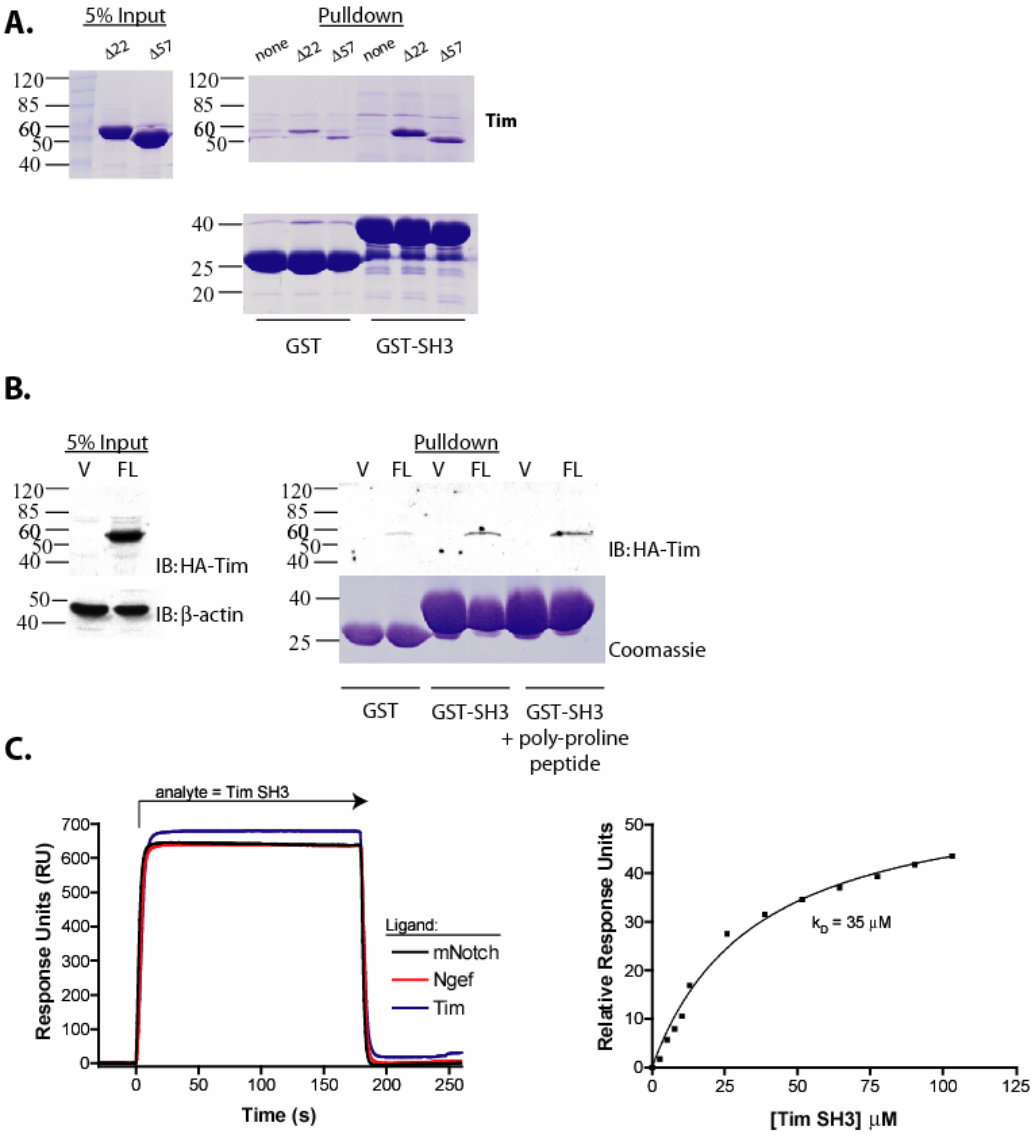

Figure 25: The SH3 domain of Tim interacts with the N-terminal poly-proline region.
(A) GST and a GST-tagged construct containing the SH3 domain of Tim (residues 434 - 519) was immobilized on glutathione-sepharose beads. Purified Tim proteins were incubated with either GST or GST-SH3 beads for a period of 1 hour. The beads were extensively washed and loaded onto an SDS-PAGE gel (right lower panel). Both Δ22 and to a lesser extent Δ57 Tim were affinity purified by GST-SH3 beads, and not GST beads (right upper panel). **(B)** GST-SH3 beads were used to affinity purify full length Tim from lysates of transiently transfected HEK 293T cells. Addition of 0.5 mM of the peptide used in panel C does not abrogate binding of the GST-SH3 to full length Tim, indicating that there are additional binding determinants for the SH3 domain besides the poly-proline region. **(C)** The isolated SH3 domain of Tim interacts with an isolated poly-proline containing peptide. Biotinylated peptides corresponding to the poly-proline region of Tim (residues 39 - 54), the poly-proline region of Ngef (residues 223-233), and a non-proline containing portion of an unrelated protein (mNotch) were synthesized commercially and immobilized to a streptavadin coated sensor chip. Various concentrations of GST-SH3 were flowed over this surface using a BIAcore 3000. The resulting binding isotherms were normalized to the signal achieved due to binding to the unrelated peptide. The apparent kD for this interaction is 35 μM.

purified, recombinant, full-length Tim by analytical ultracentrifugation (Figure 26A). The molecular mass of Tim determined by this experiment (59.8 kDa) is smaller than the calculated molecular mass of Tim (60.0 kDa), indicating that Tim is 100% monomeric in solution. To complement this result, we performed an analytical gel filtration chromatography experiment. Tim eluted as a single peak from this column at a volume corresponding to 60 kDa. In sum, these data indicate that the SH3 domain of Tim is involved in multiple auto-inhibitory intramolecular interactions.

We were unable to assess the consequences of removal of the SH3 domain on the *in vitro* exchange activity of Tim, since both truncation of the SH3 domain and mutation of a conserved tryptophan (W470R) known to be critical for poly-proline ligand binding destabilized Tim upon over-expression in *E. coli*. However, expression of Δ22+W470R Tim in NIH 3T3 cells did not induce formation of foci relative to background levels, despite the fact that Δ22 Tim did induce foci formation in the same experiment (Figure 27A). Indirect immunofluorescence experiments reveal that while Δ22 Tim co-localizes with the actin cytoskeleton in NIH 3T3 cells, Δ22+W470R Tim does not (Figure 27B). These data indicate that the SH3 domain of Tim may play a role in regulation of Tim localization in intact cells in addition to its maintenance of Tim auto-inhibition.

Discussion:

A model for the regulation of Tim by intramolecular and intermolecular interactions is depicted in Figure 28. In the basal state the exchange potential of Tim is auto-inhibited by two sets of intramolecular interactions: the auto-inhibitory helix packing into a conserved pocket on the DH domain and the SH3 domain binding to the N-terminal poly-proline region. This second interaction serves to both stabilize the auto-

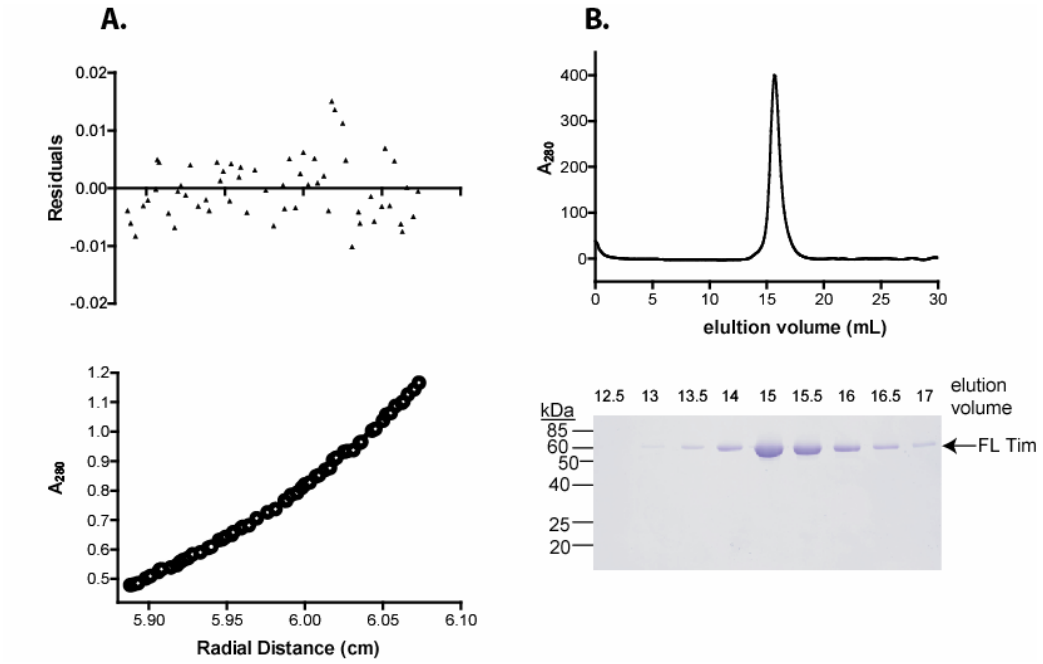

Figure 26: Tim is monomeric in solution.
(A) Residuals (upper panel) and raw data (lower panel) for a sedimentation equilibrium data generated by analytical ultracentrifugation fit to a one-state model. The molecular weight for Tim determined empirically by this experiment is 59.8 kDa. **(B)** Purified Tim elutes from an analytical gel filtration column as a single peak at a volume corresponding to a molecular weight of 60 kDa.

inhibitory helix on the DH domain and to partially occlude the DH domain. Binding of another protein to the SH3 domain, with a higher affinity than that of the SH3 domain for the poly-proline region of Tim, could serve to remove the SH3 domain from that poly-proline region (center). This binding interaction could also localize Tim to the appropriate sub-cellular compartment for nucleotide exchange. Interactions between another unidentified protein and the poly-proline region of Tim could also serve to modulate Tim exchange activity and localization.

With interactions between the SH3 domain and the poly-proline region disrupted, the auto-inhibitory helix would be unstable in the DH domain pocket, increasing frequency of time that the auto-inhibitory helix is solvent-exposed. Src could then phosphorylate the tyrosine residues in the auto-inhibitory helix as previously described (269), both preventing a rebinding event and fully activating the exchange potential of this Dbl-family GEF (Figure 28, right panel). Further work is necessary to identify potential intermolecular binding partners for the Tim SH3 domain and poly-proline region, as well as to determine the molecular details of the intramolecular interaction between the SH3 domain and regions of Tim.

Phenotypic diversity and complexity in biological systems arises from new combinations of proteins and independently-folding protein domains working together as a network, not from new protein functions (300). In fact, multiple sequence analysis of Dbl-family proteins from diverse animal species revealed that GEFs that are composed of an N-terminal SH3 domain followed by a DH/PH cassette, such as Asef1, and GEFs that are composed of a DH/PH cassette followed by an SH3 domain, such as Tim, evolved from a common ancestor composed of only a DH/PH cassette through independent

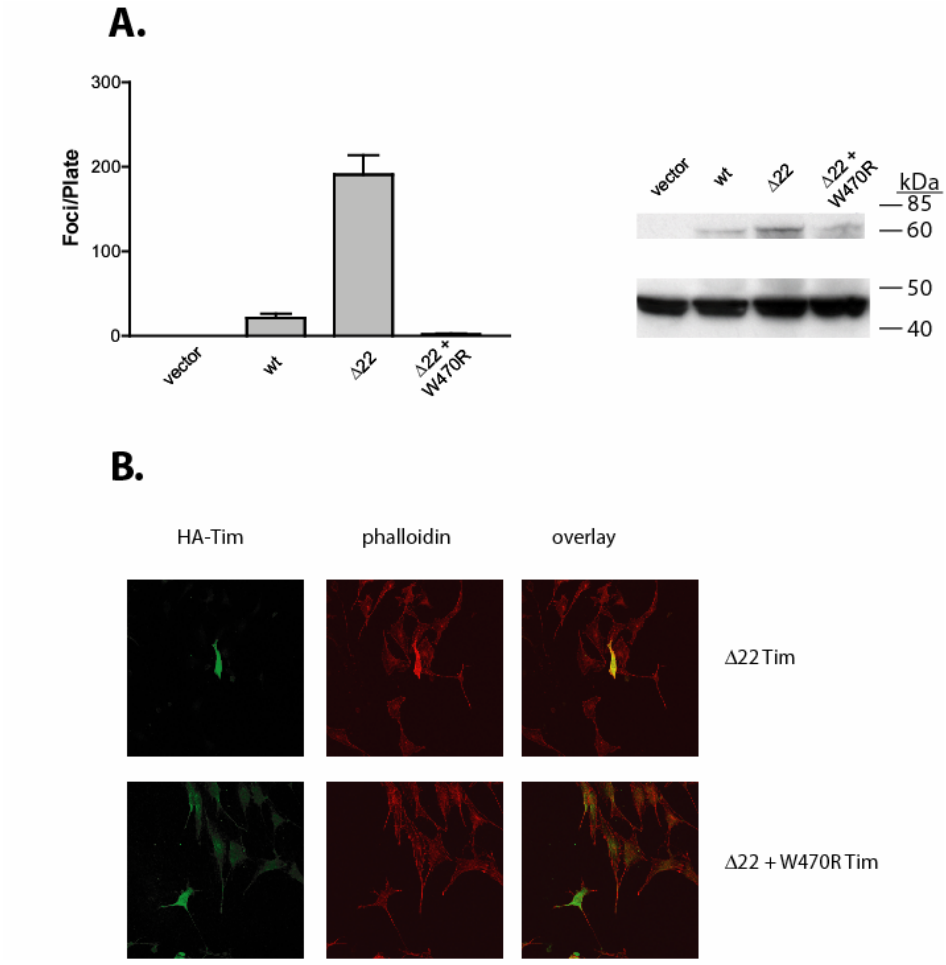

Figure 27: Tim compromised in poly-proline binding is inactive in transformation assays and mislocalized in cells.
(A) Mutation of Tim in the ligand binding pocket of the SH3 domain (W470R) abrogates transformation by Δ22 Tim. Data represent the averages of three independent experiments carried out in duplicate. Right panel verifies approximately equal expression of Tim variants used in the focus formation assays. (B) Indirect immunofluorescence experiments on transfected NIH 3T3 cells reveal that Δ22 Tim colocalizes with the actin cytoskeleton, but Δ22 + W470R Tim is cystosolic.

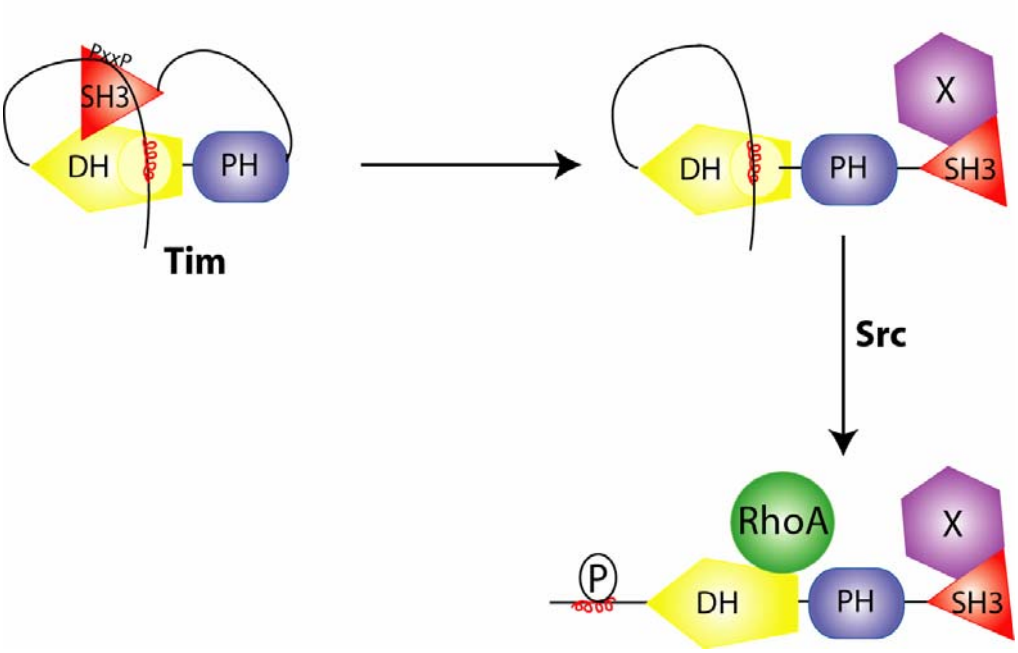

Figure 28: A model for the regulation of Tim by intramolecular and intermolecular interactions. In the basal state (left), the exchange potential of Tim is auto-inhibited by two sets of intramolecular interactions. First, the auto-inhibitory helix (red) packs against a conserved pocket on the DH domain. Second, the SH3 domain binds to the N-terminal poly-proline region. This second interaction serves to both stabilize the auto-inhibitory helix on the DH domain and to partially occlude the DH domain. Binding of protein X (purple) to the SH3 domain, with a higher affinity than that of the SH3 domain for the poly-proline region of Tim, could serve to remove the SH3 domain from that poly-proline region (center). The auto-inhibitory helix would then be unstable in the DH domain pocket, increasing frequency of time that the auto-inhibitory helix is solvent-exposed. The auto-inhibitory helix would then be able to be phosphorylated by Src, preventing a rebinding event, and fully activating the exchange potential of this Dbl-family GEF (right).

insertion of the SH3 domain (301). Since the SH3 domains of both Tim and Asef1 function to regulate the exchange potential of these GEFs by auto-inhibition, it is likely that the evolutionary pressure for the insertion of the SH3 domain was to achieve finer control of the exchange activity of these Dbl-family proteins.

The stabilization of the auto-inhibitory motif on the DH domain of Tim by SH3 domain/poly-proline region interaction, like the auto-inhibitory helix itself, is reminiscent of the mechanism of auto-inhibition of the Vav isozymes. Recent structural characterization of full-length Vav3 by electron microscopy showed that the CH domain of this protein stabilizes the acidic region, including the auto-inhibitory helix, through an intramolecular interaction with the zinc finger domain (157). For both Tim and Vav, then, multiple domains are functioning together to stabilize the inactive state of the catalytic DH domain. While the first interaction, the auto-inhibitory helix, is conserved between Tim and Vav (269), the second interaction is divergent in primary and tertiary structure. If auto-inhibition by interaction of the auto-inhibitory helix with the DH domain is a conserved mechanism of regulation among Dbl-family GEFs, perhaps the second, stabilizing interactions are the mechanism by which specificity of activation is achieved. In fact, these two sets of auto-inhibitory interactions could enable Tim, and Vav, to approximate a logical AND gate (302). In this way, full activation of Tim would not occur unless both sets of auto-inhibitory interactions were removed, thus allowing a large degree of spatiotemporal control of Tim activation.

CHAPTER 5: GENERAL CONCLUSIONS AND FUTURE DIRECTIONS

The studies described here identify a conserved mechanism for the basal auto-inhibition and phosphorylation-dependent activation of the exchange potential of Tim and Ngef. In particular, these Dbl proteins are auto-inhibited by a short N-terminal helix that directly interacts with a conserved surface of the DH domain to prevent the binding of GTPases necessary for guanine nucleotide exchange and GTPase activation. Phosphorylation of the auto-inhibitory helix disrupts interactions with the DH domain and frees the conserved surface of the DH domain for subsequent GTPase activation. This model of regulation has been borne out by several experimental lines of evidence. For example, using an *in vitro* guanine nucleotide exchange assay, cell-based GTPase activity assays, and assays for cellular transformation, we determined that auto-inhibition of Tim is relieved by truncation, mutation, and Src- or EphA4-mediated phosphorylation of the N-terminal helical motif. Similar results are seen with the Tim homolog, Ngef. Finally, we show that Tim is constitutively activated by substitutions within their DH domains designed to disrupt interactions with the N-terminal auto-inhibitory helix while preserving intrinsic exchange activity. Lines of experimentation that are designed to more fully characterize the function and regulation of Tim and Ngef are described in the following sections.

Extend the concept of auto-inhibition mediated by a small, conserved sequence motif to other Dbl-family GEFs.

Several observations presented here suggest that other Dbl-family proteins may be regulated similarly to Tim. First, one mechanism by which the distantly-related Vav isozymes are regulated is through phosphorylation of an auto-inhibitory helix homologous to that of Tim. Second, while many of the conserved surface sites on DH domains overlap with sites known to contact GTPases in nucleotide-depleted complexes, several of the most conserved positions overlap instead to points of contact between the DH domain of Vav1 and its inhibitory helix as determined by NMR. Indeed, the deep cavity used by Vav1 to sequester Tyr 174 of its auto-inhibitory helix is preserved in all of the other DH domain structures that have been solved to date (Figure 15A). It seems extremely likely that other Dbl-family proteins also use this cavity to sequester large aromatic or hydrophobic residues that are part of similar auto-inhibitory motifs. Finally, the guanine nucleotide exchange activities of a majority of Dbl-family proteins are increased upon N-terminal truncation (see Table 1). Indeed, truncated forms of many Dbl-family proteins have been isolated as oncogenes capable of constitutively activating Rho-family GTPases, leading to cellular transformation (10). It is likely that these truncation events involve the removal of short inhibitory sequences that would normally pack against the DH domain to prevent GTPase binding and activation.

Identifying other Dbl family members that are regulated by auto-inhibition and phosphorylation in a manner similar to Tim, Ngef and the Vav isozymes is an important line of future research. We would like to begin by confirming that other members of the Tim subfamily are regulated in this manner. We have extended our analysis to include

Wgef. Truncation of the auto-inhibitory helix of Wgef (Δ302) is activating *in vitro* and in affinity purification assays using nucleotide-free RhoA as the affinity matrix. In addition, Wgef behaved similarly to Tim in that mutation of its auto-inhibitory helix (Y295E, analogous to Y19E in Tim) and its DH domain (S394A; analogous to S114A in Tim) activated a truncated form of Wgef (Δ285) containing the auto-inhibitory region (Figure 29A). Wgef, like Tim and Ngef, is inhibited by a peptide derived from the auto-inhibitory helix of Tim (Figure 29C) and is activated by Src phosphorylation *in vitro* (Figure 29D).

In order to establish that all of the members of the Tim subfamily are regulated by auto-inhibition, the regulation of the remaining members of that subfamily, Sgef, Vsm-RhoGEF and neuroblastoma, must be studied. Of these three remaining Tim subfamily members, we have attempted to study only Vsm-RhoGEF and Sgef thus far. We have been unsuccessful at generating soluble Vsm-RhoGEF after expression in *E. coli*. While we are able to express and purify Sgef, we are unable to detect Sgef activity in our *in vitro* exchange assay. The regulation of these exchange factors will have to be studied in cellular assays, such as affinity purifications using nucleotide free forms of their cognate GTPases (RhoA for Vsm-RhoGEF and RhoG for Sgef).

Ultimately, in order to establish the generality that auto-inhibition as well as catalytic nucleotide exchange activity is embedded within the most conserved surface of DH domains, we must identify a Dbl-family protein outside of the Tim and Vav subfamilies that is regulated in this manner. We decided to target several Dbl-family proteins for scrutiny, namely: Tiam1, GEF-H1 and FRG. These proteins fulfill several criteria required of this hypothesis. Tiam1 (149) and FRG (46,47) are excellent

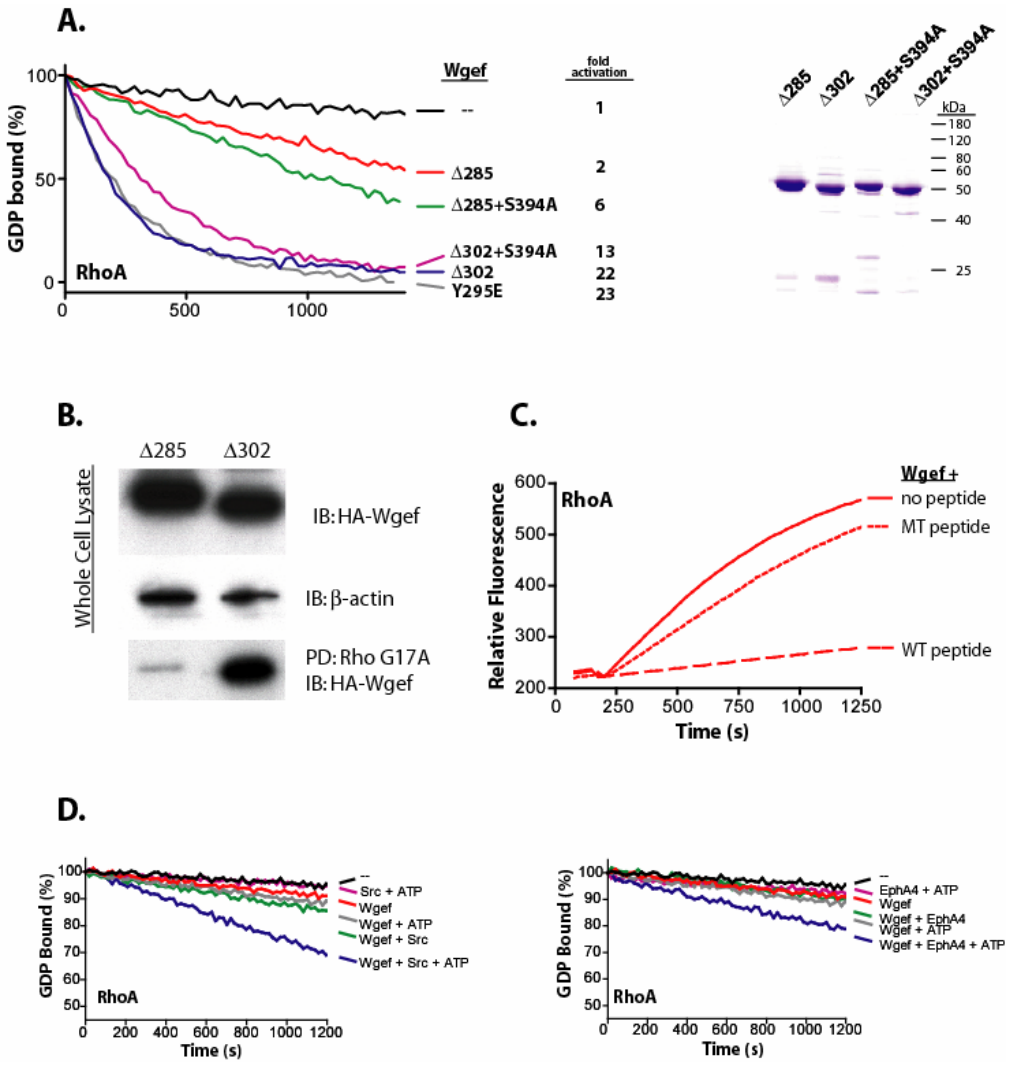

Figure 29: Wgef is regulated by auto-inhibition and phosphorylation.
(A) The exchange of GDP bound to RhoA and catalyzed by 50 nM Wgef was measured using a standard fluorescence-based assay (245,246). Fold-activation is relative to the spontaneous loading of guanine nucleotide and represents the average of two independent reactions for each trace. Equal amounts (2 μg) of purified proteins used in the exchange assays are shown at right following SDS-PAGE and staining with Coomassie brilliant blue. **(B)** The activity of Wgef constructs transiently expressed in quiescent COS7 cells was assessed by a pulldown assay using GST-tagged nucleotide-free RhoA as the affinity purification matrix. Levels of active Wgef were determined by immunoblotting the pulldown samples. Immunoblots of the total cell lysate (2.5% input shown) show approximately equal expression of the Wgef constructs. **(C)** Wgef (Δ302) was incubated with either a peptide corresponding to the N-terminal auto-inhibitory region of Tim (WT, biotin-SQLLYQEYSDV-amide) or a mutant peptide (MT, biotin-SQLLEQEYSDV-amide) at room temperature for 20 minutes. The resulting complexes were assayed for their ability to stimulate loading of mant-GTP onto RhoA. The peptide concentrations were 100 μM, Wgef concentrations were 50 nM. **(D)** Phosphorylation of Wgef by Src (left) or EphA4 (right) promotes the capacity of Wgef to catalyze nucleotide exchange on RhoA. Auto-inhibited Wgef (Δ285) was incubated with combinations of kinase and ATP as indicated for thirty minutes prior to addition of the mixtures to exchange reactions.

substrates for Src-family kinases and in both cases phosphorylation is associated with increased levels of activated GTPases. The case for the physiological relevance of Src-mediated phosphorylation is especially compelling for FRG since cell-cell adhesions initiated by homotypic clustering of nectins recruits and activates Src, which subsequently is required for the recruitment and phosphorylation of FRG. Phosphorylated FRG is then responsible for enhanced levels of GTP-bound Cdc42. The case for Tiam1 phosphorylation by Src is less clear, although stimulation of cells with BNDF leads to an association of Tiam1 with the receptor for BNDF, TrkB. TrkB directly phosphorylates Tiam1 at a tyrosine residue in the RBD, Y829, and this phosphorylation leads to an increase in Tiam1 exchange activity (150). GEF-H1 is also phosphorylated *in vivo*, although it is not known if phosphorylation correlates with active GTPase levels (85). The functional relationship between phosphorylation and GTPase activation is not understood for any of these Dbl-family GEFs.

We have identified sequence motifs in all three proteins with high conservation to the regions in Vav and Tim required for regulated auto-inhibition (Figure 30A). Consistent with a general mode of inhibition typified by Vav and supported by our preliminary data with Tim, the short spans in Tiam1, GEF-H1 and FRG are: ***a)*** located N-terminal to their respective DH domains, ***b)*** all predicted to be helical with high confidence, and ***c)*** predicted to be excellent substrates for tyrosine phosphorylation. For Tiam1 (165) and GEF-H1 (131), N-terminal truncations that remove these putative auto-inhibitory regions result in transforming phenotypes. Tiam1 also has been shown to be phosphorylated within this motif (150).

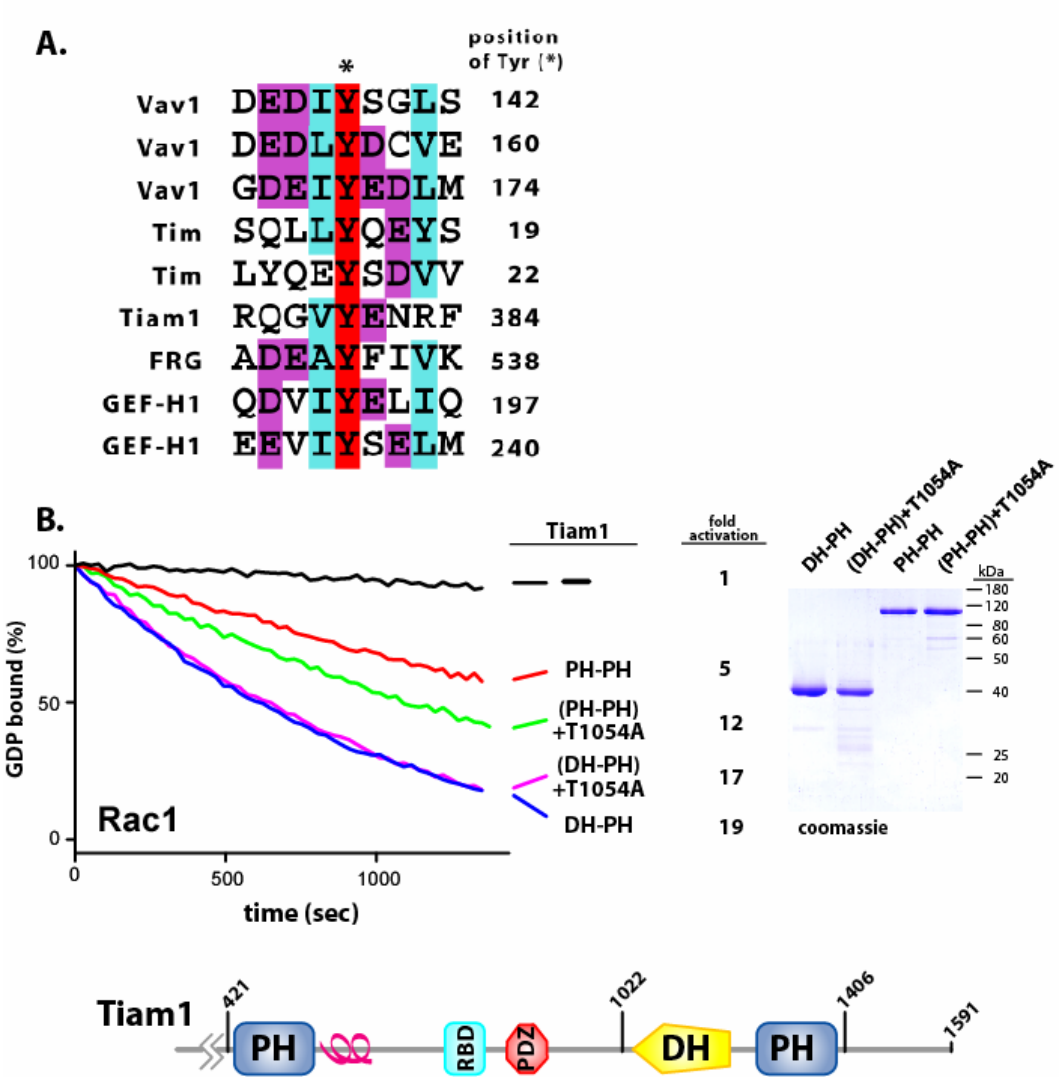

Figure 30: Tiam1 is regulated by auto-inhibition.

(A) Regions in Vav1 and Tim responsible for auto-inhibition of exchange activity were aligned with ClustalX along with similar regions in Tiam1, FRG, and GEF-H1. The asterisk above the alignment marks the tyrosines in Vav1 and Tim that when phosphorylated relieve inhibition and these positions are numbered to the right of the alignment. Analogous tyrosines in the other GEFs are also numbered. **(B)** Mutation of the Tiam1 DH domain (T1054A) is activating within a large fragment (PH-PH) of Tiam1; but has no effect on the DH-PH fragment. The domain architecture of Tiam1 is presented below. Panel to the right indicates equal amounts (2 μg) of the assayed proteins submitted to SDS-PAGE followed by staining with Coomassie brilliant blue. Also depicted is a schematic of the domain architecture of Tiam1.

Unfortunately, we have been unable to purify active forms of GEF-H1 and FRG to test the hypothesis that these Dbl-family proteins are regulated by the motifs identified in Figure 30A. However, we have been able to establish that a long form of purified Tiam1 (PH-PH; similar to the well-studied version C1199) that includes all its known domains is auto-inhibited relative to the minimal DH-PH fragment necessary for guanine nucleotide exchange (Figure 30B). We have been unable to show that introduction of a phosphomimetic mutation in the potential auto-inhibitory motif affects the exchange activity of Tiam1 (Y829E, data not shown). However, introduction of T1054A, analogous to S114A in Tim, was partially activating in the auto-inhibited form of Tiam1, while having no effect on the exchange activity of the shorter fragment (Figure 30B). These analyses indicated that Tiam1 is also auto-inhibited and that this auto-inhibition can be partially relieved by mutation of the DH domain without affecting the intrinsic exchange mechanism.

The cumulative data strongly suggest that the most conserved surface of DH domains serves two separable, but functionally linked purposes. Most obviously, this conserved surface is designed to engage Rho GTPases to catalyze nucleotide exchange and consequent GTPase activation. Second, and less obviously, this conservation appears built into DH domains in order to provide for auto-inhibition of guanine nucleotide exchange. It remains to be determined how extensively these dual functions are linked, but the preliminary data presented here suggests that this linkage may be wide-spread throughout the family of Dbl proteins and will be useful in understanding the various processes, such as truncations and phosphorylations, that are known to activate many of the Dbl-family proteins.

Define the molecular details of the auto-inhibited form of Tim or a closely related Dbl-family member using protein crystallography.

We have used site-directed mutagenesis coupled with *in vitro* and cellular functional assays to define the auto-inhibitory helix of Tim, as well as a region of the DH domain important for binding the auto-inhibitory helix to maintain a basal level of Tim activity. However, the precise composition of the DH domain pocket that accepts the auto-inhibitory helix and the nature of the auto-inhibitory interactions involving the Tim SH3 domain will not be elucidated without determining the atomic-resolution crystal structure of the auto-inhibited form of Tim or one of its closely-related homologs. Unfortunately, Tim and its homologs have been recalcitrant to crystallize in initial screens. Future crystallization experiments include attempting to improve crystallization by removing the loop region between the poly-proline region and the extended DH domain in these proteins. This region has no identifiable secondary structure and is not part of a known consensus regulatory motif or phosphorylation site, and therefore deletion of this region is not expected to activate the exchange potential of these Dbl-family proteins. Additionally, we will attempt to improve crystallization by decreasing the conformational heterogeneity of surface residues by site-directed mutagenesis (303).

Once preliminary diffraction experiments indicate that crystals are tractable, cryo-cooling conditions will be found for collection of a complete data set from a single crystal. Initial attempts to obtain phases associated with the diffraction data will involve molecular replacement using either the programs AMoRe (304) or Beast (305). Search models for molecular replacement will include isolated DH and PH domains derived from structures previously determined in this lab (94,225,245) or others (306-308), as

well as the SH3 domain of Vav1(309). If necessary, fragments encompassing both DH and PH domains will be used; however, these search models will not be favored given the unusually high degree of conformational flexibility originating from the hinge region between DH and PH domains (310).

Should molecular replacement fail, phase information will be generated using conventional techniques including heavy atom derivatization of native crystals or production of seleno-methionine incorporated proteins to be used for MAD data collection (311). Given the fact that all forms of Tim and its closely related members proposed for study in this application are currently being expressed and purified from bacteria, structure determination by MAD using seleno-methionine-incorporated proteins will be the favored route. Model building and refinement will use the interactive molecular graphics program O (312) and the X-PLOR suite of crystallographic programs. Geometry and stereochemistry of the final model will be confirmed with PROCHECK (313).

Establish the physiological relevance of Tim phosphorylation by Src.

We have shown that Tim is directly phosphorylated by Src *in vitro*, as well as when co-expressed with a constitutively active mutant of Src in SYF cells. However, whether endogenously expressed Tim is phosphorylated upon activation of endogenous tyrosine kinases has yet to be determined. To attempt to answer this question, we created and characterized a polyclonal antibody directed at full-length Tim. This antibody is capable of detecting over-expressed Tim protein in immunoblot, immunoprecipitation and indirect immunofluorescence experiments (Figure 31). In addition, the anti-Tim

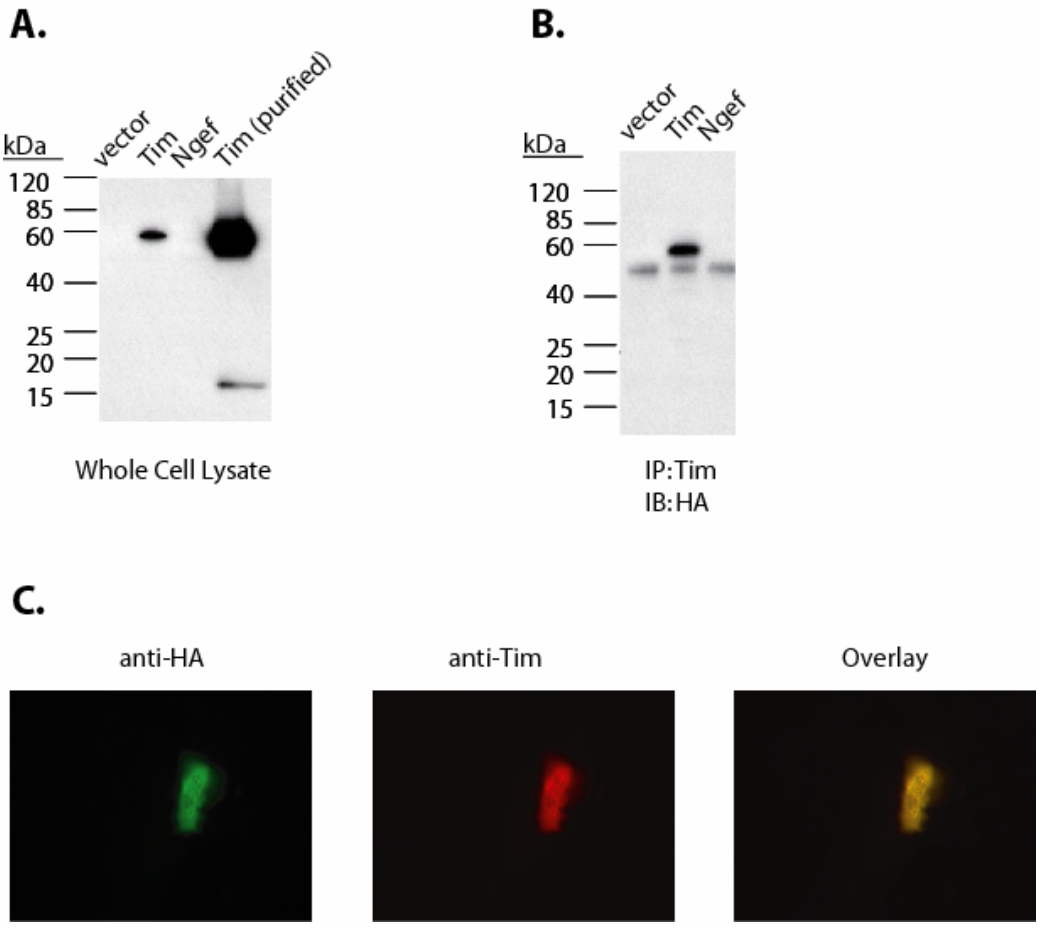

Figure 31: Characterization of a polyclonal antibody specific for Tim.

(A) A polyclonal antibody was generated using full-length Tim as the immunogen. This antibody was capable of detecting HA-tagged Tim, but not the highly related Ngef, in 1 μg of COS7 cell lysate. **(B)** 1 μL of anti-Tim antibody was able to immunoprecipitate HA-Tim from 100 μg of COS7 cell lysate, but not HA-Ngef. **(C)** HA-tagged Tim was over-expressed in COS-7 cells and visualized by indirect immunofluorescence experiments. The signal derived from the anti-HA primary antibody and Alexa 488-conjugated anti-mouse secondary antibody overlapped completely with the signal derived from the anti-Tim primary antibody and Alexa-546 conjugated anti-rabbit secondary antibody.

antibody was able to detect endogenously expressed Tim in HEK 293T cell lysates (data not shown).

To establish if endogenously expressed Tim is phosphorylated in the context of an intact cell, we treated HEK 293T cells with 10 μM pervanadate for various time points, prior to lysing the cells. We then immunoprecipitated Tim with the anti-Tim antibody and analyzed the immunoprecipitates by SDS-PAGE followed by immunoblotting with an anti-phosphotyrosine antibody. As few as ten minutes of treatment with pervanadate, which inhibits cellular tyrosine phosphatases (314), led to an increase in the amount of tyrosine phosphorylation of Tim (Figure 32). Tyrosine phosphorylation of Tim appeared to be Src-dependent, since treatment of the HEK 293T cells with PP2, a Src inhibitor, prior to the pervanadate treatment abrogated Tim tyrosine phosphorylation (Figure 32).

Although the experiments described above establish that endogenously expressed Tim is tyrosine phosphorylated in a Src-dependent manner, they do not establish the upstream signaling pathways that lead to Tim phosphorylation. Interestingly, fetal bovine serum does not contain any growth factor components that lead to Tim phosphorylation (data not shown). The Tim homologs, ephexin and Vsm-RhoGEF, interact with and are tyrosine phosphorylated downstream of the EphA4 receptor tyrosine kinase (77,80), and we have previously shown that Tim is directly phosphorylated by the kinase domain of EphA4 *in vitro*. Therefore, we anticipate that Tim phosphorylation is stimulated by an ephrin ligand binding to EphA4. This hypothesis will be tested by transfecting HEK 293 cells with an HA-tagged version of EphA4, treating these cells with an ephrinA3-Fc fusion protein that has been pre-clustered by incubation with an ant-Fc antibody, and performing immunoprecipitation and immunoblotting experiments as

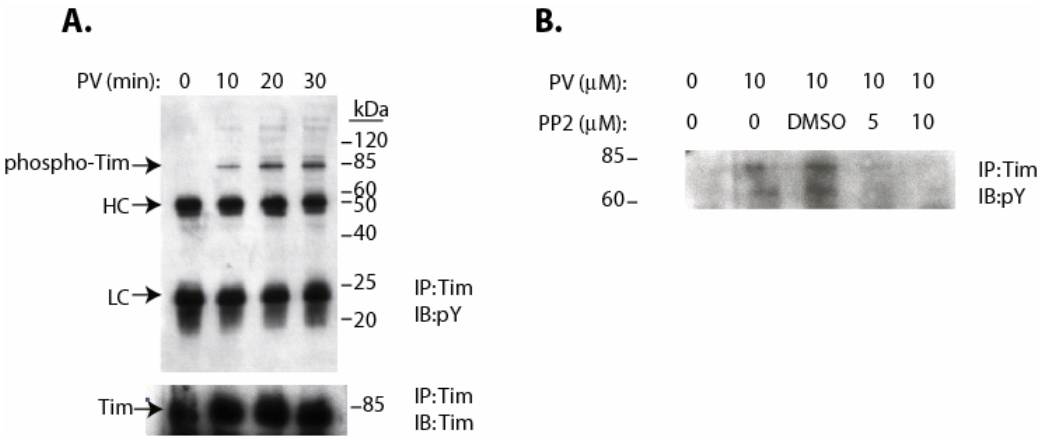

Figure 32: Phosphorylation of endogenous Tim upon activation of endogenous tyrosine kinases.

(A) HEK 293 T cells, which express Tim endogenously, were treated with pervanadate for various time periods, prior to lysis and immunoprecipitation of Tim. Immunoprecipitates were analyzed by Western blot using anti-phosphotyrosine and anti-Tim antibodies. **(B)** HEK 293 T cells were treated with various concentrations of the Src inhibitor, PP2, for two hours prior to treatment with pervanadate for 30 minutes. Tim was immunoprecipitated from the resulting cell lysates and the immunoprecipitates were analyzed as above.

were described above for pervanadate treatment. Additionally, we will identify a cell line that expresses Tim, EphA4 and Src endogenously, treat these cells with pre-clustered ephrinA3-Fc and perform similar experiments. Current candidate cell lines include the CaCo2 and MIA Paca2 cell lines, both of which are predicted to express all three proteins of interest.

Identify mechanisms for down-regulating Tim activity.

We have identified several mechanisms by which Tim exchange activity can be up-regulated, namely truncation or mutation of the auto-inhibitory helix, Src phosphorylation of the auto-inhibitory helix and mutation of the surface of the DH domain involved in binding to the auto-inhibitory helix. However, we have yet to identify mechanisms by which Tim exchange activity can be down-regulated. Importantly, a tyrosine phosphatase that might remove phosphate groups from Tyr 19 and Tyr 22 has yet to be identified.

Tim has recently been identified as a substrate for direct serine/threonine phosphorylation by Pak2 (A. Beeser and J. Chernoff, personal communication). Phosphorylation of an activated version of Tim (Y19E+Y22E) by Pak2 decreases its exchange activity *in vitro* (Figure 33). Current studies are aimed at determining the specific residue(s) of Tim that are phosphorylated by Pak, in order to define a mechanism for this inhibition of exchange activity.

Tim phosphorylation and inhibition by Pak2 would represent one of many mechanisms by which activation of Rac, for which Group I Pak family members are downstream effectors, leads to the inactivation of RhoA. Indeed, many such examples of crosstalk between the signaling pathways of the Rho GTPases have been identified. For

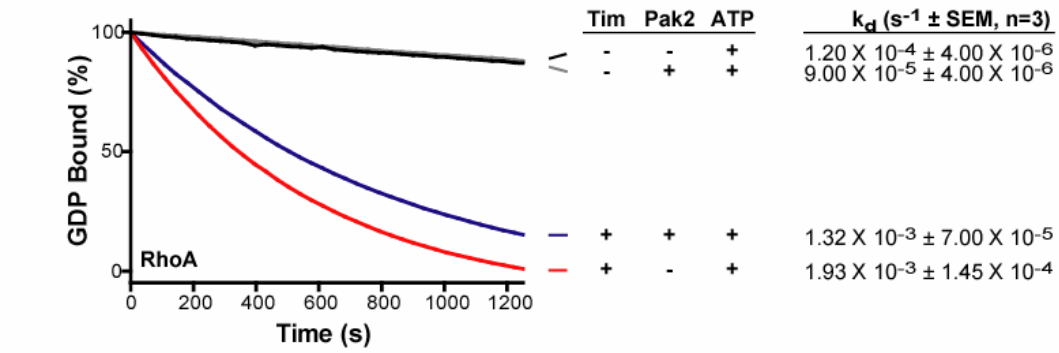

Figure 33: Tim is phosphorylated and inhibited by Pak2.

15 μg of activated Tim (Y19E+Y22E) were incubated with ATP in the presence or absence of 6 μg of Pak2 for 30 min at 30 degrees prior to analysis in a fluorescence-based guanine nucleotide exchange assay as indicated. In the exchange assay, one fifth of the kinase assay reaction (a final [Tim] of 50 nM) was added to 200 nM RhoA, which had been pre-loaded with BODIPY-labeled GDP. The rate of guanine nucleotide exchange was monitored as a decrease in fluorescence intensity over time as the labeled GDP is released into solution, where it is quenched. The resulting curves were fit to an exponential decay model, and the rate of dissociation of guanine nucleotide is shown above (values represent the mean and standard error of the mean for three independent exchange assays from the same kinase assay).

example, Rac-mediated production of reactive oxygen species (ROS) leads to inhibition of low molecular weight protein tyrosine phosphatase, an increase in phosphorylation and activation of p190-RhoGAP and subsequent inhibition of RhoA (315). Pak1 phosphorylation of the Dbl-family GEF, GEF-H1, on Ser 885 leads to a decrease in its exchange activity towards RhoA due to an increase in its association with the phospho-serine binding protein 14-3-3 (9). Most recently, Rac has been shown to inhibit Rho activation in response to thrombin stimulation of endothelial cells through activation of Pak, which phosphorylates and inactivates p115-RhoGEF (118). Interestingly, Rho activation can inhibit Rac activation in a similar manner. The Rho effector, p160-ROCK, phosphorylates and decreases the activity of the Rac specific exchange factor, Tiam2 (148). Phosphorylation of Dbl-family proteins by the serine/threonine kinase effector proteins of Rho GTPases, then, may be a general mechanism by which activation of one Rho GTPase leads to a decrease in the activity level of another Rho GTPase.

Identify a small molecule inhibitor of Tim.

We have shown that Tim (Figure 12), as well as the highly related proteins Ngef (Figure 19) and Wgef (Figure 29), is effectively inhibited by high concentrations (100 μM) of an 11-mer peptide based upon its auto-inhibitory helix. However, substitution of a key tyrosine residue within this peptide renders the peptide inactive as an inhibitor of exchange activity. In addition, this peptide inhibitor seems to be relatively selective for the Tim subfamily of exchange factors, since it is inactive on an unrelated protein, Trio (Figure 34A). Finally, the inhibition of Tim by the 11-mer peptide is sensitive to the dose of peptide used, and the IC50 for the 11-mer is approximately 50 μM. A 7-mer peptide derived from the original 11-mer sequence is 10-fold less active (Figure 34B).

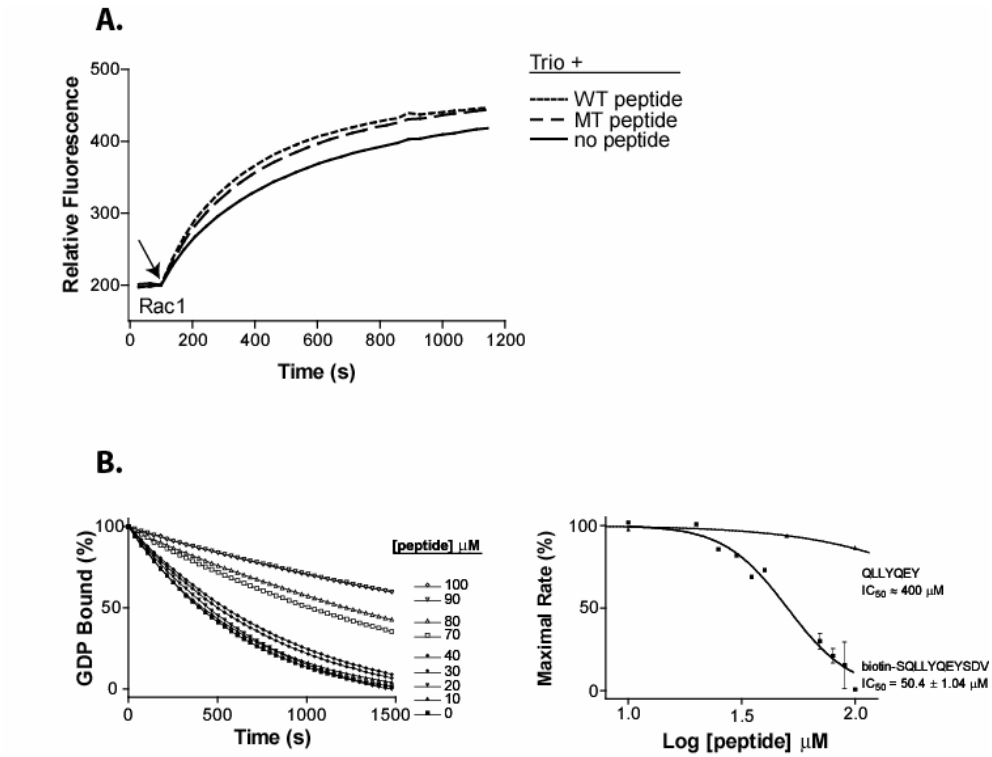

Figure 34: The peptide inhibitor is specific for Tim subfamily GEFs.

(A) Trio (DHPH1) was incubated with the WT and MT peptides used in Figure 12. The resulting complexes were assayed for their ability to stimulate loading of mant-GTP onto Rac1. **(B)** Tim (Δ22) was incubated with various concentrations of an 11-mer peptide (biotin-SQLLYQEYSDV-amide), or a 7-mer peptide (acetyl-QLLYQEY-amide). The resulting complexes were assayed for their ability to stimulate loading of GTP on RhoA that had been pre-loaded with BODIPY-labeled GDP (left). The exchange assay curves were fit to an exponential decay model. The rates of dissociation were normalized and presented at right.

Alanine scanning mutagenesis experiments have revealed that Tim is regulated in a manner similar to the Vav isozymes, and the auto-inhibitory helix of Tim exhibits significant sequence identity to the auto-inhibitory helix of Vav1. Importantly, the critical Vav residues Ile 173, Tyr 174 and Leu 177, which make hydrophobic contacts near the active site of Vav to sterically occlude the active site of the DH domain, are functionally conserved in the Tim auto-inhibitory helix by Ile 18, Tyr 19 and Tyr 22. These residues are present at positions 4, 5 and 8 of the inhibitory 11-mer peptide. A synthetic agent able to reproduce the *I Y x x Y* (where X is any amino acid) sequence while maintaining the conformation of one turn of an α-helix has the potential to also function as an inhibitor of constitutively active Tim.

Several candidate peptidomimetic compounds based on the auto-inhibitory helix of Tim were synthesized and tested for their ability to inhibit the exchange activity of Tim *in vitro* (Figure 3 A through G). Of these, one compound in particular, 3,5-benzyloxy-N-isobutyl benzamide (PW6_053) inhibited Tim in a dose-dependent manner with an IC50 of approximately 30 μM (Figure 35). In this compound, the two benzyl groups function to mimic the two tyrosines in the auto-inhibitory helix (positions *i+1* and *i+4*), with the isobutyl group mimicking the isoleucine (position *i*). Experiments are currently underway to improve the water solubility and the efficacy of this potential Tim inhibitor.

Establish a role for Tim in tumorigenesis.

We have identified several mechanisms by which Tim is regulated, auto-inhibition and tyrosine phosphorylation, however, the cellular functions of Tim are

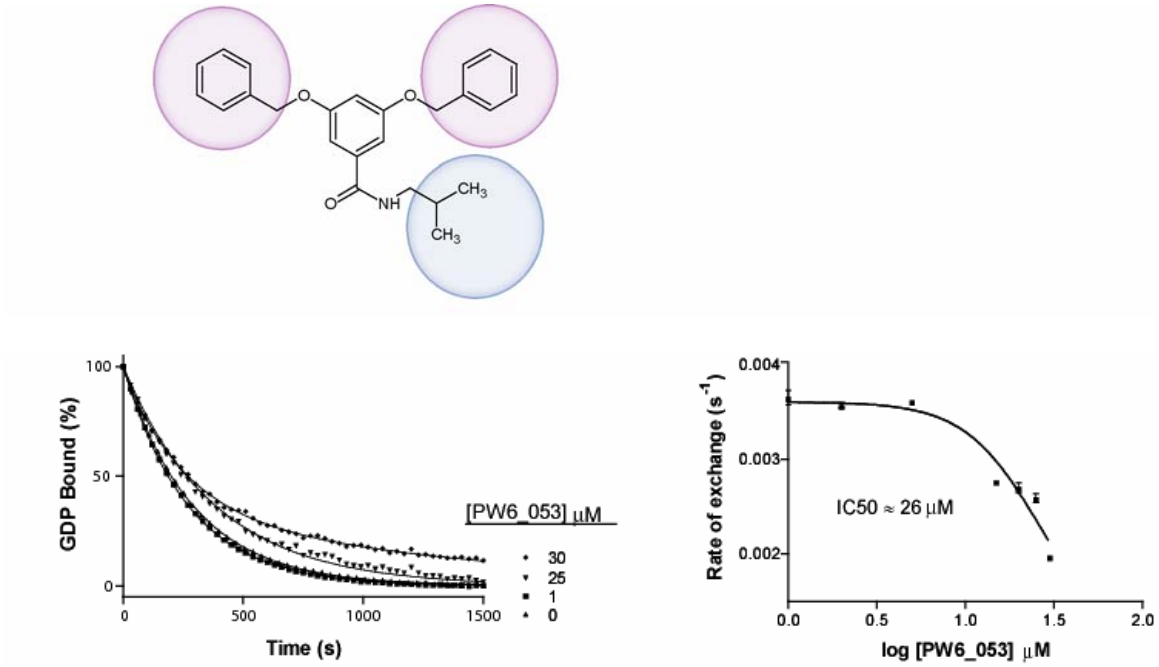

Figure 35: PW6_053 is a peptidomimetic Tim inhibitor

The ability of Tim (Δ22) to stimulate loading of GTP on RhoA that had been pre-loaded with BODIPY-labeled GDP in the presence of various concentrations of compound PW6_053 was assessed. The resulting curves were fit to an exponential decay model. The rates of dissociation are presented at right. Also depicted is the chemical structure of PW6_053. The phenyl groups (purple) function as tyrosine mimetics, while the isobutyl group (blue) functions to mimic isoleucine.

largely unknown. Importantly, although Tim was originally identified as an oncogene, its role in tumorigenesis has yet to be established.

The EphA4 receptor tyrosine kinase was recently shown to be up-regulated in pancreatic ductal adenocarcinoma (PDAC) cells. Knocking down expression of EphA4 in these cells using siRNA decreased the viability of these cells, and conversely, over-expressing EphA4 in these cells increased their growth rate. Finally, it was also established that a ligand for EphA4, ephrin A3, is also over-expressed in these cells (316). Since Tim is highly expressed in the pancreas (44), and since we believe Tim to be part of a signal transduction pathway downstream of EphA4, we would like to study the role of Tim in pancreatic cancer development.

To this end, we would like to investigate whether Tim is expressed in PDAC cell lines and primary tumors using the anti-Tim antibody described above. Affinity purification experiments using GST-tagged rhotekin could be used to ascertain the level of RhoA activity in these cell lines and tumor samples. Additionally, we would like to use RT-PCR, using previously established primers for the Tim mRNA (244), coupled with direct nucleotide sequencing to determine if the Tim expressed in PDAC cell lines and tumors harbors mutations in the auto-inhibitory helix or DH domain that we would expect to be auto-activating based upon our understanding of the mechanism by which Tim is regulated. Should we find a cell line that expresses Tim, we would like to determine if knocking down expression of Tim, or inhibition of Tim activity with a small molecule, affects the ability of this cell line to proliferate or grow in the absence of adherence to the extracellular matrix.

Identify the functional consequences of Ngef activation of Rac1 in neurons.

We have used functional *in vitro* and cellular assays to show that truncation, mutation or phosphorylation of the auto-inhibitory helix of Ngef activates this Dbl-family GEF toward its entire repertoire of cognate GTPases, RhoA, Rac1 and Cdc42. These data are in contrast with experiments describing the regulation of the mouse paralog of Ngef, ephexin. Several lines of future experimentation are aimed at resolving this discrepancy. We will study the spatio-temporal dynamics of Ngef localization in primary cortical neuron progenitor cells in order to determine if Ngef is properly localized in the cell to activate Cdc42 as well as RhoA. We are working in collaboration with Dr. Prithwish Pal in the laboratory of Dr. Klaus Hahn to develop novel fluorescent biosensors for Ngef in the activated state. These sensors will be used in conjunction with the biosensors for activated RhoA and Cdc42 previously developed in the Hahn lab (317), as well as with traditional immunofluorescence techniques to resolve the localization of the total pools of RhoA, Cdc42 and Ngef in these cells.

In addition, it has been shown that ephrin induced growth cone collapse is dependent on Vav2 activation of Rac1. Active Rac1 in this context promotes internalization of the membranes in which both the ligand ephrin and the receptor EphA4 are localized via a unique endocytosis event (282). Our future experiments include investigating if ephexin/Ngef activation of Rac1 can function in this pathway. We will treat primary cortical neuron progenitor cells from ephexin -/- knockout mice with either pre-clustered ephrin A1-Fc or Fc alone prior to fixing the cells and blocking them in either the presence or absence of a permeabilizing agent, the detergent, TritonX-100. We will then visualize the surface (unpermeabilized cells) or total (permeabilized cells)

ephrin A1-Fc by indirect immunofluorescence using a Cy3-conjugated anti-human Fc antibody. We anticipate that the cells derived from the ephexin -/- mice will display more surface ephrin A1-Fc than cells derived from wild type mice due to impairment of activation of Rac1 and subsequent inhibition of Rac1-mediated endocytosis of the ephrin/Eph complex.

Identify binding partners for the SH3 domain and poly-proline region of Tim.

We have established that the exchange potential of Tim is auto-inhibited by two sets of intramolecular interactions: the auto-inhibitory helix packing into a conserved pocket on the DH domain and the SH3 domain binding to the N-terminal poly-proline region. Binding of another protein to either the poly-proline region or the SH3 domain, could serve to activate the exchange potential of Tim. The identification of such interacting proteins is an important future aim.

We plan to transfect HEK 293T cells, which express Tim endogenously and therefore are likely to also express proteins that interact with Tim, with HA-tagged wild type Tim, or HA-tagged versions of Tim with mutations in the poly-proline region (P49A) or the SH3 domain (W470R) that are expected to prevent these regions from binding to proteins containing SH3 domains or poly-proline regions, respectively. We will then affinity purify Tim-containing protein complexes on an anti-HA matrix, and analyze these protein complexes by SDS-PAGE followed by Coomassie or silver staining. Bands present in the immunoprecipitates of HA-Tim, but not HA-Tim (P49A) or HA-Tim (W470R) will be trypsin digested and identified by liquid chromatography and mass spectrometry.

Summary:

We have shown that the Dbl-family protein, Tim, is a RhoA, RhoB and RhoC-specific GEF that is auto-inhibited by a putative helix N-terminal to the DH domain, which directly binds the DH domain to sterically exclude Rho GTPases and prevent their activation. This auto-inhibition is relieved by truncation, mutation, or phosphorylation of the auto-inhibitory helix, or by mutation of the conserved surface of the DH domain to disrupt interactions with the auto-inhibitory helix. Since inhibition of Tim can be restored by addition of the auto-inhibitory helix *in trans*, the auto-inhibitory helix is necessary and sufficient for maintenance of a basal state of Tim activation.

We have also demonstrated that Ngef is activated towards its full repertoire of cognate GTPases, namely RhoA, Rac1 and Cdc42, by removal, substitution or Src-dependent tyrosine phosphorylation of a small, conserved sequence N-terminal to its DH domain. This work is in contrast to published studies, which show that phosphorylation of the mouse paralog of Ngef, ephexin, activates this GEF toward only RhoA. Ngef exchange activity is inhibited by a peptide derived from the auto-inhibitory sequence of Tim, indicating that these two proteins are regulated in a near identical manner. The exchange activity of Ngef, and its Rho-specific exchange activity in particular, functions to inhibit axon outgrowth in developing neurons.

Finally, we have shown preliminary data that indicate that Tim is also auto-inhibited by the SH3 domain binding to the N-terminal poly-proline region. This second interaction serves to both stabilize the auto-inhibitory helix on the DH domain and to partially occlude the DH domain. Future studies will identify other Dbl-family members regulated in a manner similar to Tim, define the precise molecular details of Tim auto-

inhibition and rationally design small molecule inhibitors of Tim activity. They will also define the intracellular signaling pathways regulating Tim under normal conditions and during tumorigenesis. Finally, future studies will establish the physiological role for Ngef activation of multiple GTPases.

REFERENCES

1. Wennerberg, K., and Der, C. J. (2004) *J Cell Sci* **117**, 1301-1312

2. Etienne-Manneville, S., and Hall, A. (2002) *Nature* **420**, 629-635

3. Sahai, E., and Marshall, C. J. (2002) *Nat Rev Cancer* **2**, 133-142

4. Ramakers, G. J. (2002) *Trends Neurosci* **25**, 191-199

5. Rossman, K. L., Der, C. J., and Sondek, J. (2005) *Nat Rev Mol Cell Biol* **6**, 167-180

6. Yoshizuka, N., Moriuchi, R., Mori, T., Yamada, K., Hasegawa, S., Maeda, T., Shimada, T., Yamada, Y., Kamihira, S., Tomonaga, M., and Katamine, S. (2004) *J Biol Chem* **279**, 43998-44004

7. Vanni, C., Mancini, P., Gao, Y., Ottaviano, C., Guo, F., Salani, B., Torrisi, M. R., Zheng, Y., and Eva, A. (2002) *J Biol Chem* **277**, 19745-19753

8. Lopez-Lago, M., Lee, H., Cruz, C., Movilla, N., and Bustelo, X. R. (2000) *Mol Cell Biol* **20**, 1678-1691

9. Zenke, F. T., Krendel, M., DerMardirossian, C., King, C. C., Bohl, B. P., and Bokoch, G. M. (2004) *J Biol Chem* **279**, 18392-18400

10. Schmidt, A., and Hall, A. (2002) *Genes Dev* **16**, 1587-1609

11. Schultz, J., Copley, R. R., Doerks, T., Ponting, C. P., and Bork, P. (2000) *Nucleic Acids Res* **28**, 231-234

12. Pasteris, N. G., Cadle, A., Logie, L. J., Porteous, M. E., Schwartz, C. E., Stevenson, R. E., Glover, T. W., Wilroy, R. S., and Gorski, J. L. (1994) *Cell* **79**, 669-678

13. Pasteris, N. G., and Gorski, J. L. (1999) *Genomics* **60**, 57-66

14. Pasteris, N. G., Nagata, K., Hall, A., and Gorski, J. L. (2000) *Gene* **242**, 237-247

15. Obaishi, H., Nakanishi, H., Mandai, K., Satoh, K., Satoh, A., Takahashi, K., Miyahara, M., Nishioka, H., Takaishi, K., and Takai, Y. (1998) *J Biol Chem* **273**, 18697-18700

16. Olson, M. F., Pasteris, N. G., Gorski, J. L., and Hall, A. (1996) *Curr Biol* **6**, 1628-1633

17. Nagata, K., Driessens, M., Lamarche, N., Gorski, J. L., and Hall, A. (1998) *J Biol Chem* **273**, 15453-15457

18. Whitehead, I. P., Abe, K., Gorski, J. L., and Der, C. J. (1998) *Mol Cell Biol* **18**, 4689-4697

19. Orrico, A., Galli, L., Falciani, M., Bracci, M., Cavaliere, M. L., Rinaldi, M. M., Musacchio, A., and Sorrentino, V. (2000) *FEBS Lett* **478**, 216-220

20. Estrada, L., Caron, E., and Gorski, J. L. (2001) *Hum Mol Genet* **10**, 485-495

21. Hou, P., Estrada, L., Kinley, A. W., Parsons, J. T., Vojtek, A. B., and Gorski, J. L. (2003) *Hum Mol Genet* **12**, 1981-1993

22. Hayakawa, M., Kitagawa, H., Miyazawa, K., Kitagawa, M., and Kikugawa, K. (2005) *Genes Cells* **10**, 241-251

23. Umikawa, M., Obaishi, H., Nakanishi, H., Satoh-Horikawa, K., Takahashi, K., Hotta, I., Matsuura, Y., and Takai, Y. (1999) *J Biol Chem* **274**, 25197-25200

24. Nakahara, H., Otani, T., Sasaki, T., Miura, Y., Takai, Y., and Kogo, M. (2003) *Genes Cells* **8**, 1019-1027

25. Chen, X. M., Splinter, P. L., Tietz, P. S., Huang, B. Q., Billadeau, D. D., and LaRusso, N. F. (2004) *J Biol Chem* **279**, 31671-31678

26. Kawasaki, Y., Senda, T., Ishidate, T., Koyama, R., Morishita, T., Iwayama, Y., Higuchi, O., and Akiyama, T. (2000) *Science* **289**, 1194-1197

27. Koyano, Y., Kawamoto, T., Kikuchi, A., Shen, M., Kuruta, Y., Tsutsumi, S., Fujimoto, K., Noshiro, M., Fujii, K., and Kato, Y. (2001) *Osteoarthritis Cartilage* **9 Suppl A**, S64-68

28. Bi, F., Debreceni, B., Zhu, K., Salani, B., Eva, A., and Zheng, Y. (2001) *Mol Cell Biol* **21**, 1463-1474

29. Kostenko, E. V., Mahon, G. M., Cheng, L., and Whitehead, I. P. (2005) *J Biol Chem* **280**, 2807-2817

30. Saito, S., Liu, X. F., Kamijo, K., Raziuddin, R., Tatsumoto, T., Okamoto, I., Chen, X., Lee, C. C., Lorenzi, M. V., Ohara, N., and Miki, T. (2004) *J Biol Chem* **279**, 7169-7179

31. Ren, Y., Li, R., Zheng, Y., and Busch, H. (1998) *J Biol Chem* **273**, 34954-34960

32. Hussain, N. K., Jenna, S., Glogauer, M., Quinn, C. C., Wasiak, S., Guipponi, M., Antonarakis, S. E., Kay, B. K., Stossel, T. P., Lamarche-Vane, N., and McPherson, P. S. (2001) *Nat Cell Biol* **3**, 927-932

33. Chikumi, H., Barac, A., Behbahani, B., Gao, Y., Teramoto, H., Zheng, Y., and Gutkind, J. S. (2004) *Oncogene* **23**, 233-240

34. Olson, M. F., Sterpetti, P., Nagata, K., Toksoz, D., and Hall, A. (1997) *Oncogene* **15**, 2827-2831

35. Chan, A. M., Takai, S., Yamada, K., and Miki, T. (1996) *Oncogene* **12**, 1259-1266

36. Rodrigues, N. R., Theodosiou, A. M., Nesbit, M. A., Campbell, L., Tandle, A. T., Saranath, D., and Davies, K. E. (2000) *Genomics* **65**, 53-61

37. Niu, J., Profirovic, J., Pan, H., Vaiskunaite, R., and Voyno-Yasenetskaya, T. (2003) *Circ Res* **93**, 848-856

38. van Horck, F. P., Ahmadian, M. R., Haeusler, L. C., Moolenaar, W. H., and Kranenburg, O. (2001) *J Biol Chem* **276**, 4948-4956

39. Xiang, S., Kim, E. Y., Connelly, J. J., Nassar, N., Kirsch, J., Winking, J., Schwarz, G., and Schindelin, H. (2006) *J Mol Biol* **359**, 35-46

40. Hill, K., Krugmann, S., Andrews, S. R., Coadwell, W. J., Finan, P., Welch, H. C., Hawkins, P. T., and Stephens, L. R. (2005) *J Biol Chem* **280**, 4166-4173

41. Yang, H., and Mattingly, R. R. (2006) *Mol Biol Cell* **17**, 2177-2189

42. Ellerbroek, S. M., Wennerberg, K., Arthur, W. T., Dunty, J. M., Bowman, D. R., DeMali, K. A., Der, C., and Burridge, K. (2004) *Mol Biol Cell* **15**, 3309-3319

43. Matsuo, N., Hoshino, M., Yoshizawa, M., and Nabeshima, Y. (2002) *J Biol Chem* **277**, 2860-2868

44. Xie, X., Chang, S. W., Tatsumoto, T., Chan, A. M., and Miki, T. (2005) *Cell Signal* **17**, 461-471

45. Zugaza, J. L., Lopez-Lago, M. A., Caloca, M. J., Dosil, M., Movilla, N., and Bustelo, X. R. (2002) *J Biol Chem* **277**, 45377-45392

46. Miyamoto, Y., Yamauchi, J., and Itoh, H. (2003) *J Biol Chem* **278**, 29890-29900

47. Fukuhara, T., Shimizu, K., Kawakatsu, T., Fukuyama, T., Minami, Y., Honda, T., Hoshino, T., Yamada, T., Ogita, H., Okada, M., and Takai, Y. (2004) *J Cell Biol* **166**, 393-405

48. Fukuyama, T., Ogita, H., Kawakatsu, T., Fukuhara, T., Yamada, T., Sato, T., Shimizu, K., Nakamura, T., Matsuda, M., and Takai, Y. (2005) *J Biol Chem* **280**, 815-825

49. Murata, T., Ohnishi, H., Okazawa, H., Murata, Y., Kusakari, S., Hayashi, Y., Miyashita, M., Itoh, H., Oldenborg, P. A., Furuya, N., and Matozaki, T. (2006) *J Neurosci* **26**, 12397-12407

50. Innocenti, M., Zippel, R., Brambilla, R., and Sturani, E. (1999) *FEBS Lett* **460**, 357-362

51. Kiyono, M., Satoh, T., and Kaziro, Y. (1999) *Proc Natl Acad Sci U S A* **96**, 4826-4831

52. Anborgh, P. H., Qian, X., Papageorge, A. G., Vass, W. C., DeClue, J. E., and Lowy, D. R. (1999) *Mol Cell Biol* **19**, 4611-4622

53. Forlani, G., Baldassa, S., Lavagni, P., Sturani, E., and Zippel, R. (2006) *Febs J* **273**, 2127-2138

54. Innocenti, M., Tenca, P., Frittoli, E., Faretta, M., Tocchetti, A., Di Fiore, P. P., and Scita, G. (2002) *J Cell Biol* **156**, 125-136

55. Scita, G., Tenca, P., Areces, L. B., Tocchetti, A., Frittoli, E., Giardina, G., Ponzanelli, I., Sini, P., Innocenti, M., and Di Fiore, P. P. (2001) *J Cell Biol* **154**, 1031-1044

56. Scita, G., Nordstrom, J., Carbone, R., Tenca, P., Giardina, G., Gutkind, S., Bjarnegard, M., Betsholtz, C., and Di Fiore, P. P. (1999) *Nature* **401**, 290-293

57. Khanday, F. A., Santhanam, L., Kasuno, K., Yamamori, T., Naqvi, A., Dericco, J., Bugayenko, A., Mattagajasingh, I., Disanza, A., Scita, G., and Irani, K. (2006) *J Cell Biol* **172**, 817-822

58. Nimnual, A. S., Yatsula, B. A., and Bar-Sagi, D. (1998) *Science* **279**, 560-563

59. Rameh, L. E., Ak, A., Carraway, K. L., 3rd, Couvillon, A. D., Rathbun, G., Crompton, A., VanRenterghem, B., Czech, M. P., Ravichandran, K. S., Burakoff, S. J., Wang, D. S., Chen, C. S., and Cantley, L. C. (1997) *J Biol Chem* **272**, 22059-22066

60. Das, B., Shu, X., Day, G. J., Han, J., Krishna, U. M., Falck, J. R., and Broek, D. (2000) *J Biol Chem* **275**, 15074-15081

61. Innocenti, M., Frittoli, E., Ponzanelli, I., Falck, J. R., Brachmann, S. M., Di Fiore, P. P., and Scita, G. (2003) *J Cell Biol* **160**, 17-23

62. Sini, P., Cannas, A., Koleske, A. J., Di Fiore, P. P., and Scita, G. (2004) *Nat Cell Biol* **6**, 268-274

63. Yang, L., and Bashaw, G. J. (2006) *Neuron* **52**, 595-607

64. Tatsumoto, T., Xie, X., Blumenthal, R., Okamoto, I., and Miki, T. (1999) *J Cell Biol* **147**, 921-928

65. Kimura, K., Tsuji, T., Takada, Y., Miki, T., and Narumiya, S. (2000) *J Biol Chem* **275**, 17233-17236

66. Solski, P. A., Wilder, R. S., Rossman, K. L., Sondek, J., Cox, A. D., Campbell, S. L., and Der, C. J. (2004) *J Biol Chem* **279**, 25226-25233

67. Kim, J. E., Billadeau, D. D., and Chen, J. (2005) *J Biol Chem* **280**, 5733-5739

68. Nishimura, Y., and Yonemura, S. (2006) *J Cell Sci* **119**, 104-114

69. Chalamalasetty, R. B., Hummer, S., Nigg, E. A., and Sillje, H. H. (2006) *J Cell Sci* **119**, 3008-3019

70. Wolf, A., Keil, R., Gotzl, O., Mun, A., Schwarze, K., Lederer, M., Huttelmaier, S., and Hatzfeld, M. (2006) *Nat Cell Biol* **8**, 1432-1440

71. Scoumanne, A., and Chen, X. (2006) *Cancer Res* **66**, 6271-6279

72. Eguchi, T., Takaki, T., Itadani, H., and Kotani, H. (2007) *Oncogene* **26**, 509-520

73. Reiter, L. T., Seagroves, T. N., Bowers, M., and Bier, E. (2006) *Hum Mol Genet* **15**, 2825-2835

74. Clemens, F., Verma, R., Ramnath, J., and Landolph, J. R. (2005) *Toxicol Appl Pharmacol* **206**, 138-149

75. Niiya, F., Tatsumoto, T., Lee, K. S., and Miki, T. (2006) *Oncogene* **25**, 827-837

76. Knoll, B., and Drescher, U. (2004) *J Neurosci* **24**, 6248-6257

77. Shamah, S. M., Lin, M. Z., Goldberg, J. L., Estrach, S., Sahin, M., Hu, L., Bazalakova, M., Neve, R. L., Corfas, G., Debant, A., and Greenberg, M. E. (2001) *Cell* **105**, 233-244

78. Sahin, M., Greer, P. L., Lin, M. Z., Poucher, H., Eberhart, J., Schmidt, S., Wright, T. M., Shamah, S. M., O'Connell, S., Cowan, C. W., Hu, L., Goldberg, J. L., Debant, A., Corfas, G., Krull, C. E., and Greenberg, M. E. (2005) *Neuron* **46**, 191-204

79. Fu, W. Y., Chen, Y., Sahin, M., Zhao, X. S., Shi, L., Bikoff, J. B., Lai, K. O., Yung, W. H., Fu, A. K., Greenberg, M. E., and Ip, N. Y. (2007) *Nat Neurosci* **10**, 67-76

80. Ogita, H., Kunimoto, S., Kamioka, Y., Sawa, H., Masuda, M., and Mochizuki, N. (2003) *Circ Res* **93**, 23-31

81. Qi, H., Fournier, A., Grenier, J., Fillion, C., Labrie, Y., and Labrie, C. (2003) *Endocrinology* **144**, 1742-1752

82. Wang, Y., Suzuki, H., Yokoo, T., Tada-Iida, K., Kihara, R., Miura, M., Watanabe, K., Sone, H., Shimano, H., Toyoshima, H., and Yamada, N. (2004) *Biochem Biophys Res Commun* **324**, 1053-1058

83. Chan, A. M., McGovern, E. S., Catalano, G., Fleming, T. P., and Miki, T. (1994) *Oncogene* **9**, 1057-1063

84. Takai, S., Chan, A. M., Yamada, K., and Miki, T. (1995) *Cancer Genet Cytogenet* **83**, 87-89

85. Benais-Pont, G., Punn, A., Flores-Maldonado, C., Eckert, J., Raposo, G., Fleming, T. P., Cereijido, M., Balda, M. S., and Matter, K. (2003) *J Cell Biol* **160**, 729-740

86. Schmidt, A., and Hall, A. (2002) *J Biol Chem* **277**, 14581-14588

87. Zhang, H., and Macara, I. G. (2006) *Nat Cell Biol* **8**, 227-237

88. Ten Klooster, J. P., Evers, E. E., Janssen, L., Machesky, L. M., Michiels, F., Hordijk, P., and Collard, J. G. (2006) *Biochem J* **397**, 39-45

89. Otani, T., Ichii, T., Aono, S., and Takeichi, M. (2006) *J Cell Biol* **175**, 135-146

90. Okamoto, M., Schoch, S., and Sudhof, T. C. (1999) *J Biol Chem* **274**, 18446-18454

91. Yamabhai, M., Hoffman, N. G., Hardison, N. L., McPherson, P. S., Castagnoli, L., Cesareni, G., and Kay, B. K. (1998) *J Biol Chem* **273**, 31401-31407

92. Snyder, J. T., Rossman, K. L., Baumeister, M. A., Pruitt, W. M., Siderovski, D. P., Der, C. J., Lemmon, M. A., and Sondek, J. (2001) *J Biol Chem* **276**, 45868-45875.

93. Pruitt, W. M., Karnoub, A. E., Rakauskas, A. C., Guipponi, M., Antonarakis, S. E., Kurakin, A., Kay, B. K., Sondek, J., Siderovski, D. P., and Der, C. J. (2003) *Biochim Biophys Acta* **1640**, 61-68

94. Snyder, J. T., Worthylake, D. K., Rossman, K. L., Betts, L., Pruitt, W. M., Siderovski, D. P., Der, C. J., and Sondek, J. (2002) *Nat Struct Biol* **9**, 468-475

95. Kim, S., Lee, S. H., and Park, D. (2001) *J Biol Chem* **276**, 10581-10584

96. Zhu, K., Debreceni, B., Bi, F., and Zheng, Y. (2001) *Mol Cell Biol* **21**, 425-437

97. Sterpetti, P., Hack, A. A., Bashar, M. P., Park, B., Cheng, S. D., Knoll, J. H., Urano, T., Feig, L. A., and Toksoz, D. (1999) *Mol Cell Biol* **19**, 1334-1345

98. Nishimura, T., Yamaguchi, T., Tokunaga, A., Hara, A., Hamaguchi, T., Kato, K., Iwamatsu, A., Okano, H., and Kaibuchi, K. (2006) *Mol Biol Cell* **17**, 1273-1285

99. Wang, J. B., Wu, W. J., and Cerione, R. A. (2005) *J Biol Chem* **280**, 22883-22891

100. Irie, F., and Yamaguchi, Y. (2002) *Nat Neurosci* **5**, 1117-1118

101. Alberts, A. S., and Treisman, R. (1998) *EMBO J* **17**, 4075-4085

102. Arthur, W. T., Ellerbroek, S. M., Der, C. J., Burridge, K., and Wennerberg, K. (2002) *J Biol Chem* **277**, 42964-42972

103. Qin, H., Carr, H. S., Wu, X., Muallem, D., Tran, N. H., and Frost, J. A. (2005) *J Biol Chem* **280**, 7603-7613

104. Jaffe, A. B., Hall, A., and Schmidt, A. (2005) *Curr Biol* **15**, 405-412

105. Alberts, A. S., Qin, H., Carr, H. S., and Frost, J. A. (2005) *J Biol Chem* **280**, 12152-12161

106. Fukuhara, S., Murga, C., Zohar, M., Igishi, T., and Gutkind, J. S. (1999) *J Biol Chem* **274**, 5868-5879

107. Hart, M. J., Jiang, X., Kozasa, T., Roscoe, W., Singer, W. D., Gilman, A. G., Sternweis, P. C., and Bollag, G. (1998) *Science* **280**, 2112-2114

108. Booden, M. A., Siderovski, D. P., and Der, C. J. (2002) *Mol Cell Biol* **22**, 4053-4061

109. Wells, C. D., Gutowski, S., Bollag, G., and Sternweis, P. C. (2001) *J Biol Chem* **276**, 28897-28905.

110. Bhattacharyya, R., and Wedegaertner, P. B. (2000) *J Biol Chem* **275**, 14992-14999

111. Bhattacharyya, R., and Wedegaertner, P. B. (2003) *Biochem J* **371**, 709-720

112. Perrot, V., Vazquez-Prado, J., and Gutkind, J. S. (2002) *J Biol Chem* **277**, 43115-43120

113. Oinuma, I., Katoh, H., Harada, A., and Negishi, M. (2003) *J Biol Chem* **278**, 25671-25677

114. Yamada, T., Ohoka, Y., Kogo, M., and Inagaki, S. (2005) *J Biol Chem* **280**, 19358-19363

115. Taya, S., Inagaki, N., Sengiku, H., Makino, H., Iwamatsu, A., Urakawa, I., Nagao, K., Kataoka, S., and Kaibuchi, K. (2001) *J Cell Biol* **155**, 809-820

116. Holinstat, M., Mehta, D., Kozasa, T., Minshall, R. D., and Malik, A. B. (2003) *J Biol Chem* **278**, 28793-28798

117. Suzuki, N., Nakamura, S., Mano, H., and Kozasa, T. (2003) *Proc Natl Acad Sci U S A* **100**, 733-738

118. Rosenfeldt, H., Castellone, M. D., Randazzo, P. A., and Gutkind, J. S. (2006) *J Mol Signal* **1**, 8

119. Barac, A., Basile, J., Vazquez-Prado, J., Gao, Y., Zheng, Y., and Gutkind, J. S. (2004) *J Biol Chem* **279**, 6182-6189

120. Meyer, D., Liu, A., and Margolis, B. (1999) *J Biol Chem* **274**, 35113-35118

121. Toksoz, D., and Williams, D. A. (1994) *Oncogene* **9**, 621-628

122. Zheng, Y., Olson, M. F., Hall, A., Cerione, R. A., and Toksoz, D. (1995) *J Biol Chem* **270**, 9031-9034

123. Dutt, P., Nguyen, N., and Toksoz, D. (2004) *Cell Signal* **16**, 201-209

124. Majumdar, M., Seasholtz, T. M., Buckmaster, C., Toksoz, D., and Brown, J. H. (1999) *J Biol Chem* **274**, 26815-26821

125. Baisamy, L., Jurisch, N., and Diviani, D. (2005) *J Biol Chem* **280**, 15405-15412

126. Rubino, D., Driggers, P., Arbit, D., Kemp, L., Miller, B., Coso, O., Pagliai, K., Gray, K., Gutkind, S., and Segars, J. (1998) *Oncogene* **16**, 2513-2526

127. Kino, T., Souvatzoglou, E., Charmandari, E., Ichijo, T., Driggers, P., Mayers, C., Alatsatianos, A., Manoli, I., Westphal, H., Chrousos, G. P., and Segars, J. H. (2006) *J Biol Chem* **281**, 9118-9126

128. Diviani, D., Soderling, J., and Scott, J. D. (2001) *J Biol Chem* **276**, 44247-44257

129. Diviani, D., Abuin, L., Cotecchia, S., and Pansier, L. (2004) *Embo J* **23**, 2811-2820

130. Iwashita, S., Fujii, M., Mukai, H., Ono, Y., and Miyamoto, M. (2004) *Biochem Biophys Res Commun* **320**, 1063-1068

131. Brecht, M., Steenvoorden, A. C., Collard, J. G., Luf, S., Erz, D., Bartram, C. R., and Janssen, J. W. (2005) *Int J Cancer* **113**, 533-540

132. Krendel, M., Zenke, F. T., and Bokoch, G. M. (2002) *Nat Cell Biol* **4**, 294-301

133. Aijaz, S., D'Atri, F., Citi, S., Balda, M. S., and Matter, K. (2005) *Dev Cell* **8**, 777-786

134. Chang, Y. C., Lee, H. H., Chen, Y. J., Bokoch, G. M., and Chang, Z. F. (2006) *Cell Death Differ* **13**, 2023-2032

135. Matsuzawa, T., Kuwae, A., Yoshida, S., Sasakawa, C., and Abe, A. (2004) *Embo J* **23**, 3570-3582

136. Callow, M. G., Zozulya, S., Gishizky, M. L., Jallal, B., and Smeal, T. (2005) *J Cell Sci* **118**, 1861-1872

137. Mizuarai, S., Yamanaka, K., and Kotani, H. (2006) *Cancer Res* **66**, 6319-6326

138. Frolov, A., Chahwan, S., Ochs, M., Arnoletti, J. P., Pan, Z. Z., Favorova, O., Fletcher, J., von Mehren, M., Eisenberg, B., and Godwin, A. K. (2003) *Mol Cancer Ther* **2**, 699-709

139. Shin, E. Y., Woo, K. N., Lee, C. S., Koo, S. H., Kim, Y. G., Kim, W. J., Bae, C. D., Chang, S. I., and Kim, E. G. (2004) *J Biol Chem* **279**, 1994-2004

140. Chahdi, A., Miller, B., and Sorokin, A. (2005) *J Biol Chem* **280**, 578-584

141. Feng, Q., Baird, D., Peng, X., Wang, J., Ly, T., Guan, J. L., and Cerione, R. A. (2006) *Nat Cell Biol* **8**, 945-956

142. Kato, J., Kaziro, Y., and Satoh, T. (2000) *Biochem Biophys Res Commun* **268**, 141-147

143. Yamauchi, J., Hirasawa, A., Miyamoto, Y., Kokubu, H., Nishii, H., Okamoto, M., Sugawara, Y., Tsujimoto, G., and Itoh, H. (2002) *Biochem Biophys Res Commun* **296**, 85-92

144. Yamauchi, J., Chan, J. R., Miyamoto, Y., Tsujimoto, G., and Shooter, E. M. (2005) *Proc Natl Acad Sci U S A* **102**, 5198-5203

145. Penzes, P., Beeser, A., Chernoff, J., Schiller, M. R., Eipper, B. A., Mains, R. E., and Huganir, R. L. (2003) *Neuron* **37**, 263-274

146. Mayeenuddin, L. H., McIntire, W. E., and Garrison, J. C. (2006) *J Biol Chem* **281**, 1913-1920

147. Kiyono, M., Kaziro, Y., and Satoh, T. (2000) *J Biol Chem* **275**, 5441-5446

148. Takefuji, M., Mori, K., Morita, Y., Arimura, N., Nishimura, T., Nakayama, M., Hoshino, M., Iwamatsu, A., Murohara, T., Kaibuchi, K., and Amano, M. (2007) *Biochem Biophys Res Commun*

149. Servitja, J. M., Marinissen, M. J., Sodhi, A., Bustelo, X. R., and Gutkind, J. S. (2003) *J Biol Chem* **278**, 34339-34346

150. Miyamoto, Y., Yamauchi, J., Tanoue, A., Wu, C., and Mobley, W. C. (2006) *Proc Natl Acad Sci U S A* **103**, 10444-10449

151. Forsthoefel, D. J., Liebl, E. C., Kolodziej, P. A., and Seeger, M. A. (2005) *Development* **132**, 1983-1994

152. Bustelo, X. R. (2000) *Mol Cell Biol* **20**, 1461-1477

153. Fernandez-Zapico, M. E., Gonzalez-Paz, N. C., Weiss, E., Savoy, D. N., Molina, J. R., Fonseca, R., Smyrk, T. C., Chari, S. T., Urrutia, R., and Billadeau, D. D. (2005) *Cancer Cell* **7**, 39-49

154. Aghazadeh, B., Lowry, W. E., Huang, X. Y., and Rosen, M. K. (2000) *Cell* **102**, 625-633

155. Schiller, M. R. (2006) *Cell Signal* **18**, 1834-1843

156. Han, J., Luby-Phelps, K., Das, B., Shu, X., Xia, Y., Mosteller, R. D., Krishna, U. M., Falck, J. R., White, M. A., and Broek, D. (1998) *Science* **279**, 558-560

157. Llorca, O., Arias-Palomo, E., Zugaza, J. L., and Bustelo, X. R. (2005) *Embo J* **24**, 1330-1340

158. Oh, W. K., Yoo, J. C., Jo, D., Song, Y. H., Kim, M. G., and Park, D. (1997) *Biochem Biophys Res Commun* **235**, 794-798

159. Bagrodia, S., Taylor, S. J., Jordon, K. A., Van Aelst, L., and Cerione, R. A. (1998) *J Biol Chem* **273**, 23633-23636

160. Manser, E., Loo, T. H., Koh, C. G., Zhao, Z. S., Chen, X. Q., Tan, L., Tan, I., Leung, T., and Lim, L. (1998) *Mol Cell* **1**, 183-192

161. Feng, Q., Baird, D., and Cerione, R. A. (2004) *Embo J* **23**, 3492-3504

162. Kutsche, K., Yntema, H., Brandt, A., Jantke, I., Nothwang, H. G., Orth, U., Boavida, M. G., David, D., Chelly, J., Fryns, J. P., Moraine, C., Ropers, H. H., Hamel, B. C., van Bokhoven, H., and Gal, A. (2000) *Nat Genet* **26**, 247-250

163. Feng, Q., Albeck, J. G., Cerione, R. A., and Yang, W. (2002) *J Biol Chem* **277**, 5644-5650

164. Baird, D., Feng, Q., and Cerione, R. A. (2005) *Curr Biol* **15**, 1-10

165. Habets, G. G., van der Kammen, R. A., Stam, J. C., Michiels, F., and Collard, J. G. (1995) *Oncogene* **10**, 1371-1376.

166. Muroya, K., Kawasaki, Y., Hayashi, T., Ohwada, S., and Akiyama, T. (2007) *Biochem Biophys Res Commun*

167. Cheng, L., Mahon, G. M., Kostenko, E. V., and Whitehead, I. P. (2004) *J Biol Chem* **279**, 12786-12793

168. Chakrabarti, K., Lin, R., Schiller, N. I., Wang, Y., Koubi, D., Fan, Y. X., Rudkin, B. B., Johnson, G. R., and Schiller, M. R. (2005) *Mol Cell Biol* **25**, 5106-5118

169. Welch, H. C., Coadwell, W. J., Ellson, C. D., Ferguson, G. J., Andrews, S. R., Erdjument-Bromage, H., Tempst, P., Hawkins, P. T., and Stephens, L. R. (2002) *Cell* **108**, 809-821

170. Das, B., Shu, X., Day, G. J., Han, J., Krishna, U. M., Falck, J. R., and Broek, D. (2000) *J Biol Chem* **275**, 15074-15081.

171. Bellanger, J. M., Astier, C., Sardet, C., Ohta, Y., Stossel, T. P., and Debant, A. (2000) *Nat Cell Biol* **2**, 888-892.
taf/DynaPage.taf?file=/ncb/journal/v882/n812/full/ncb1200_1888.html
taf/DynaPage.taf?file=/ncb/journal/v1202/n1212/abs/ncb1200_1888.html

172. Michiels, F., Habets, G. G., Stam, J. C., van der Kammen, R. A., and Collard, J. G. (1995) *Nature* **375**, 338-340.

173. Engers, R., Zwaka, T. P., Gohr, L., Weber, A., Gerharz, C. D., and Gabbert, H. E. (2000) *Int J Cancer* **88**, 369-376

174. Engers, R., Mueller, M., Walter, A., Collard, J. G., Willers, R., and Gabbert, H. E. (2006) *Br J Cancer* **95**, 1081-1086

175. Mertens, A. E., Roovers, R. C., and Collard, J. G. (2003) *FEBS Lett* **546**, 11-16

176. Qi, H., Juo, P., Masuda-Robens, J., Caloca, M. J., Zhou, H., Stone, N., Kazanietz, M. G., and Chou, M. M. (2001) *Cell Growth Differ* **12**, 603-611

177. Malliri, A., van Es, S., Huveneers, S., and Collard, J. G. (2004) *J Biol Chem* **279**, 30092-30098

178. Buchanan, F. G., Elliot, C. M., Gibbs, M., and Exton, J. H. (2000) *J Biol Chem* **275**, 9742-9748

179. Michiels, F., Stam, J. C., Hordijk, P. L., van der Kammen, R. A., Ruuls-Van Stalle, L., Feltkamp, C. A., and Collard, J. G. (1997) *J Cell Biol* **137**, 387-398

180. Sander, E. E., van Delft, S., ten Klooster, J. P., Reid, T., van der Kammen, R. A., Michiels, F., and Collard, J. G. (1998) *J Cell Biol* **143**, 1385-1398

181. Fleming, I. N., Batty, I. H., Prescott, A. R., Gray, A., Kular, G. S., Stewart, H., and Downes, C. P. (2004) *Biochem J* **382**, 857-865

182. Buchsbaum, R. J., Connolly, B. A., and Feig, L. A. (2003) *J Biol Chem* **278**, 18833-18841

183. Crompton, A. M., Foley, L. H., Wood, A., Roscoe, W., Stokoe, D., McCormick, F., Symons, M., and Bollag, G. (2000) *J Biol Chem* **275**, 25751-25759

184. Baumeister, M. A., Martinu, L., Rossman, K. L., Sondek, J., Lemmon, M. A., and Chou, M. M. (2003) *J Biol Chem* **278**, 11457-11464

185. Nishida, K., Kaziro, Y., and Satoh, T. (1999) *FEBS Lett* **459**, 186-190

186. Lutz, S., Freichel-Blomquist, A., Yang, Y., Rumenapp, U., Jakobs, K. H., Schmidt, M., and Wieland, T. (2005) *J Biol Chem* **280**, 11134-11139

187. Fleming, I. N., Elliott, C. M., Collard, J. G., and Exton, J. H. (1997) *J Biol Chem* **272**, 33105-33110

188. Fleming, I. N., Elliott, C. M., and Exton, J. H. (1998) *FEBS Lett* **429**, 229-233

189. Tanaka, M., Ohashi, R., Nakamura, R., Shinmura, K., Kamo, T., Sakai, R., and Sugimura, H. (2004) *Embo J* **23**, 1075-1088

190. Tolias, K. F., Bikoff, J. B., Burette, A., Paradis, S., Harrar, D., Tavazoie, S., Weinberg, R. J., and Greenberg, M. E. (2005) *Neuron* **45**, 525-538

191. Malliri, A., van der Kammen, R. A., Clark, K., van der Valk, M., Michiels, F., and Collard, J. G. (2002) *Nature* **417**, 867-871

192. Lambert, J. M., Lambert, Q. T., Reuther, G. W., Malliri, A., Siderovski, D. P., Sondek, J., Collard, J. G., and Der, C. J. (2002) *Nat Cell Biol* **4**, 621-625

193. Wohlgemuth, S., Kiel, C., Kramer, A., Serrano, L., Wittinghofer, F., and Herrmann, C. (2005) *J Mol Biol* **348**, 741-758

194. Arthur, W. T., Quilliam, L. A., and Cooper, J. A. (2004) *J Cell Biol* **167**, 111-122

195. Snyder, J. T., Singer, A. U., Wing, M. R., Harden, T. K., and Sondek, J. (2003) *J Biol Chem* **278**, 21099-21104

196. Nishimura, T., Yamaguchi, T., Kato, K., Yoshizawa, M., Nabeshima, Y., Ohno, S., Hoshino, M., and Kaibuchi, K. (2005) *Nat Cell Biol* **7**, 270-277

197. Curtis, C., Hemmeryckx, B., Haataja, L., Senadheera, D., Groffen, J., and Heisterkamp, N. (2004) *Mol Cancer* **3**, 10

198. Freedman, T. S., Sondermann, H., Friedland, G. D., Kortemme, T., Bar-Sagi, D., Marqusee, S., and Kuriyan, J. (2006) *Proc Natl Acad Sci U S A* **103**, 16692-16697

199. Hamann, M. J., Lubking, C. M., Luchini, D. N., and Billadeau, D. D. (2007) *Mol Cell Biol* **27**, 1380-1393

200. Reid, T., Bathoorn, A., Ahmadian, M. R., and Collard, J. G. (1999) *J Biol Chem* **274**, 33587-33593

201. Kins, S., Betz, H., and Kirsch, J. (2000) *Nat Neurosci* **3**, 22-29

202. Kawasaki, Y., Sato, R., and Akiyama, T. (2003) *Nat Cell Biol* **5**, 211-215

203. Murayama, K., Shirouzu, M., Kawasaki, Y., Kato-Murayama, M., Hanawa-Suetsugu, K., Sakamoto, A., Katsura, Y., Suenaga, A., Toyama, M., Terada, T., Taiji, M., Akiyama, T., and Yokoyama, S. (2007) *J Biol Chem* **282**, 4238-4242

204. Kamynina, E., Kauppinen, K., Duan, F., Muakkassa, N., and Manor, D. (2007) *Mol Cell Biol* **27**, 1809-1822

205. Rosenfeldt, H., Vazquez-Prado, J., and Gutkind, J. S. (2004) *FEBS Lett* **572**, 167-171

206. Donald, S., Hill, K., Lecureuil, C., Barnouin, R., Krugmann, S., John Coadwell, W., Andrews, S. R., Walker, S. A., Hawkins, P. T., Stephens, L. R., and Welch, H. C. (2004) *FEBS Lett* **572**, 172-176

207. Joseph, R. E., and Norris, F. A. (2005) *J Biol Chem* **280**, 27508-27512

208. Yoshizawa, M., Kawauchi, T., Sone, M., Nishimura, Y. V., Terao, M., Chihama, K., Nabeshima, Y., and Hoshino, M. (2005) *J Neurosci* **25**, 4406-4419

209. Zhao, T., Nalbant, P., Hoshino, M., Dong, X., Wu, D., and Bokoch, G. M. (2007) *J Leukoc Biol*

210. Kovacs, E. M., Makar, R. S., and Gertler, F. B. (2006) *J Cell Sci* **119**, 2715-2726

211. Salazar, M. A., Kwiatkowski, A. V., Pellegrini, L., Cestra, G., Butler, M. H., Rossman, K. L., Serna, D. M., Sondek, J., Gertler, F. B., and De Camilli, P. (2003) *J Biol Chem* **278**, 49031-49043

212. Borisov, A. B., Raeker, M. O., Kontrogianni-Konstantopoulos, A., Yang, K., Kurnit, D. M., Bloch, R. J., and Russell, M. W. (2003) *Biochem Biophys Res Commun* **310**, 910-918

213. Young, P., Ehler, E., and Gautel, M. (2001) *J Cell Biol* **154**, 123-136

214. Eva, A., and Aaronson, S. A. (1985) *Nature* **316**, 273-275

215. Ron, D., Tronick, S. R., Aaronson, S. A., and Eva, A. (1988) *Embo J* **7**, 2465-2473

216. Russo, C., Gao, Y., Mancini, P., Vanni, C., Porotto, M., Falasca, M., Torrisi, M. R., Zheng, Y., and Eva, A. (2001) *J Biol Chem* **276**, 19524-19531.

217. Zheng, Y., Zangrilli, D., Cerione, R. A., and Eva, A. (1996) *J Biol Chem* **271**, 19017-19020

218. Ron, D., Graziani, G., Aaronson, S. A., and Eva, A. (1989) *Oncogene* **4**, 1067-1072

219. Kauppinen, K. P., Duan, F., Wels, J. I., and Manor, D. (2005) *J Biol Chem* **280**, 21638-21644

220. Whitehead, I. P., Kirk, H., and Kay, R. (1995) *Oncogene* **10**, 713-721

221. Cheng, L., Rossman, K. L., Mahon, G. M., Worthylake, D. K., Korus, M., Sondek, J., and Whitehead, I. P. (2002) *Mol Cell Biol* **22**, 6895-6905

222. Whitehead, I. P., Lambert, Q. T., Glaven, J. A., Abe, K., Rossman, K. L., Mahon, G. M., Trzaskos, J. M., Kay, R., Campbell, S. L., and Der, C. J. (1999) *Mol Cell Biol* **19**, 7759-7770

223. Rossman, K. L., Cheng, L., Mahon, G. M., Rojas, R. J., Snyder, J. T., Whitehead, I. P., and Sondek, J. (2003) *J Biol Chem* **278**, 18393-18400

224. Baumeister, M. A., Rossman, K. L., Sondek, J., and Lemmon, M. A. (2006) *Biochem J* **400**, 563-572

225. Rossman, K. L., Worthylake, D. K., Snyder, J. T., Siderovski, D. P., Campbell, S. L., and Sondek, J. (2002) *Embo J* **21**, 1315-1326.

226. Kostenko, E. V., Olabisi, O. O., Sahay, S., Rodriguez, P. L., and Whitehead, I. P. (2006) *Mol Cell Biol* **26**, 8964-8975

227. Souchet, M., Portales-Casamar, E., Mazurais, D., Schmidt, S., Leger, I., Javre, J. L., Robert, P., Berrebi-Bertrand, I., Bril, A., Gout, B., Debant, A., and Calmels, T. P. (2002) *J Cell Sci* **115**, 629-640

228. Guo, X., Stafford, L. J., Bryan, B., Xia, C., Ma, W., Wu, X., Liu, D., Songyang, Z., and Liu, M. (2003) *J Biol Chem* **278**, 13207-13215

229. Bryan, B., Kumar, V., Stafford, L. J., Cai, Y., Wu, G., and Liu, M. (2004) *J Biol Chem* **279**, 45824-45832

230. Lutz, S., Freichel-Blomquist, A., Rumenapp, U., Schmidt, M., Jakobs, K. H., and Wieland, T. (2004) *Naunyn Schmiedebergs Arch Pharmacol* **369**, 540-546

231. Bryan, B. A., Mitchell, D. C., Zhao, L., Ma, W., Stafford, L. J., Teng, B. B., and Liu, M. (2005) *Mol Cell Biol* **25**, 11089-11101

232. Debant, A., Serra-Pagès, C., Seipel, K., O'Brien, S., Tang, M., Park, S.-H., and Steuli, M. (1996) *Proc Natl Acad Sci* **93**, 5466-5471

233. Newsome, T. P., Schmidt, S., Dietzl, G., Keleman, K., Asling, B., Debant, A., and Dickson, B. J. (2000) *Cell* **101**, 283-294

234. Estrach, S., Schmidt, S., Diriong, S., Penna, A., Blangy, A., Fort, P., and Debant, A. (2002) *Curr Biol* **12**, 307-312

235. Bellanger, J. M., Estrach, S., Schmidt, S., Briancon-Marjollet, A., Zugasti, O., Fromont, S., and Debant, A. (2003) *Biol Cell* **95**, 625-634

236. Liebl, E. C., Forsthoefel, D. J., Franco, L. S., Sample, S. H., Hess, J. E., Cowger, J. A., Chandler, M. P., Shupert, A. M., and Seeger, M. A. (2000) *Neuron* **26**, 107-118

237. Sun, Y. J., Nishikawa, K., Yuda, H., Wang, Y. L., Osaka, H., Fukazawa, N., Naito, A., Kudo, Y., Wada, K., and Aoki, S. (2006) *Mol Cell Biol* **26**, 6923-6935

238. Alam, M. R., Johnson, R. C., Darlington, D. N., Hand, T. A., Mains, R. E., and Eipper, B. A. (1997) *J Biol Chem* **272**, 12667-12675

239. Johnson, R. C., Penzes, P., Eipper, B. A., and Mains, R. E. (2000) *J Biol Chem* **275**, 19324-19333

240. Penzes, P., Johnson, R. C., Kambampati, V., Mains, R. E., and Eipper, B. A. (2001) *J Neurosci* **21**, 8426-8434

241. Penzes, P., Johnson, R. C., Sattler, R., Zhang, X., Huganir, R. L., Kambampati, V., Mains, R. E., and Eipper, B. A. (2001) *Neuron* **29**, 229-242

242. May, V., Schiller, M. R., Eipper, B. A., and Mains, R. E. (2002) *J Neurosci* **22**, 6980-6990

243. Schiller, M. R., Chakrabarti, K., King, G. F., Schiller, N. I., Eipper, B. A., and Maciejewski, M. W. (2006) *J Biol Chem* **281**, 18774-18786

244. Debily, M. A., Camarca, A., Ciullo, M., Mayer, C., El Marhomy, S., Ba, I., Jalil, A., Anzisi, A., Guardiola, J., and Piatier-Tonneau, D. (2004) *Hum Mol Genet* **13**, 323-334

245. Worthylake, D. K., Rossman, K. L., and Sondek, J. (2000) *Nature* **408**, 682-688

246. Rojas, R. J., Kimple, R. J., Rossman, K. L., Siderovski, D. P., and Sondek, J. (2003) *Comb Chem High Throughput Screen* **6**, 409-418

247. Rost, B. (1996) *Methods Enzymol* **266**, 525-539

248. Blom, N., Gammeltoft, S., and Brunak, S. (1999) *J Mol Biol* **294**, 1351-1362

249. Miranti, C. K., Leng, L., Maschberger, P., Brugge, J. S., and Shattil, S. J. (1998) *Curr Biol* **8**, 1289-1299

250. Salojin, K. V., Zhang, J., Meagher, C., and Delovitch, T. L. (2000) *J Biol Chem* **275**, 5966-5975

251. Teramoto, H., Salem, P., Robbins, K. C., Bustelo, X. R., and Gutkind, J. S. (1997) *J Biol Chem* **272**, 10751-10755

252. Han, J., Das, B., Wei, W., Van Aelst, L., Mosteller, R. D., Khosravi-Far, R., Westwick, J. K., Der, C. J., and Broek, D. (1997) *Mol Cell Biol* **17**, 1346-1353

253. Crespo, P., Schuebel, K. E., Ostrom, A. A., Gutkind, J. S., and Bustelo, X. R. (1997) *Nature* **385**, 169-172

254. Fischer, K. D., Zmuldzinas, A., Gardner, S., Barbacid, M., Bernstein, A., and Guidos, C. (1995) *Nature* **374**, 474-477

255. Deprez, C., Lloubes, R., Gavioli, M., Marion, D., Guerlesquin, F., and Blanchard, L. (2005) *J Mol Biol* **346**, 1047-1057

256. DeLano, W. L. (2002) *The PyMOL Molecular Graphics System*, DeLano Scientific, San Carlos, CA, USA

257. Boettner, B., and Van Aelst, L. (2002) *Gene* **286**, 155-174

258. Hornstein, I., Pikarsky, E., Groysman, M., Amir, G., Peylan-Ramu, N., and Katzav, S. (2003) *J Pathol* **199**, 526-533

259. Schmidt, S., Diriong, S., Mery, J., Fabbrizio, E., and Debant, A. (2002) *FEBS Lett* **523**, 35-42

260. Akbar, H., Cancelas, J., Williams, D. A., Zheng, J., and Zheng, Y. (2006) *Methods Enzymol* **406**, 554-565

261. Gao, Y., Dickerson, J. B., Guo, F., Zheng, J., and Zheng, Y. (2004) *Proc Natl Acad Sci U S A* **101**, 7618-7623

262. Zeeh, J. C., Zeghouf, M., Grauffel, C., Guibert, B., Martin, E., Dejaegere, A., and Cherfils, J. (2006) *J Biol Chem* **281**, 11805-11814

263. Chen, L., Liao, G., Yang, L., Campbell, K., Nakafuku, M., Kuan, C. Y., and Zheng, Y. (2006) *Proc Natl Acad Sci U S A* **103**, 16520-16525

264. Cappello, S., Attardo, A., Wu, X., Iwasato, T., Itohara, S., Wilsch-Brauninger, M., Eilken, H. M., Rieger, M. A., Schroeder, T. T., Huttner, W. B., Brakebusch, C., and Gotz, M. (2006) *Nat Neurosci* **9**, 1099-1107

265. Pucharcos, C., Fuentes, J. J., Casas, C., de la Luna, S., Alcantara, S., Arbones, M. L., Soriano, E., Estivill, X., and Pritchard, M. (1999) *Eur J Hum Genet* **7**, 704-712

266. Hadano, S., Hand, C. K., Osuga, H., Yanagisawa, Y., Otomo, A., Devon, R. S., Miyamoto, N., Showguchi-Miyata, J., Okada, Y., Singaraja, R., Figlewicz, D. A., Kwiatkowski, T., Hosler, B. A., Sagie, T., Skaug, J., Nasir, J., Brown, R. H., Jr., Scherer, S. W., Rouleau, G. A., Hayden, M. R., and Ikeda, J. E. (2001) *Nat Genet* **29**, 166-173

267. Kubo, T., Yamashita, T., Yamaguchi, A., Sumimoto, H., Hosokawa, K., and Tohyama, M. (2002) *J Neurosci* **22**, 8504-8513

268. Toyofuku, T., Yoshida, J., Sugimoto, T., Zhang, H., Kumanogoh, A., Hori, M., and Kikutani, H. (2005) *Nat Neurosci* **8**, 1712-1719

269. Yohe, M. E., Rossman, K. L., Gardner, O. S., Karnoub, A. E., Snyder, J. T., Gershburg, S., Graves, L. M., Der, C. J., and Sondek, J. (2007) *J Biol Chem* **in press**

270. Hand, R., Bortone, D., Mattar, P., Nguyen, L., Heng, J. I., Guerrier, S., Boutt, E., Peters, E., Barnes, A. P., Parras, C., Schuurmans, C., Guillemot, F., and Polleux, F. (2005) *Neuron* **48**, 45-62

271. Solski, P. A., Wilder, R. S., Rossman, K. L., Sondek, J., Cox, A. D., Campbell, S. L., and Der, C. J. (2004) *J Biol Chem*

272. Polleux, F., and Ghosh, A. (2002) *Sci STKE* **2002**, PL9

273. Luo, L. (2000) *Nat Rev Neurosci* **1**, 173-180

274. Chen, T. J., Gehler, S., Shaw, A. E., Bamburg, J. R., and Letourneau, P. C. (2006) *J Neurobiol* **66**, 103-114

275. Hirose, M., Ishizaki, T., Watanabe, N., Uehata, M., Kranenburg, O., Moolenaar, W. H., Matsumura, F., Maekawa, M., Bito, H., and Narumiya, S. (1998) *J Cell Biol* **141**, 1625-1636

276. Kozma, R., Sarner, S., Ahmed, S., and Lim, L. (1997) *Mol Cell Biol* **17**, 1201-1211

277. Giniger, E. (2002) *Differentiation* **70**, 385-396

278. Dickson, B. J. (2001) *Curr Opin Neurobiol* **11**, 103-110

279. Woo, S., and Gomez, T. M. (2006) *J Neurosci* **26**, 1418-1428

280. Kuhn, T. B., Brown, M. D., Wilcox, C. L., Raper, J. A., and Bamburg, J. R. (1999) *J Neurosci* **19**, 1965-1975

281. Noren, N. K., and Pasquale, E. B. (2004) *Cell Signal* **16**, 655-666

282. Cowan, C. W., Shao, Y. R., Sahin, M., Shamah, S. M., Lin, M. Z., Greer, P. L., Gao, S., Griffith, E. C., Brugge, J. S., and Greenberg, M. E. (2005) *Neuron* **46**, 205-217

283. Jurney, W. M., Gallo, G., Letourneau, P. C., and McLoon, S. C. (2002) *J Neurosci* **22**, 6019-6028

284. Thies, E., and Davenport, R. W. (2003) *J Neurobiol* **54**, 358-369

285. Cesareni, G., Panni, S., Nardelli, G., and Castagnoli, L. (2002) *FEBS Lett* **513**, 38-44

286. Sicheri, F., and Kuriyan, J. (1997) *Curr Opin Struct Biol* **7**, 777-785

287. Moarefi, I., LaFevre-Bernt, M., Sicheri, F., Huse, M., Lee, C. H., Kuriyan, J., and Miller, W. T. (1997) *Nature* **385**, 650-653

288. Lerner, E. C., and Smithgall, T. E. (2002) *Nat Struct Biol* **9**, 365-369

289. Pursglove, S. E., Mulhern, T. D., Mackay, J. P., Hinds, M. G., and Booker, G. W. (2002) *J Biol Chem* **277**, 755-762

290. Andreotti, A. H., Bunnell, S. C., Feng, S., Berg, L. J., and Schreiber, S. L. (1997) *Nature* **385**, 93-97

291. Hansson, H., Smith, C. I., and Hard, T. (2001) *FEBS Lett* **508**, 11-15

292. Hansson, H., Okoh, M. P., Smith, C. I., Vihinen, M., and Hard, T. (2001) *FEBS Lett* **489**, 67-70

293. Brazin, K. N., Fulton, D. B., and Andreotti, A. H. (2000) *J Mol Biol* **302**, 607-623

294. Nagar, B., Hantschel, O., Seeliger, M., Davies, J. M., Weis, W. I., Superti-Furga, G., and Kuriyan, J. (2006) *Mol Cell* **21**, 787-798

295. Pluk, H., Dorey, K., and Superti-Furga, G. (2002) *Cell* **108**, 247-259

296. Zamanian, J. L., and Kelly, R. B. (2003) *Mol Biol Cell* **14**, 1624-1637

297. Gentry, H. R., Singer, A. U., Betts, L., Yang, C., Ferrara, J. D., Sondek, J., and Parise, L. V. (2005) *J Biol Chem* **280**, 8407-8415

298. Snow, B. E., Brothers, G. M., and Siderovski, D. P. (2002) *Methods Enzymol* **344**, 740-761

299. Johnston, C. A., Willard, F. S., Jezyk, M. R., Fredericks, Z., Bodor, E. T., Jones, M. B., Blaesius, R., Watts, V. J., Harden, T. K., Sondek, J., Ramer, J. K., and Siderovski, D. P. (2005) *Structure* **13**, 1069-1080

300. Bhattacharyya, R. P., Remenyi, A., Yeh, B. J., and Lim, W. A. (2006) *Annu Rev Biochem*

301. Sun, Q. L., Zhou, H. J., and Lin, K. (2005) *Genomics Proteomics Bioinformatics* **3**, 94-106

302. Lim, W. A. (2002) *Curr Opin Struct Biol* **12**, 61-68

303. Derewenda, Z. S. (2004) *Structure* **12**, 529-535

304. Navaza, J., and Saludjian, P. (1997) *Methods Enzymol* **276**, 581-594

305. Read, R. J. (2001) *Acta Crystallogr D Biol Crystallogr* **57**, 1373-1382

306. Derewenda, U., Oleksy, A., Stevenson, A. S., Korczynska, J., Dauter, Z., Somlyo, A. P., Otlewski, J., Somlyo, A. V., and Derewenda, Z. S. (2004) *Structure (Camb)* **12**, 1955-1965

307. Kristelly, R., Gao, G., and Tesmer, J. J. (2004) *J Biol Chem*

308. Skowronek, K. R., Guo, F., Zheng, Y., and Nassar, N. (2004) *J Biol Chem*

309. Nishida, M., Nagata, K., Hachimori, Y., Horiuchi, M., Ogura, K., Mandiyan, V., Schlessinger, J., and Inagaki, F. (2001) *Embo J* **20**, 2995-3007

310. Worthylake, D. K., Rossman, K. L., and Sondek, J. (2004) *Structure (Camb)* **12**, 1078-1086

311. Hendrickson, W. A., Horton, J. R., and LeMaster, D. M. (1990) *Embo J* **9**, 1665-1672

312. Jones, T. A., Zou, J. Y., Cowan, S. W., and Kjeldgaard. (1991) *Acta Crystallogr A* **47**, 110-119

313. Laskowski, R. A., MacArthur, M. W., Moss, D. S., and Thorton, J. M. (1993) *J Appl Crystallogr* **26**, 283-291

314. Radha, V., Rajanna, A., and Swarup, G. (2004) *BMC Cell Biol* **5**, 31

315. Wildenberg, G. A., Dohn, M. R., Carnahan, R. H., Davis, M. A., Lobdell, N. A., Settleman, J., and Reynolds, A. B. (2006) *Cell* **127**, 1027-1039

316. Iiizumi, M., Hosokawa, M., Takehara, A., Chung, S., Nakamura, T., Katagiri, T., Eguchi, H., Ohigashi, H., Ishikawa, O., Nakamura, Y., and Nakagawa, H. (2006) *Cancer Sci* **97**, 1211-1216

317. Pertz, O., and Hahn, K. M. (2004) *J Cell Sci* **117**, 1313-1318